MULTI-AGENT OPEN ARCHITECTURE FOR PROCESS MONITORING AND PART CERTIFICATION

A Dissertation
Presented to
The Academic Faculty

by

Kyle Scott Saleeby

In Partial Fulfillment
of the Requirements for the Degree
Doctor of Philosophy in the
George W. Woodruff School of Mechanical Engineering

Georgia Institute of Technology
May 2021

MULTI-AGENT OPEN ARCHITECTURE FOR PROCESS MONITORING AND PART CERTIFICATION

Approved by:

Dr. Thomas Kurfess, Advisor
School of Mechanical Engineering
Georgia Institute of Technology

Dr. Vincent Paquit
Energy Systems Analytics Group
Oak Ridge National Laboratory

Dr. Christopher Saldana
School of Mechanical Engineering
Georgia Institute of Technology

Dr. Lonnie Love
Manufacturing Science Division
Oak Ridge National Laboratory

Dr. Katherine Fu
School of Mechanical Engineering
Georgia Institute of Technology

Dr. Thomas Gardner
Chief Technical Officer
Hewlett-Packard Federal

Date Approved: 11 February 2021

To my wife Regan,

my parents Nancy and Charlie Saleeby,

and my grandmother Helen Diggers.

I love you all.

ACKNOWLEDGEMENTS

First and foremost, I would like to thank Dr. Tom Kurfess, who not only advised this research but generously shares his time as a tremendous engineering mentor and personal friend. Thank you for taking me on as a student, researcher, and of course, as an ME2110 Head TA.

Thank you as well to Dr. Lonnie Love and Dr. Vincent Paquit for the opportunity to complete this research at the world-class Manufacturing Demonstration Facility. It is truly an honor to work with an such an incredible team of researchers, innovators, and engineers. I would also like to thank my reading committee, Dr. Chris Saldana, Dr. Kate Fu, and Dr. Tommy Gardner for their caring guidance, expert advice, and unique perspective. Learning from each of you has been an invaluable experience.

None of this work would be possible without my brilliant and beautiful wife, Regan. Thank you for your endless wisdom, patience, love, and support. The joy you bring to my life cannot be captured in words. Go Big Red.

It is hard to overstate my thanks and respect for Dr. Tom Feldhausen, whom I consider a friend, mentor, and partner-in-crime for the dangerous phrase "What if…?" A big thank you as well to Dennis, Rebecca, and the MDF's Hybrid Manufacturing Team, who all bring exceptional skill, perceptive insight, and witty humor to any challenge.

Finally, I'd like to thank my loving parents. I am truly blessed by and thankful for the many sacrifices you made for me. It all began with a series of crazy science fair experiments, a uniquely strange JASON speech, and countless hours laughing over The Far Side comics. Thank you to my mother, Nancy Saleeby, who always encourages me to "be happy, and smile", and to my father, Charlie Saleeby, who always catches the first, the most, and the biggest fish.

TABLE OF CONTENTS

LIST OF TABLES

LIST OF FIGURES

LIST OF SYMBOLS AND ABBREVIATIONS

CAM	Computer Aided Manufacturing
CC	Cloud Computing
CNC	Compute Numerical Control
CPS	Cyber-Physical System
DCS	Distributed Control System
DED	Direct Energy Deposition
EC	Edge Computing
FC	Fog Computing
HTTP	Hypertext Transfer Protocol
HWD	Hot-Wire Deposition
IoT	Internet of Things
JSON	JavaScript Object Notation
MDF	Manufacturing Demonstration Facility
MQTT	Message Queue Telemetry Transport
OEE	Overall Equipment Effectiveness
OPC-UA	Open Platform Communications – Unified Architecture
ORNL	Oak Ridge National Laboratory
PLC	Programable Logic Controller
SCADA	Supervisory Control and Data Acquisition
XML	Extensible Markup Language

SUMMARY

Methods to connect manufacturing machines, processes, and sensors have rapidly developed through the fourth industrial revolution, known as Industry 4.0. Data collection is now possible at every point in a production process, providing exceptional analysis opportunities to monitor and affect manufacturing operations. Digital manufacturing technologies can be applied to computer numeric control (CNC) manufacturing processes to measure and improve component quality. Various architectures have been proposed to leverage machine connection mechanisms and extract information in a logical manner. However, these architectures often rely on proprietary software, restricting flexibility for future changes and upgrades. Furthermore, additional capabilities are needed to combine data collected from different sensing modalities and provide a method of *in-situ* geometric verification. A multi-agent open architecture is proposed to collect, analyze, and communicate information of different formats and sampling characteristics in a strategic manner. This body of work evaluates the strategic combination and synchronization of information from multiple sensing modalities to improve the accuracy of digital twin models. A voxel modelling methodology is developed and investigated to create a digital twin of the component being produced. Information describing the machine's current operations is strategically combined with information from additional sensing modalities, improving the accuracy of *in-situ* digital twin models by up to 52%. This research results in (1) a method to geometrically compare features of *in-situ* components from multiple sensing modalities against desired specifications, (2) a multi-agent architecture to support efficient communication, storage, and use of this information, resulting in (3) feedback methodologies for commercial CNC systems to affect the *in-situ* manufacturing process and correct geometric deviations.

CHAPTER 1. INTRODUCTION AND BACKGROUND

The integration of digital manufacturing technologies with traditional manufacturing systems has enabled revolutionary advances in manufacturing process control. Digital manufacturing technologies can be applied to computer numeric control (CNC) manufacturing processes to gain a better understanding of processing conditions. When strategically leveraged, these technologies enable the creation of a digital twin, an *in-situ* virtual representation of the manufactured component that allows for a comparison of accuracy between the realized part and desired specifications. The goal of this dissertation is to evaluate combinations of process monitoring techniques, information architectures, and process feedback methodologies to increase the geometric accuracy and process control of components fabricated with CNC manufacturing systems. This project is fundamentally different from previous investigations because it evaluates the combination of multiple sensor information sources to increase the accuracy of digital twin models, resulting in feedback methodologies for i*n-situ* process and component modifications.

1.1 Introduction to Digital Manufacturing

The manufacturing industry has experienced several significant changes over the past two centuries. Three primary industrial revolutions can be seen, each focused on mechanization, large-scale production, and automation, respectively [1]. The shift towards connected manufacturing processes with feedback methods represents the 4th Industrial Revolution, commonly referred to as Industry 4.0 [2]. This new paradigm of connected machines and processes enable the generation of tremendous amounts of data describing manufacturing operations [3].

Industry 4.0 technologies span a wide range of digital technologies including sensors, data communication mechanisms, storage capabilities, machine learning and artificial intelligence algorithms, and process feedback methods. Small-footprint implementations can consist of monitoring machine production status, whether the machine is running or idle, to calculate Overall Equipment Effectiveness (OEE) analytics [4]. These implementations are often used to monitor a single mission-critical machine, decreasing bottlenecks in the production line. Large footprint implementations can consist of data streams from hundreds of machines, each sampling up to 1kHz frequency. These implementations are often used in the continuous manufacturing industry, such as pulp and paper manufacturers, where mis-matches in roll speed between two paper dryers are detected, preventing the sheet from tearing. The combination of digital communication technologies with traditional manufacturing systems created a new classification of equipment, termed Cyber-Physical Systems (CPS), which depend on synergy of computational and physical components for standard operations [5]. CPS frameworks have become integral to the manufacturing industry. Technologies developed in support of the Industry 4.0 revolution have enabled significant opportunities to monitor manufacturing processes.

1.2 Introduction to Hybrid Manufacturing

Hybrid manufacturing is the combination of additive manufacturing (AM) and subtractive manufacturing (SM) capabilities within the same build volume. Together, these capabilities enable additive, subtractive, and inspection operations to be interchangeably used throughout the build process in a single machine setup. While hybrid manufacturing technologies have existed for two decades, they have only recently found momentum in commercial applications [6].

Hybrid manufacturing technologies are often integrated into standard subtractive CNC machining centers, commonly referred to as CNC machines. Machine tool manufactures such as Mazak, Okuma, and DMG-Mori have produced integrated systems with a variety of material deposition and removal capabilities [7-9]. These manufacturers often include additive capabilities offset as a parallel column next to standard subtractive machining spindles, as displayed in Figure 1 [8]. Other manufacturers such as Hybrid Manufacturing Technologies have developed deposition systems that can be retrofitted on existing commercial CNC machines by developing additive deposition heads as removable tools placed coaxially in standard subtractive spindles [10].

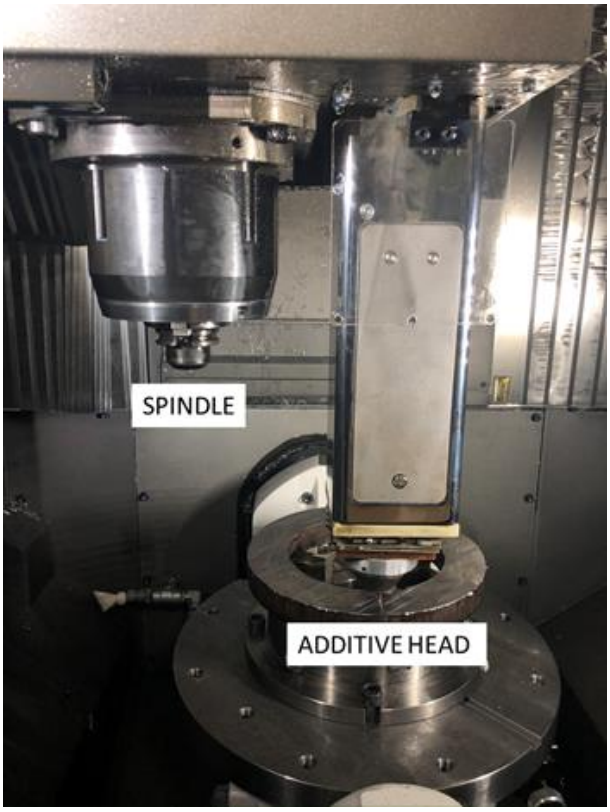

Figure 1: Subtractive Spindle (left) and Additive Head (right) [8].

While the results of this research are applicable to any commercial CNC system, including standard subtractive systems as well as hybrid systems, this body of work leverages a Mazak VC-500A/5X AM HWD hybrid CNC machine. Additive capabilities are achieved with a laser hotwire directed-energy deposition (DED) system, where standard welding wire is melted and fused to substrate through a combination of resistive and lased-based thermal heating [11]. The inclusion of additional processing techniques within standard subtractive systems has driven the need for increased processes monitoring and feedback control capabilities. These efforts are assisted by numerous information streams produced by modern CNC manufacturing systems.

1.3 Sensing Modalities

Multiple sensing modalities exist for CNC machines. These modalities can be categorized into two main clarifications based on the source of information, (1) machine-direct information, including any information that is generated, calculated, or measured by the primary machine controller and, (2) external sensor information including sensors that are retrofitted on the CNC system and do not have any direct line of communication to the primacy machine controller.

Multiple protocols exist for capturing machine-direct communication, including MTConnect, OPC-UA, and Haas Connect [12-14]. These protocols provide information such as current machine position, feed rate, spindle speed, and machine state. Some protocols such as MTConnect defines a common formatting standard for the information, increasing flexibility over multiple systems. Others, such as OPC-UA, do not include a lexicon-based formatting standard, decreasing interoperability between separate systems.

A third category includes machine monitoring protocols such as Haas Connect that only allow a user to view machine usage analytics with little opportunity for further development.

External sensing modalities often consist of retrofit sensors added by the machine tool user. Most implementations are driven by the specific need of the manufacturing process. Common external sensing modalities include thermocouples and thermal infrared imaging systems, accelerometers, acoustic systems, and environmental sensors.

1.4 Technological Deficiencies

Metrics of component verification and statistical process control are integral to any manufacturing process. However, these methods are often evaluated in aggregate, abstracted away from variations of an individual unit with Shewart control charts [15]. The integration of CPS with manufacturing production lines enable opportunities to include digital verification methods for every single part that is produced. The capability to leverage *in-situ* certification methods enables increased assurance of part quality and authenticity for mission-critical components, such as high pressure turbine blades, where a single failure is catastrophic.

1.4.1 Component Certification

The need for and benefits of component certification can be most easily observed in hybrid manufacturing. While subtractive machining is a well-understood and controlled process, the inclusion of additive technologies in hybrid manufacturing creates a new set of process parameters, techniques, and potential defects that must be investigated and

controlled. In an additive manufacturing regime, geometric accuracy continues to be an active research area to mitigate effects such as overbuilding, underbuilding, and thermal distortion. When subtractive capabilities are included, these problems are exacerbated as error accumulates across different processing segments. Recent advancements in digital manufacturing technologies and digital twin modelling may enable greater monitoring capabilities to detect and mitigate these geometric errors. While methods of geometric verification and process improvement are necessary to the success and industry adoption of hybrid systems, implications of these technologies include mechanisms for cyber security and verification of a component's authentic fabrication.

1.4.2 Process Monitoring Information

The information produced as part of the machine monitoring technologies is often under-utilized or unused altogether due to a variety of factors. Significant infrastructure such as information architectures, communication mechanisms, and storage capabilities are needed to apply this information and make actionable changes in the production line. Additionally, significant technological deficiencies exist withing the process monitoring capabilities. The MTConnect protocol is one of the most used machine monitoring technologies in the machining industry. However, it was primarily designed to provide manufacturing supervisors with operational efficiency metrics such as Overall Equipment Effectiveness (OEE) and machine operational time logs.

Recent versions of the MTConnect protocol have included additional machine state information such as current machine position, feed rate, and spindle speed. This information can be applied to digital twin modeling methods to for a digital representation of the fabricated component.

Subtractive CNC machines typically update the MTConnect information at rates between 2 Hz and 10 Hz. Given a standard component processed with subtractive machining at a rate of 1000 mm/min, and MTConnect information update rate of 2 Hz, the minimum distance between recorded points in 8.3mm. With common dimensional tolerances of 0.127mm (0.005 in) on standard manufacturing components, additional information is needed to verify the accuracy of fabricated components from digital twin modelling methods. Minimum recorded distance combinations of refresh rates and feed rates are displayed in Table 1.

Table 1: Minimum Recorded Distance for MTConnect Sample Rates

Sample Frequency	2Hz	3Hz	5Hz
Travel Time	9.0 s	9.0 s	9.0 s
Datapoints	18 pts.	27 pts.	45 pts.
Minimum Distance	**8.3 mm**	**5.5 mm**	3.3 mm

1.4.3 Advanced Process Control

Subtractive machining has been heavily investigated over the past century and underlying scientific principles are well-known [16]. Common areas of research in the field of subtractive processing parameters are cutting parameters (depth of cut, feed rate, and spindle speed), tool stability, and surface finish [17]. However, process parameters for the additive manufacturing are not well understood [18]. While additive manufacturing enables the production of complex geometries that are unobtainable by traditional manufacturing technologies, significant work remains to identify reliable processing parameters for an arbitrary combination of geometry and material. Feldhausen demonstrated that no one set of processing parameters is sufficient for all geometries [19]. Additionally, previous work has demonstrated that static processing parameters may not

be suitable for some geometries due to thermal overheating [20]. Geometric inaccuracies are further exacerbated when additive and subtractive processes are interchangeably used as enabled by hybrid CNC machines.

1.5 Summary

This research investigates three technologies to improve process monitoring and part certification;

(1) A method to geometrically compare features of *in-situ* components from the combination of multiple sensing modalities against desired specifications;

(2) A multi-agent architecture to support efficient communication, storage, and use of manufacturing information, resulting in;

(3) Feedback methodologies for commercial CNC systems to affect the *in-situ* manufacturing process and correct geometric deviations.

These technologies are developed and investigated with hybrid manufacturing; however, they are applicable to any CNC manufacturing process. These contributions further enable industry adoption of hybrid manufacturing technology, and verification of component accuracy through digital twin modelling techniques.

CHAPTER 2. PROJECT DESCRIPTION

This chapter outlines the body of research conducted to advance the understanding and applications of digital monitoring technologies with feedback methodologies for CNC manufacturing systems. This project is different than previous research because it evaluates the combination of multiple sensor modality techniques to increase the geometric understanding of the fabricated component *in-situ*, resulting in feedback actions to affect the processes for a more desirable outcome with commercially available CNC manufacturing systems. It is hypothesized that the strategic combination and synchronization of information from multiple sensing modalities can be leveraged to improve the accuracy of *in-situ* digital twins, resulting in a smaller measure of error between the fabricated component and intended specifications. This error in turn can be mitigated by the development of closed-loop control methodologies to affect the manufacturing process. This research is conducted with hybrid manufacturing operations, where additive, subtractive, and inspection capabilities can be used interchangeably to affect the component. This body of work will result in methodologies for *in-situ* process monitoring, information communication architectures, and closed-loop control operations for reliable, efficient, and consistent CNC manufacturing operations.

2.1 Introduction

This project consists of three phases for the evaluation and development of digital process monitoring and feedback systems. Each phase of research builds upon the previous phase, leveraging subsequent advances to culminate in process control feedback mechanisms for improved geometric component fabrication.

Phase I evaluates combination and synchronization of information from multiple sensing modalities to improve the accuracy of digital twin models of *in-situ* components. This body of work investigates the accuracy of the digital representation of the *in-situ* component, created from the combination of information from multiple digital and physical sources, enabling a numerical comparison mechanism to desired specifications.

Phase II investigates information architectures required to support operations developed in Phase I. This body of work explores multi-agent open architectures needed to capture, communicate, and store information from multiple sensing modalities. Additionally, this body of work evaluates compression mechanisms for sensing modality information in coordination with architecture size and digital footprint.

Phase III investigates methods of process feedback control for commercial CNC manufacturing systems. A machine-agnostic feedback framework is developed and evaluated for three levels of feedback control, each focused on a different timescale of operational processes. Three distinct applications of closed-loop control are implemented and demonstrated.

This dissertation results in a framework for process monitoring and evaluation, an information communication architecture to support monitoring and evaluation operations, and feedback methods for closed-loop control of CNC manufacturing processes on commercially available equipment. This research is conducted with hybrid manufacturing processes due to process monitoring information availability, and the need for improved geometric control through dynamic processing conditions with hybrid operations. The

results of this work increase fabrication accuracy and process control of commercial CNC machines.

2.2 Phase I – Data Synchronization for Geometric Accuracy

2.2.1 Summary

Previous research has demonstrated that components fabricated with hybrid manufacturing often experience significant geometric deviations from engineered specifications [19]. These deviations can be detrimental to future additive and subtractive processing operations, particularly when fabricating large-scale components. Underbuilt structures do not provide the expected foundation for deposition of future geometries. In the subtractive part of the hybrid process, overbuilt structures result in machining passes that are deeper than expected, decreasing tool life (if not breaking the tool entirely). Deviations between engineered specification and realized components can be detected in process through a variety of sensing modalities. It is hypothesized that the strategic combination and synchronization of sensing modalities results in a more accurate understanding of the *in-situ* component, resulting in a comparison between intended and realized geometry. This numerical comparison enables future corrective actions.

Experiments with four strategically chosen geometries will be performed to determine the capabilities and limitations of detecting the accuracy of the desired component through *in-situ* voxel modelling techniques. Information from the initial programmed G-code instructions, MTConnect process data, and *in-situ* probing data will be used to form a digital model of the experiment geometry using voxel methods. The resulting geometries will be compared for accuracy against specified dimensions. Finally, *ex-situ* measurements were taken to provide a ground-truth comparison.

2.2.2 Experiment 1.1: Subtractive NIST Geometry

Experiment 1.1 consists of the subtractive fabrication and digital detection of an AM test article developed by the National Institute of Standards and Technology (NIST) [21]. This article is designed to test the dimensional accuracy of features that are difficult to manufacture with AM methods. For this experiment, a subset of features are extracted and placed on round substrate, displayed in Figure 2.

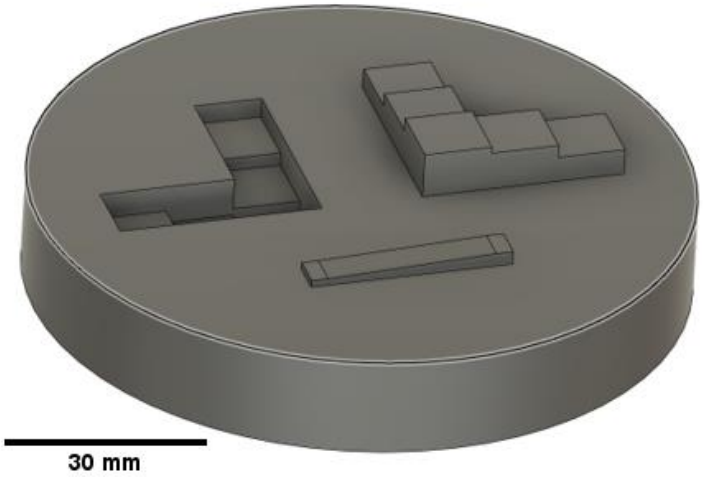

Figure 2: NIST Subtractive Test Geometry

NIST allows for uniform scaling of the geometry to a size appropriate for the machine in question [21]. These features are scaled appropriately and manufactured with subtractive methods only (additive and hybrid features are evaluated in Experiment 1.2.)

2.2.3 Experiment 1.2: Additive and Hybrid NIST Geometry

Experiment 1.2 consists of the hybrid fabrication of geometry sources from the NIST test article in Experiment 1.1. The selected geometry is scaled appropriately for additive methods and placed on round substrate, displayed in Figure 3.

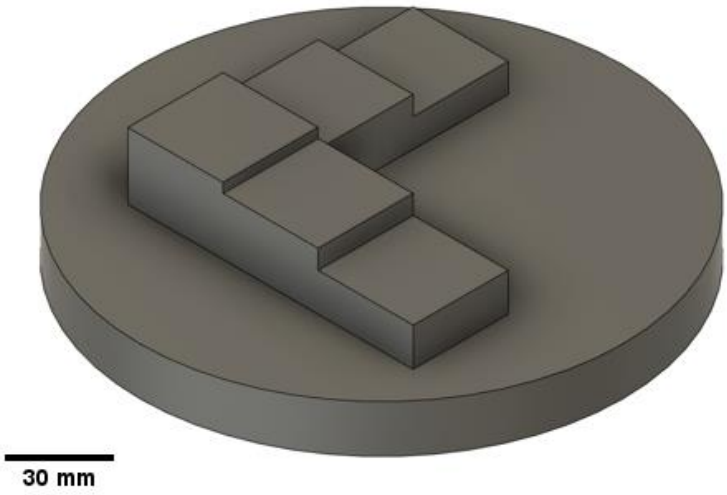

Figure 3: NIST Additive and Hybrid Test Geometry

This scale is different from Experiment 1.1 due to bead geometry constraints. Two identical components will be manufactured for this experiment. Component A was fabricated solely with additive methods. Component B will be manufactured with additive methods before subtractive machining to final dimensions. Component B is designed to be overbuilt by 2mm on every planar face, then machined to final dimensions, enabling an investigation to detect overbuild structures. Additive process parameters will be held constant through these experiments.

2.2.4 Experiment 1.3: Organic Surface Geometry

Experiment 1.3 consists of the hybrid fabrication of a raised organic surface of varying curvatures. The organic surface geometry is displayed in Figure 4.

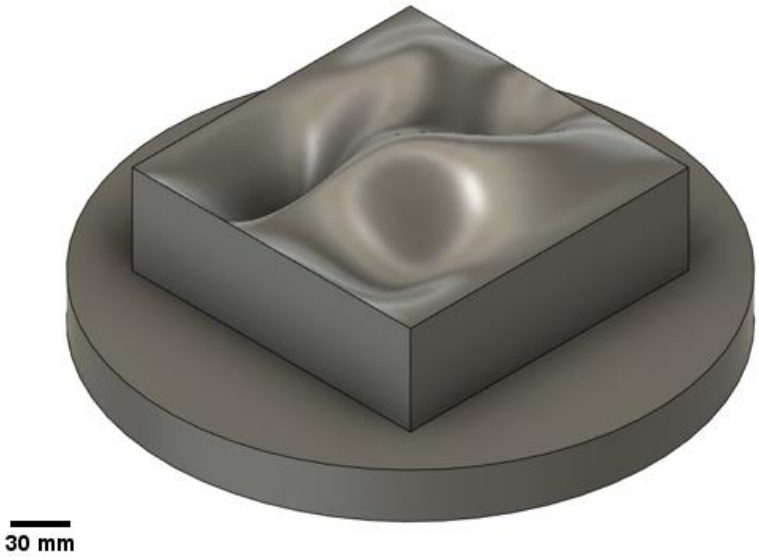

Figure 4: Organic Surface Test Geometry

This test article is designed to test the inspection and accuracy methods on 3D non-planar features, as is common with tooling molds and dies. Due to inherent workspace discretization of voxelized modelling techniques, this geometry is intended to investigate the accuracy of voxel modelling methods as the geometry continuously changes in each coordinate axis. This test article was strategically designed to have various points of curvature, ranging from perfectly horizontal to perfectly vertical.

2.2.5 Experiment 1.4: ISO-10791-7 Standard Geometry

Experiment 1.4 consists of the fabrication and digital detection of geometric features defined as part of the ISO-10791-7 standard for machine precision and accuracy [22]. This test article contains a series of circle, diamond, and square features (abbreviated as CDS geometry) that indicate a measure of the CNC machining equipment's capabilities to fabricate components with perpendicularity, concentricity, and flatness Geometric

Dimensioning and Tolerance (GD&T) specifications [23]. The geometry is displayed in Figure 5.

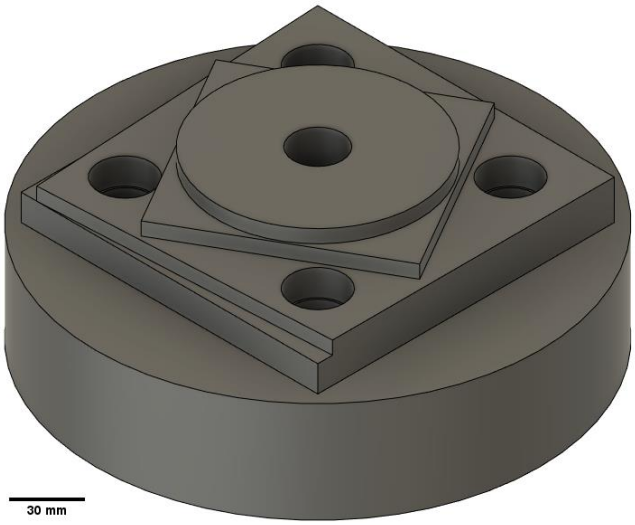

Figure 5: ISO-10791-7 Standard Machine Precision (CDS) Test Geometry [22].

This component was strategically chosen to provide an evaluation of accuracy for the methods by which other geometries are inspected in this experiment. The CDS geometry will be fabricated on the Mazak hybrid system. GD&T specifications as defined in the ISO-10791-7 standard will be evaluated on a Zeiss Calypso CMM to provide a ground truth reference. The component will be inspected with a Renishaw RMP-60 radio transmission inspection probing system on a Haas VF-5 to provide an measure of accuracy of the inspection methods used as part of this research [24, 25].

2.3 Phase II – Multi-Agent Open Architectures

2.3.1 Summary

The second phase of this dissertation explores the underlying information architectures needed to support the efficient capture, communication, storage, and analysis of manufacturing data produced in Phase I. A necessary component of this research is an evaluation of the bandwidth, computational time, and digital storage footprint needed to govern manufacturing data at various scales. Furthermore, various communication architectures are needed to send information both to and from the manufacturing system. The development of two-way dynamic communication mechanisms is essential to lay the foundation for more advances control schemes evaluated in Phase III.

2.3.2 Experiment 2.1: Multi-Agent Architectures

Experiment 2.1 investigates and develops multi-agent open architectures for two-way information communication of manufacturing process data. This experiment tests the capabilities of control units at different levels within the multi-agent architecture to analyze current machine operations, providing the groundwork for feedback of machine instructions.

Over the past decade, numerous solutions have been proposed to capture and store data from vast numbers of sources [26-29]. This presents a range of options for an end-user where advantages and disadvantages are not immediately clear. The digital storage footprint is an inherent problem in any information architecture. Dynamic compression

mechanisms are explored and evaluated for manufacturing data produced as part of standard hybrid operations, as outlined in Phase I.

2.3.3 Experiment 2.2: Information Compression Methods

Experiment 2.2 evaluates the compression algorithms for different classifications and combinations of hybrid manufacturing data. Hybrid manufacturing data produced in Phase I is categorized based on the number of axes used and the type of operation (subtractive, additive, or hybrid). Two formatting and storage methods are used with five compression algorithms to determine the most efficient methods with respect to compression ratio and compression time.

The results of Experiment 2.1 and Experiment 2.2 provide (1) a understanding of the design choices in implementing multi-agent architectures for dynamic two-way communication of manufacturing information, and (2) a methodology to determine the most efficient information compression algorithm for arbitrary manufacturing data.

2.4 Phase III – Feedback Methods for Adaptive Processing

2.4.1 Summary

Previous research has shown the material property benefits when advanced control capabilities are used in additive manufacturing and demonstrated the need for dynamic processing capabilities for increased geometric control in hybrid manufacturing [19, 30]. However, necessary monitoring, analysis, and resulting feedback methods are not typically included in commercial hybrid manufacturing systems. Phase III develops three levels of feedback methods that enable monitoring and analysis results of Phase I and Phase II to be

utilized *in-situ* with the current component. This phase explores methods that enable feedback capabilities for commercially available hybrid manufacturing systems. Three levels of feedback are explored and developed for different operational timescales.

2.4.2 Experiments 3.1-3.3: Feedback Control Methods

Three experiments using the feedback methodology are performed to evaluate the feedback methodology. Experiment 3.1 enables dynamic dwell conditions with additive operations in hybrid manufacturing. Experiment 3.2 evaluates operations on multiple components within the same build chamber, increasing operational efficiency. Experiment 3.3 explores subtractive machining stability determination with feedback methods. This experiment results in a stability map describing stable and unstable regions with varied cutting parameters. In summary, Phase III explores, develops, and implements feedback methods on three distinct timescales to enable advanced control of commercial CNC manufacturing systems. This technology is applied to hybrid manufacturing process to enable the production of more accurate components with control schemes that are otherwise impossible with the current capabilities of CNC manufacturing systems.

2.5 Conclusion

This dissertation will result in the following contributions:

(1) A method to monitor CNC manufacturing operations *in-situ*, resulting in voxel-based digital twin modelling methods for geometric comparison;

(2) A method to capture, govern, and efficiently store the manufacturing information with a multi-agent open architecture in support of digital twin modelling and analysis methods and distributed feedback control capabilities;

(3) A method for discrete, *in-situ* feedback control to update instructions on commercial CNC machines, enabling dynamic processing conditions to correct geometric deviations.

These methods will be investigated, developed, and demonstrated on a hybrid manufacturing system. A series of strategic experiments are performed to investigate specific aspects of the additive and subtractive process. This project will result in methods to measure and control unintended effects within commercial CNC manufacturing systems.

CHAPTER 3. PHASE I – DATA SYNCHRONIZATION FOR GEOMETRIC ACCURACY

Components fabricated through hybrid manufacturing processes, the combination of additive and subtractive processes within the same build chamber, often experience significant geometric deviations from engineered specifications [19]. However, hybrid CNC manufacturing centers (hybrid systems) produce multiple streams of information describing the machine's state, actions, and operations throughout the manufacturing process. This information can be used to create a digital representation of the fabricated component, known as a "digital twin" model. This body of research evaluates the strategic combination and synchronization of information from multiple sensing modalities to improve the accuracy of digital twin models. A voxel modelling methodology is developed and investigated to create a digital twin of the component being produced. Information describing the machine's current operations is strategically combined with information from additional sensing modalities to increase the accuracy of the *in-situ* digital twin model. This work results in a method to geometrically compare features of *in-situ* components against desired specifications. Research conducted as part of Phase II and Phase III builds on this body of work to support the communication, storage, and use of this information, resulting in feedback methodologies to affect the hybrid manufacturing process *in-situ* and correct geometric deviations.

3.1 Introduction

This chapter evaluates methods to leverage manufacturing data from hybrid systems for creation of a digital twin model of the *in-situ* fabricated component. Hybrid systems produce multiple streams of information from different sensing modalities throughout the manufacturing process. This information is generated by features built-in to standard commercial subtractive CNC systems (the foundation on which hybrid systems are built) as well as external auxiliary sensors that are installed by the user. Combined, this information can be used to create a digital twin model of the part currently in production. This chapter developed methods by which a voxel digital model can be created through the combination of multiple sensing modalities, and the accuracy of the digital model when compared with desired feature specifications.

3.2 Literature Review

3.2.1 Hybrid Manufacturing

While hybrid manufacturing has existed for over two decades, the capability to both deposit and remove material in commercial systems has only recently gained traction in the commercial space. The first hybrid machines were typically created from standard subtractive CNC machine bases with the custom retrofit of additive capabilities. These include metal-inter gas (MIG) welders mounted to standard tool holding, polymer deposition heads fixed to a spindle housing, and laser-based directed energy deposition (DED) attachments motion control systems [31-33]. Commercial machine tool manufacturers such as Mazak, Okuma, and DMG-Mori have more recently produced integrated systems by including additive technologies with existing subtractive CNC

frames to enable control of hybrid fabrication techniques within a single system [7-9]. Although this integration is a necessary step in the path to industry adoption of hybrid technologies, significant problems in process control remain.

With the inclusion of additive manufacturing techniques in traditional subtractive machining centres, hybrid manufacturing enables the production of complex geometries that were previously unavailable with a single machine setup [34]. However, a fundamental assumption in the operational paradigm of standard subtractive machines is the reliance on highly accurate modelling techniques to produce cutting toolpaths. Computer-Aided Manufacturing (CAM) programs such as Autodesk's Fusion 360 and OpenMind's HyperMILL, responsible for generating subtractive tool paths for precision machining, often rely on low-tolerance models of the machine, work holding, initial stock, and in-process component to appropriately select cutting parameters [35, 36]. These models also inform collision checking algorithms to prevent unintended contact between the tool and workpiece. Errors between CAD models and reality are often disastrous to an optimized production line. At best, subtractive tools can be broken mid-process while at worst, the machine can crash into the stock or workpiece resulting in costly damage and machine downtime. Therefore, it is imperative that geometric models are accurate within well-defined tolerances.

3.2.2 Geometric Effects in Hybrid Manufacturing

Additive manufacturing methods are notorious for producing geometries that are not within desired geometric specifications. Components produced by Powder Bed Fusion (PBF) and Directed Energy Deposition (DED) often experience features that are overbuilt

(exceeding the specified dimensions) or underbuilt (not reaching the specified dimensions. Different processes result in geometric errors of different order of magnitude. Additionally, components manufactured with additive methods are often subject to thermal distortion both during fabrication and while cooling, immediately following fabrication, displayed in Figure 6 [19]. Thermal stresses created by the hybrid manufacturing have been documented and are a fundamental technical challenges to the successful adoption of hybrid as an industry standard fabrication process [37].

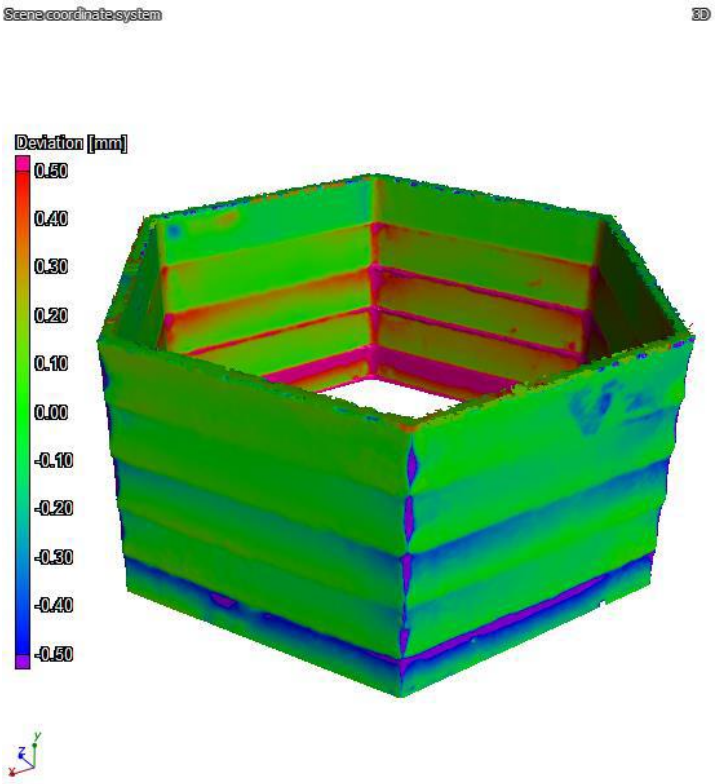

Figure 6: Distortion of Hexagon Geometry with Hybrid Manufacturing [19].

3.2.3 Digital Twin Research

Digital twin modelling efforts aim to create a virtual representation of the manufacturing equipment, processes, and fabricated components. Cai et. al. defines a

digital twin as “virtual machine tools of physical machines for cyber-physical manufacturing by using sensory data and information fusion integration techniques” [38]. These methods have been applied to several different continuous and discrete manufacturing techniques.

Simple implementations of digital twin modelling rely on the input of a few select sources for open-loop monitoring solutions. This is common in continuous manufacturing environments such as liquid chemical and pulp & paper industries where high-volume processes must be continuously adjusted. In these processes, only future product can be controlled - the current material cannot be adjusted to correct for previous operations. However, the results of information collected to monitor the process can be used to grade the material quality, enabling more efficient sorting and costing models.

More advanced digital twin models are often the result of the combination of information from physical processes and computational simulations. DebRoy provides an outline of this framework while justifying the need for digital twin modelling in purely additive systems to predict final microstructure properties of the material [39]. Knapp et. al. expands DebRoy’s concept by integrating temperature and velocity information from both experimental measurements and computational simulations for DED systems [40]. This digital twin is used to provide the CAM programmer with a more accurate cooling rate and temperature gradient prediction for the fabricated geometry.

3.2.4 Voxel Model Research

Significant research has been conducted with voxel-based modelling techniques. Similar to a pixel representing a discrete 2-dimensional area with a single color, a voxel is

the 3-dimensional expansion to a discrete cube of volume. Recent CAM software such as SculptPrint has been developed to model solid objects with voxels, enabling the representation of features and geometrical aberrations that are not easily modelled with traditional parametric CAD techniques [41]. Lynn et. al. demonstrated the use of voxel models for subtractive machining by leveraging graphics processing units to enhance computation time [42, 43].

Voxel-based modelling also provides an interesting technique for hybrid manufacturing due to ease of volume representation for arbitrary additive and subtractive tasks. Common CAM simulations such as those in Autodesk's Fusion 360 rely on parametric modelling techniques to display a prediction of in-process components. Hybrid manufacturing with DED-based additive techniques provides a difficult challenge to CAD modelling due to the highly varied nature of the deposited geometry. Recent research investigating DED processing parameters find that the geometry of deposited material is variable with regard to the underlying CAD shape, feedstock distributions, and processing parameters [20, 44]. Unlike in a purely subtractive regime where removed material is often consistent and of normal geometry, deposited material is highly variable. This is further complicated by random effects, often leading the geometrical defects that are difficult to predict.

Voxel modelling offers a solution to model some of these features and non-ideal effects without significant changes to the underlying modelling framework. Since a voxel-based modelling system relies on determining if a discrete point of volume is filled or unfilled the representation of these features is more easily achieved.

3.3 Sources of Data

Numerous sources of information exist from which operations on a CNC machine can be monitored. These information sources are often a combination of functionality built into the machine, ‘Machine-direct information’, and auxiliary sensors that have been added to the system by end-users, ‘external information’. Common examples of machine-direct information sources include MTConnect, OPC-UA, and Haas Connect [12-14]. Probing and inspection capabilities are also considered machine-direct information sources since they are usually integrated with and accessible through the machine controller. Examples of common external information sources are thermal cameras for temperature information, environmental sensors such as humidity measurements, and feedstock monitoring systems. Information sources used in this body of work are described below. However, supporting architecture methods to capture, communicate, and store produced data are described in Chapter 4.

3.3.1 G-code Machine Instructions

G-code is the industry-standard method for providing input instructions to CNC machines [45]. G-code is a text-based interpretation language that provides a linear set of instructions for the machine to follow. Advanced implementations of g-code allow for low-level programming such as logic and conditional operations, however, the most used functionality is limited to position and speed information. A sample g-code snippet with commented commands is shown in Figure 7.

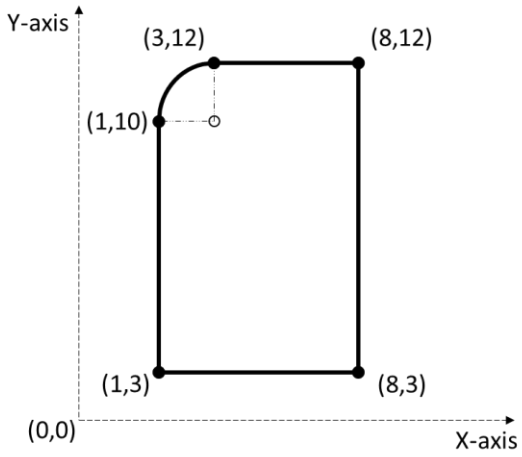


```
N1  G0 X1.0 Y3.0              Setup move, Rapid motion
N2  G1 X1.0 Y10.0 F100.0      Linear move, Feed = 100 mm/min
N3  G2 X3.0 Y12.0 I2.0 J0.0   CW circle, Feed = 100 mm/min
N4  G1 X8.0 Y12.0 F50.0       Linear move, Feed = 50 mm/min
N5  G1 X8.0 Y3.0              Linear move, Feed = 50 mm/min
N6  G1 X1.0 Y3.0              Linear move, Feed = 50 mm/min
```

Figure 7: G-Code Example with Motion and Feed Comments

However, G-code is not a complete record of the motion required to fabricate a part. G-code only describes the beginning and end points of each linear or arc segment. It is assumed that the CNC machine controller interpolates between these two points to generation motion paths. The exact interpolation, and therefore the accuracy of the final component, is not defined by the G-code. Additional information is needed to generate a Voxelized digital twin to represent actual operation within the CNC manufacturing system.

3.3.2 MTConnect Process Data

Information about the machine's operations, state, and current position is collected through the MTConnect protocol. The MTConnect protocol is standardized "semantic vocabulary for manufacturing equipment to provide structured, contextualized data with no proprietary format" [12]. MTConnect variables such as machine position, tool number,

and feed rate were collected for this research. A complete description for data acquisition, communication, and storage methods is included in Chapter 4.

3.3.3 Renishaw Inspection Data

Geometric inspection data was collected with a Renishaw RMP-60 onboard probing system. This system uses low-force contact methods to detect and measure the relative position between a geometric feature and a pre-defined origin. Resulting inspection data can be made available to the machine controller, accessible via MTConnect, or stored locally in a text file. A complete description for data acquisition, communication, and storage methods is included in Chapter 4.

3.4 Methodology

3.4.1 Summary

Each of the experiment geometries were fabricated on a Mazak VC-500A/5X AM HWD laser-hotwire hybrid CNC machining center. A digital voxel model representing the outcome of the manufacturing operation was created from process information. A method to compute discrete voxel models of solid geometry was developed. For subtractive methods, tool geometry was measured with the machine's on-board length and diameter inspection capabilities. For additive methods, standard bead geometry was assumed from previous research [19].

MTConnect information was the primary source of information used to model actual machine actions and operations. However, models created from MTConnect information alone are limited in fidelity due to information shortcomings. Information from

other sensing modalities, such as on-machine probing systems, were used to increase the accuracy of these models. Caliper measurements of key features was used to provide ground-truth measurements. Additionally, a laser line scanner was used to provide ground truth measurements of complex geometries.

For methodology descriptions, matrix operations and dataframe operations are jointly used. Matrix math is used to describe the underlying mathematical functions for voxel model creation, displayed with standard linear algebra equations. However, as this process was implemented in Python using a variety of numerical process, dataframe operations are used to implement the computational process.

3.4.2 Experiment Geometry

Four test geometries were selected for fabrication in this research. Each geometry was designed to produce a representative dataset utilizing different machine capabilities. One geometry was produced with only subtractive methods, providing a control for standard subtractive CNC machines. The remaining three models were produced with various combinations of additive and subtractive processes, utilizing the full scope of fabrication capabilities included in a hybrid system.

3.4.2.1 Subtractive NIST Geometry

The National Institute for Standards and Technology (NIST) published an additive test piece intended to serve as a uniform comparison for additive processes for resolution, stepover, dimensional accuracy, and overhangs [21]. The original NIST additive test piece is displayed in Figure 8A. The NIST additive sample geometry was modified for use as a

test piece for subtractive and wire-based hybrid operations. The modified subtractive NIST geometry is displayed in Figure 8B, and a diagram with dimensioned features is displayed in Figure 9.

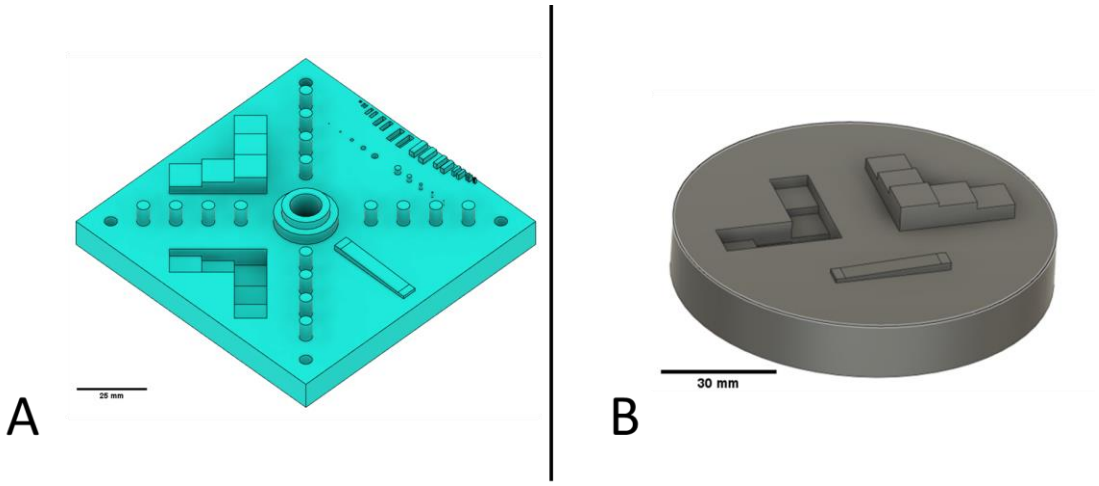

Figure 8: (A) NIST Additive Test Article (B) Subtractive NIST Geometry

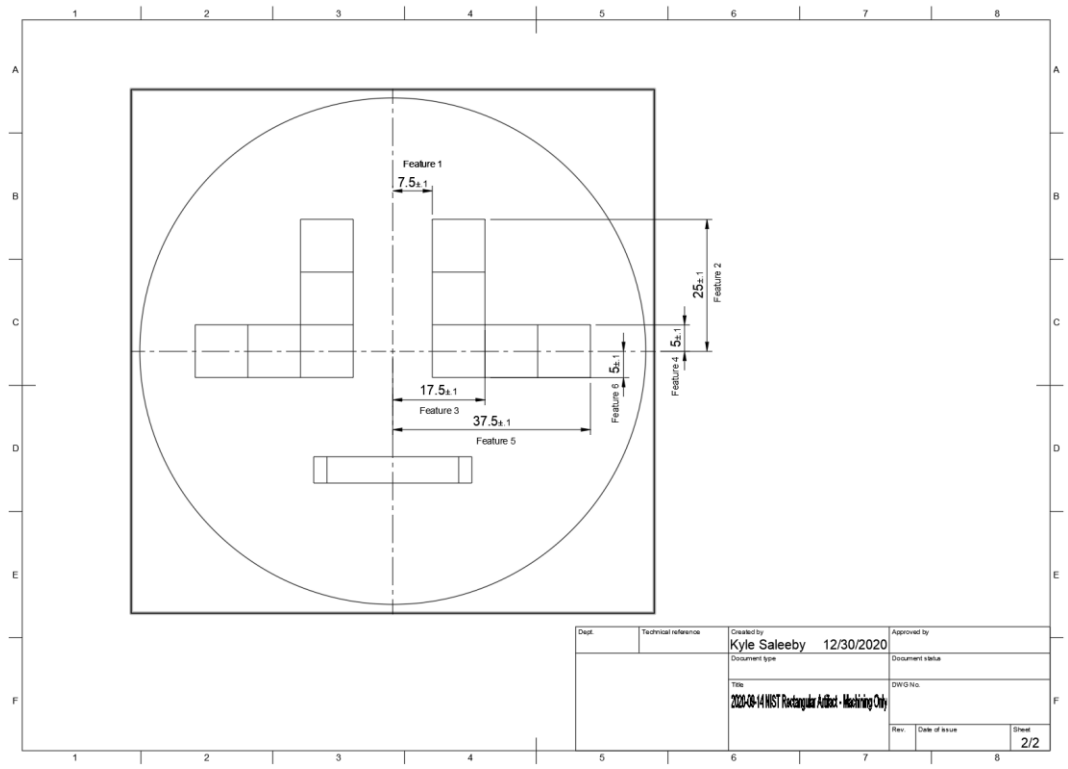

Figure 9: NIST Subtractive Geometry Engineering Diagram [units: mm]

This diagram presented in Figure 9 provides supplemental callouts for specific features that will be the focus of measurement for this experiment. Features 1 – 6 will be modelled and measured from MTConnect data. Increases in accuracy will be measured form the addition of inspection probe data. Feature dimensions and tolerances for the subtractive NIST geometry are displayed in Table 2.

Table 2: Subtractive NIST Geometry Feature Dimensions

	Dimension (mm)	Tolerance (mm)
Feature 1	17.5	±0.1
Feature 2	25.0	±0.1
Feature 3	17.5	±0.1
Feature 4	5.0	±0.1
Feature 5	37.5	±0.1
Feature 6	5.0	±0.1

Common tolerance bands for standard precision CNC subtractive parts range from ±0.127 mm (0.005 in) to ±0.0254 mm (0.001 in). High-precision part tolerances can fall below ±12.7µm (0.0005 in), while ultra-precision CNC components may require tolerances smaller than 5 µm (less than 0.0002 in). For this experiment, a tolerance band of ±0.1 mm (0.004 in) was chosen as a mid-point for common components.

It is hypothesized that the use of MTConnect data and addition of inspection data will increase the accuracy of the digital model, decreasing geometric error when compared with ground truth measurements.

3.4.2.2 Additive and Hybrid NIST Geometry

The stepped feature of the standard NIST additive test article was segmented and scaled for a size appropriate for the Mazak VC-500A/5X AM HWD hybrid machine and placed on 152 mm round stock [21]. A CAD model and dimensioned drawing are presented in Figure 10. This geometry was selected to test the digital modelling process against 2.5-Axis components as the feature can be fabricated in incremental Z-layers.

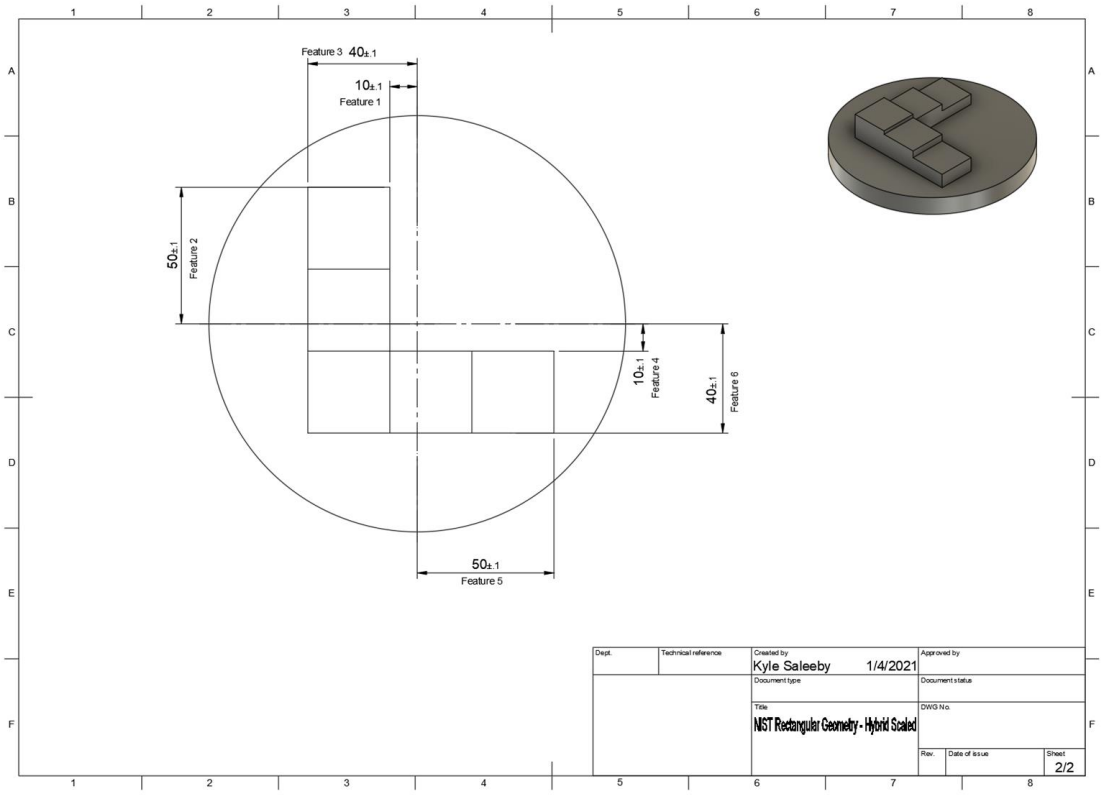

Figure 10: Additive and Hybrid NIST Geometry Specifications [units: mm]

Two versions of this geometry were fabricated under different conditions to evaluate accuracy of digital voxel modelling methods. The first version was produced with only additive methods. The second version was additively manufactured with a 2 mm overbuild on every planar face. The resulting pre-form was machined to the original feature's standard dimensions with the same tool path as in Experiment 3.

3.4.2.3 Organic Surface Geometry

The four previous geometries were designed to test voxel models created for 2.5-axis toolpaths. Full 3-axis toolpaths are commonly used for complex geometry fabrications. A fifth components was designed to evaluate the accuracy of voxel models created for organic surfaces. This experiment geometry was designed with a continuously changing

curvature in two dimensions, smoothly transitioning from perfectly horizontal tangents at the edges of the part to perfectly vertical tangents in one location. The geometry is presented in Figure 11.

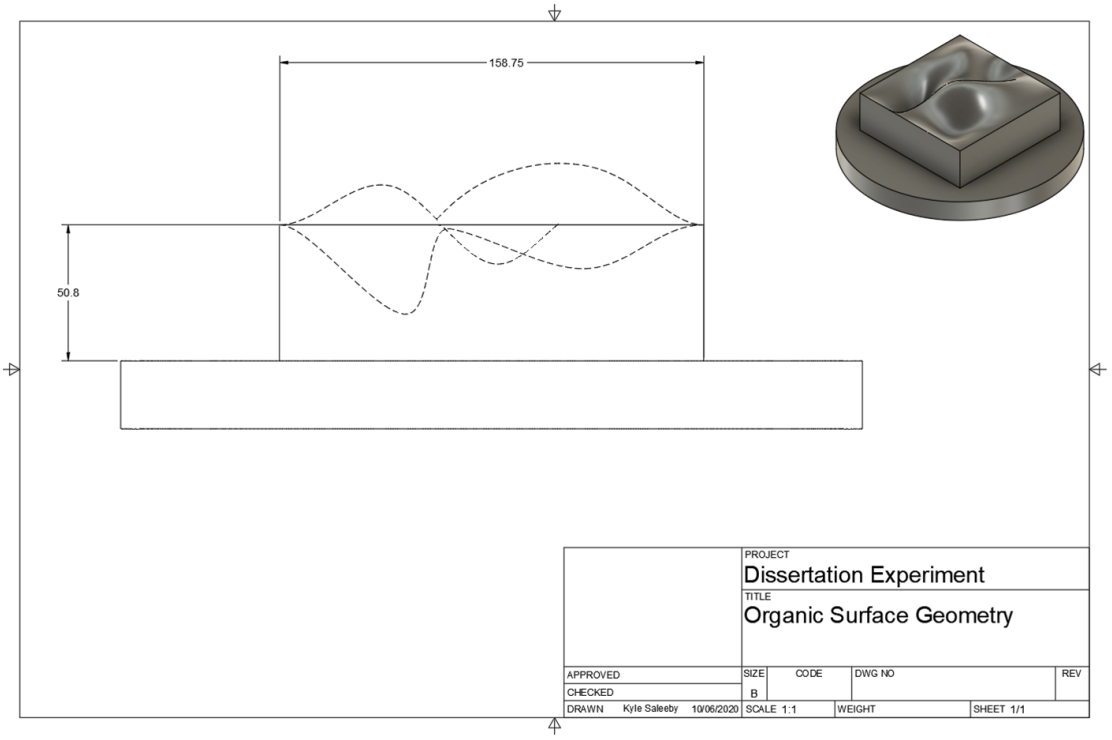

Figure 11: Organic 3-Axis Experiment Geometry [units: mm]

3.4.2.4 ISO-10791-7 Geometry

The final experiment geometry was designed to match standards set forth by the ISO-10791-7 machining precision specifications. This experiment was designed to determine the accuracy of probing measurements when compared against certified CMM measurements. The geometry is presented in Figure 12.

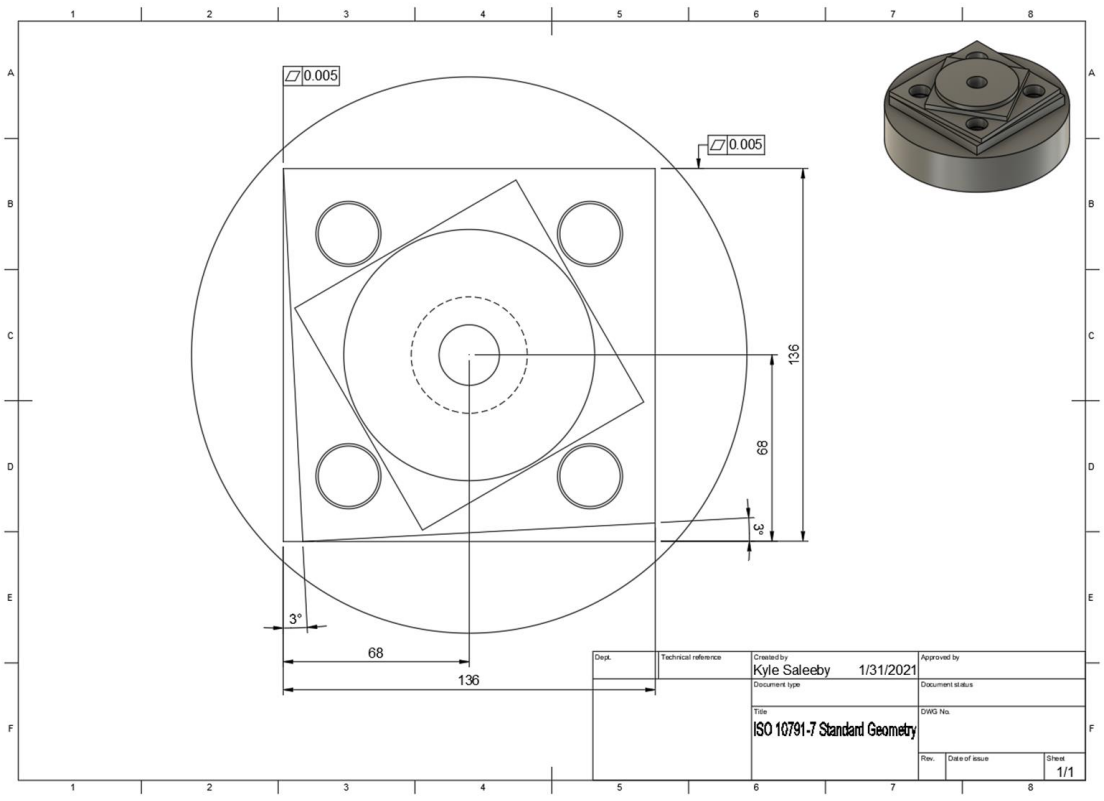

Figure 12: ISO-10791-7 Machine Precision Geometry [units: mm]

3.4.3 Voxel Model Creation

To create a voxel model, information about the initial stock size and additive subtractive operations must be known. If a subtractive operation is being modelled, the tool diameter and length must be known. If the model is representing an additive operation, bead geometry must be known. For the following process, we assume subtractive operations. Additive operations will be a modification to the initial framework used for subtractive operations.

Two primary pieces of information are used to create the stock model, the machine's XYZ position and active tool number. The XYZ position is split into the first three columns of an N x 4 matrix, where N is the number of position points, displayed in

Equation 1. Tool number is stored in the fourth column. This information can be provided from multiple sources, as described in Section 3.3 – Information Sources.

$$P_{Nx4} = \begin{bmatrix} X & Y & Z & T \\ -33.201 & -20.492 & -5.394 & 7 \\ \vdots & \vdots & \vdots & \vdots \end{bmatrix} \quad (1)$$

The maximum and minimum positions of the X-axis are computed from the columns of the matrix, shown in Equation 2 and Equation 3. Similar equations are used for the Y-axis and Z-axis.

$$X_{min} = Min(P_{1x4,X}) \quad (2)$$

$$X_{max} = Max(P_{1x4,X}) \quad (3)$$

These boundaries are used to create a digital stock. The digital stock is always represented as rectangular dimensions, regardless of actual stock used in the physical process. However, the rectangular digital stock always encapsulates the physical stock through this methodology. The digital stock model is used to create associated dataframes to store this information.

After stock dimensions have been determined, the resulting shape is used to create three dataframes of matching shape to store the voxel information. The first two data frames hold indices for the X-axis and Y-axis positions of one Z-level slice of the voxel stock. As the stock model represents a finite series of discrete volume locations, a resolution factor must be chosen. The standard resolution used is 0.05mm (slightly under 0.002 in.) This resolution provides a compromise between computation time and

dimensional resolution. The X-axis and Y-axis index dataframes are created with Numpy's meshgrid function. The number of points, X_{ind} and Y_{ind}, is computed from the resolution factor, Res, shown in Equation 4 and Equation 5.

$$X_{ind} = (X_{max} - X_{min}) * \frac{1}{Res_{XY}} \tag{4}$$

$$Y_{ind} = (Y_{max} - Y_{min}) * \frac{1}{Res_{XY}} \tag{5}$$

The index values for the X and Y axes are used to generate square index matrices, $\bar{X}_{ixj}$ and $\bar{Y}_{jxi}$, corresponding to the discrete X and Y positions of each voxel, shown in Equation 6 and Equation 7.

$$\bar{X}_{ixj} = \begin{bmatrix} 0 & \cdots & i \\ 0 & \cdots & i \\ 0 & \cdots & i \end{bmatrix} \tag{6}$$

$$\bar{Y}_{jxi} = \begin{bmatrix} 0 & 0 & 0 \\ \vdots & \vdots & \vdots \\ j & j & j \end{bmatrix} \tag{7}$$

While the XY stock limits are generated from analysis of MTConnect X-, Y-, and Z- axis limits, the user must specify the number of layers to consider in the Z-axis, Z_k, similar to the choice of resolution in the X- and Y- axes, displayed in Equation 8.

$$Z_{ind} = (Z_{max} - Z_{min}) * \frac{1}{Z_k} \tag{8}$$

The underlying voxel model is based on a Boolean masking operation, where a 2D matrix of the same shape as the rectangular stock records True for filled voxels and False for empty voxels. This can be expanded to a 3D matrix where planar indices have with the same dimensions as the X- and Y-index matrices, and adding a third dimension of length k for the Z-layers. The matrix is uniformly filled with Boolean values, displayed in Equation 8. This is referred to as the mask dataframe, $\bar{M}_{ixjxk}$.

$$\bar{M}_{ixjxk} = \begin{bmatrix} True & True & True \\ \vdots & \vdots & \vdots \\ True & True & True \end{bmatrix} \tag{9}$$

In subtractive operations, the dataframe is initialized with $True$ values, representing solid volume at each discrete voxel location. This is accomplished with Python Numpy's full method, creating a meshgrid with Boolean variables of one value. In additive operations, the dataframe is initialized with $False$ values, indicating that there is not volume at those locations. Volume will be selectively removed or added in the following steps to model the machine's operations. A visualization of the workspace digitization method is displayed in Figure 13.

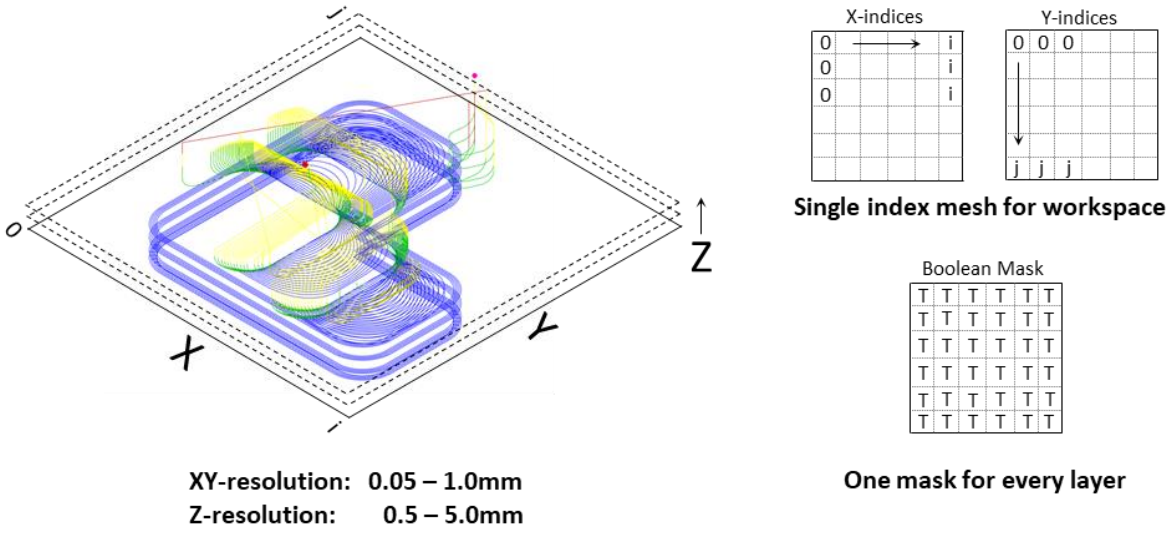

Figure 13: Workspace Digitization for Voxel Model

Throughout this process, we assume the stock is of uniform shape and does not change throughout different Z-layers. Therefore, the same index matrix can be used for all Z-layers. Once the digital voxel model is created, subtractive and additive operations can be applied to model the fabricated component. Subtractive operations require knowing the tool diameter. Common tools can be represented by a circle of diameter D and center (X_0, Y_0) as shown in Equation 10. While other tools with specialized exits, this analysis is limited to standard flat endmills, displayed in Figure 14.

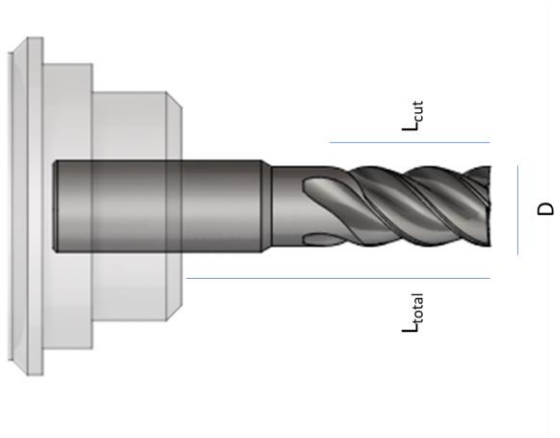

Figure 14: Flat Endmill with Diameter D

$$\frac{D}{2} = \sqrt[2]{(X - X_0)^2 + (Y - Y_0)^2} \tag{10}$$

To perform a digital subtractive operation, the center point of the tool set to match the point of interest by updating the (X_0, Y_0) values, as shown in Equation 11.

$$\bar{R}_{compare} = \sqrt[2]{\left(X_{ind} - X_{point}\right)^2 + \left(Y_{ind} - Y_{point}\right)^2} \tag{11}$$

In this form, the X and Y points used are dataframes on index values. Given a center point, (X_{point}, Y_{point}), a grid of radius values is generated and saved in the $R_{compare}$ matrix. Note, this operation results in a matrix of values, where every X and Y index point is computed against the equation.

Finally, this matrix of radius values is subtracted from the matrix mask with Boolean comparisons, as shown in Equation 12, and visualized in Figure 15.

$$\bar{M}_{k=a}^{i,j} = \bar{M}_{k=a-1}^{i,j} \,\&\, (\bar{R}_{compare} > \frac{D}{2}) \tag{12}$$

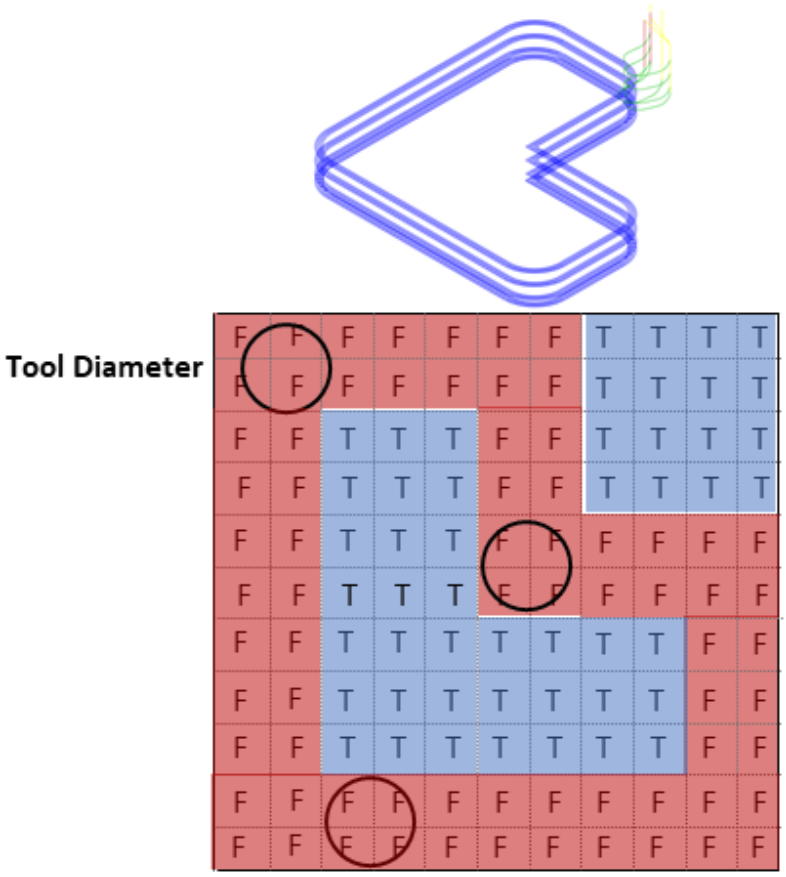

Figure 15: Subtractive Operations with Boolean Mask

This process is iteratively repeated with the next provided point for the subtractive operation. By comparing the previous Boolean mask with the current radius affected by the new subtractive point, a digital layer is created reflecting the subtractive operation. The subtractive layer process is subsequently repeated for each Z-layer. After all layers have been processed for all subtractive points, The Boolean masks represent slices of a 3D voxel model, displayed in Figure 16.

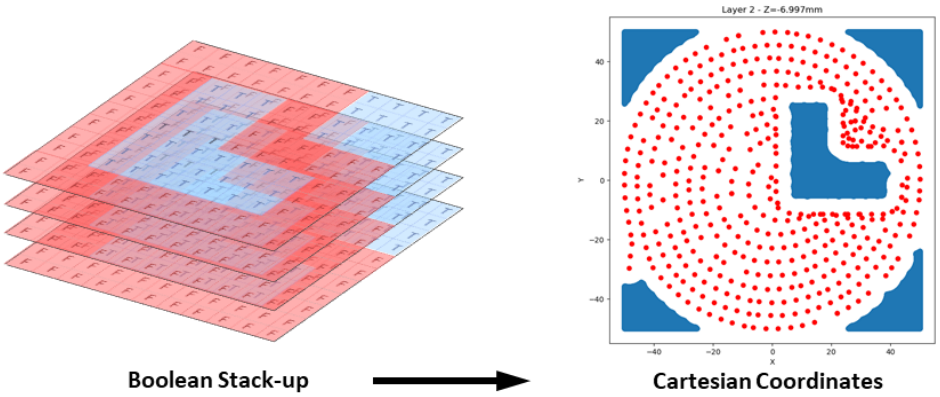

Figure 16: Voxel Model Stackup for Z-layers

Each of these masks are processed to provide a list of cartesian coordinates in (X, Y, Z) form of True values. These points are plotted for a visualization of the digital voxel model. A visualization of an example voxel model is displayed in Figure 17. A low resolution was chosen to visualize and demonstrate the use of discrete voxel volumes.

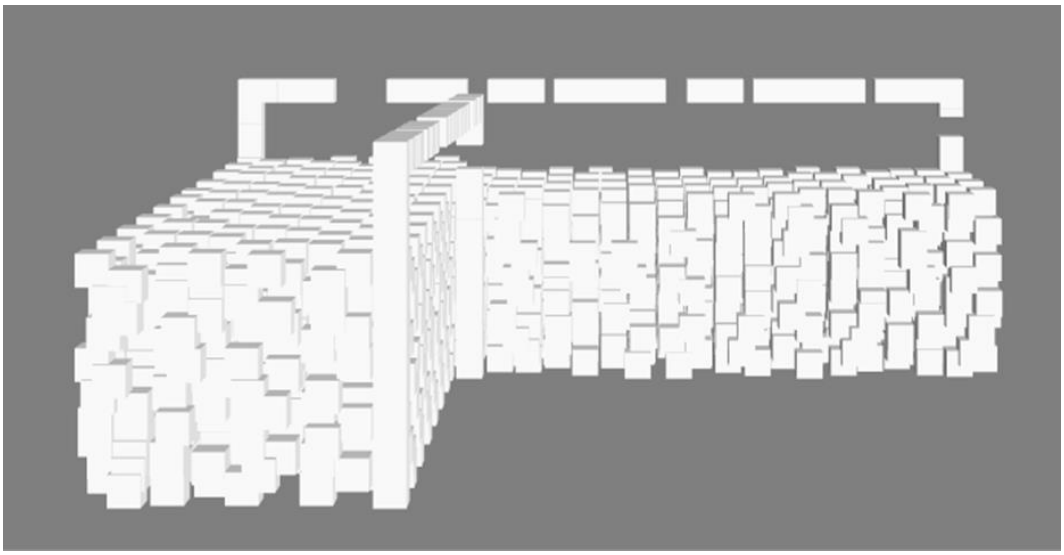

Figure 17: Voxel Model from Cartesian Coordinates

Additive operations can be modeled with the same methodology. A standard bead geometry is assumed to be a circle, similar to Equation 10, based on research by Feldhausen et. al. [19]. It is noted that this assumption is less accurate for certain scenarios due to a lack of documented research linking process parameters to bead geometry. In the same manner as subtractive operations, a stock volume is created. Often, it is useful to only create a stock for the initial substrate, instead of the full range of operation points as in the subtractive modelling process. After the stock is created, the circle approximating bead geometry is shifted to specific locations by adjusting the (X_0, Y_0) coordinates. However, the additive operation is modeled by changing values within the bead geometry circle to True, instead of False, representing the addition of volume to the stock model. This process is visualized in Figure 18.

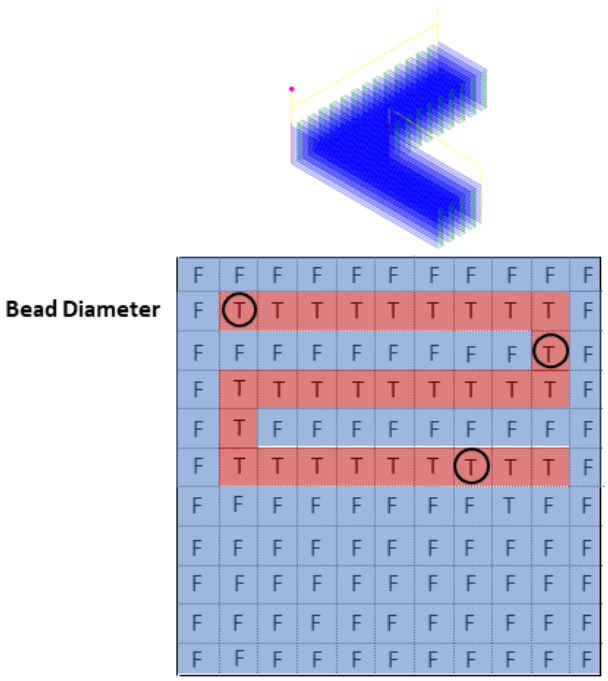

Figure 18: Additive Operations with Boolean Mask

The same process is followed to combined Boolean masks and form a 3D representation of the digital voxel model.

3.4.4 Modelling Machine Actions - MTConnect

The voxel modelling method described in predicting the output of the manufacturing operations. This provides a valuable tool to monitor the actions and processes ongoing in a machine and make a digital representation of the resulting component. MTConnect information must be captured, processed, and stored in a common format like JSON or CSV. The collection and communication process is covered in Chapter 4. After collection, it can be imported into a pandas dataframe to serve as the input to the voxel modelling process.

MTConnect provides two measures of the machine's position, (1) absolute machine position and (2) work-coordinate position. The absolute machine position is with respect to the machine's home origin. This is commonly located the intersection of a machines' table front-left corner and top surface. The absolute position is not affected by any machine operation. The Work-coordinate position is given with respect to an origin set by the operator. Common uses are to set the origin at a corner of the initial stock, or at the center of table rotation. For all voxel modelling processes, the work-coordinate system is used for simplicity.

3.4.5 Onboard Machine Probing

Many modern CNC machining systems have onboard probing systems for part setup, such as the Renishaw RMP60 system displayed in Figure 19 [46]. The probing systems operate by sensing force at the end of a touch stylus. The probe is moved at a known speed along a vector direction. Once the stylus collides with the object, the probe is retracted a short distance, and moved back in the same direction at a slower speed. The second collision is more accurate due to the reduced speed. The detected location is reported back to the CNC machine controller and saved in a specific user variable.

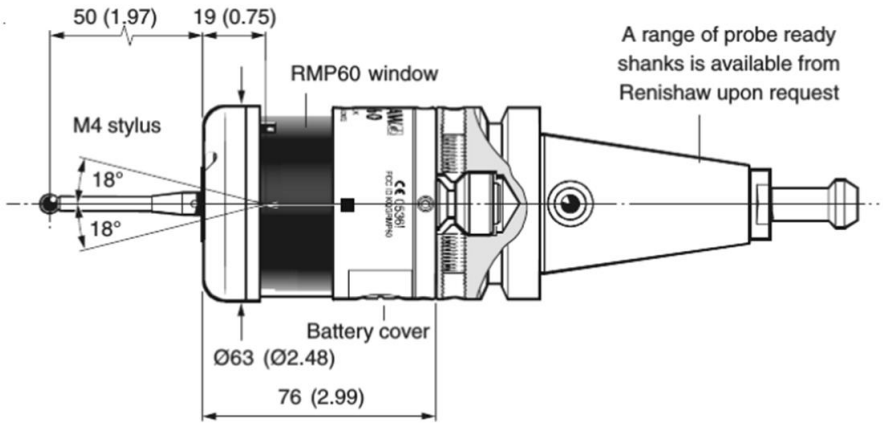

STYLUS OVERTRAVEL LIMITS		
Stylus length	±X / ±Y	Z
50 (1.96)	21 (0.82)	11 (0.43)
100 (3.93)	37 (1.45)	11 (0.43)

Figure 19: Renishaw RMP60 Inspection Probe with overtravel limits [46]

Touch probes are commonly used for workpiece setup operations, such as finding and recording the work-piece coordinate system described in the previous chapter. However, they can be programmed for inspection operations. The probe can be

commanded to inspect a pre-defined geometric feature, such as a plane, circular boss, or pocket. After reaching a setup location, the probe is used to measure the actual position of these features. The error between programmed and actual measurements is reported back to the controller.

Multiple software components were used to program the inspection operations for this research. Fusion 360 was used to generate inspection cycles for complex features such as bosses and pockets [35]. A custom python script was developed to generate inspection cycles for planar faces in an axial orientation.

3.5 Results

3.5.1 Subtractive NIST Geometry

Subtractive fabrication of the NIST subtractive geometry, Experiment 1 was performed on the Mazak VC-500A/5X AM HWD CNC machine. Tool paths were generated in Fusion 360, consisting of the following operations:

1. Facing operation to prepare the stock
2. Adaptive cutting operation for the rough profile
3. Contour operation for finish machining of the part's boss features
4. Pocket operation for finish machining of the geometry's inset features.

A summary of the operations is displayed in Figure 20A-D. These operations were posted with Fusion 360's standard Mazak VC-500A post processor and executed on the Mazak hybrid system. Finally, a series of inspection operations were programmed using Fusion 360, displayed in Figure 20E-F. The final component is displayed in Figure 21.

Initial G-code instructions and MTConnect data produced as a result of the experiment were captured and recorded with the multi-agent architecture developed as part of Phase II. Additionally, inspection data was collected and analysed to determine the improvement in accuracy of the digital voxel model. A selection of three points was measured for each feature of interest. Each of these three points were measured 4 times, providing an indication of uncertainty. The fabricated geometry was laser scanned and measured with calipers calibrated with NIST traceable equipment to provide ground truth dimensions.

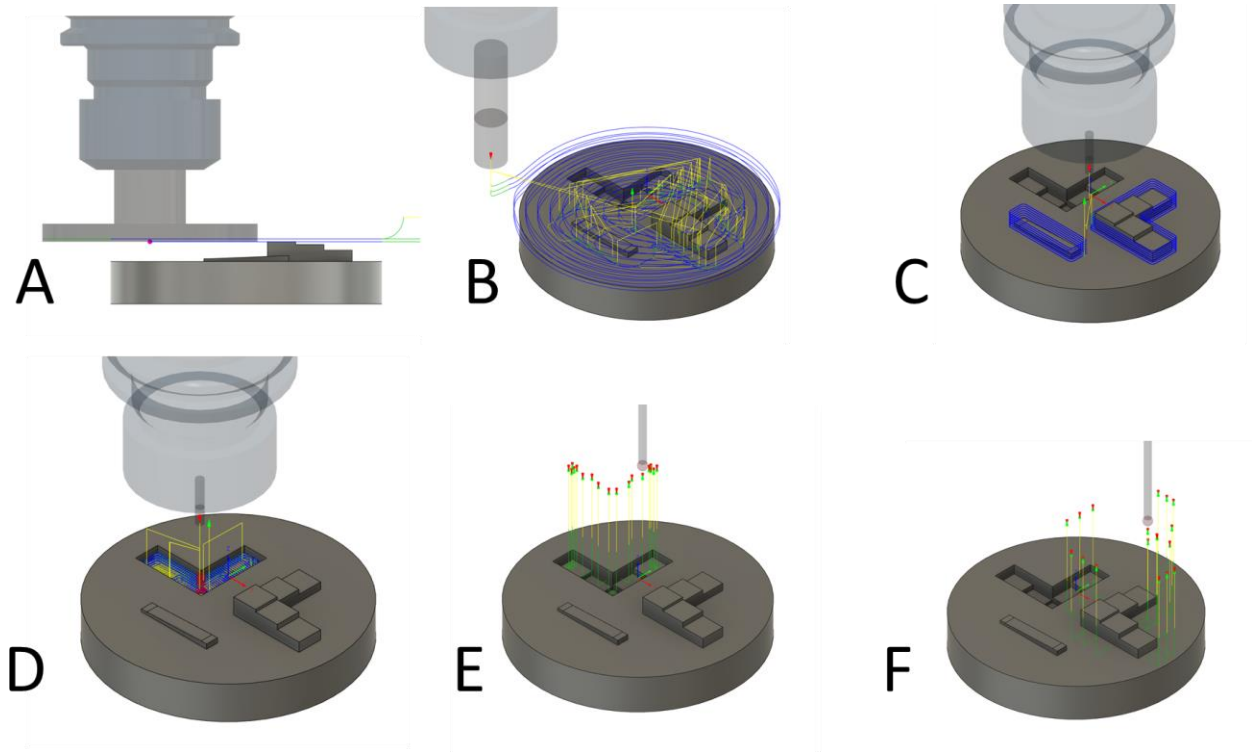

Figure 20: Subtractive NIST Geometry Machining and Inspection Operations

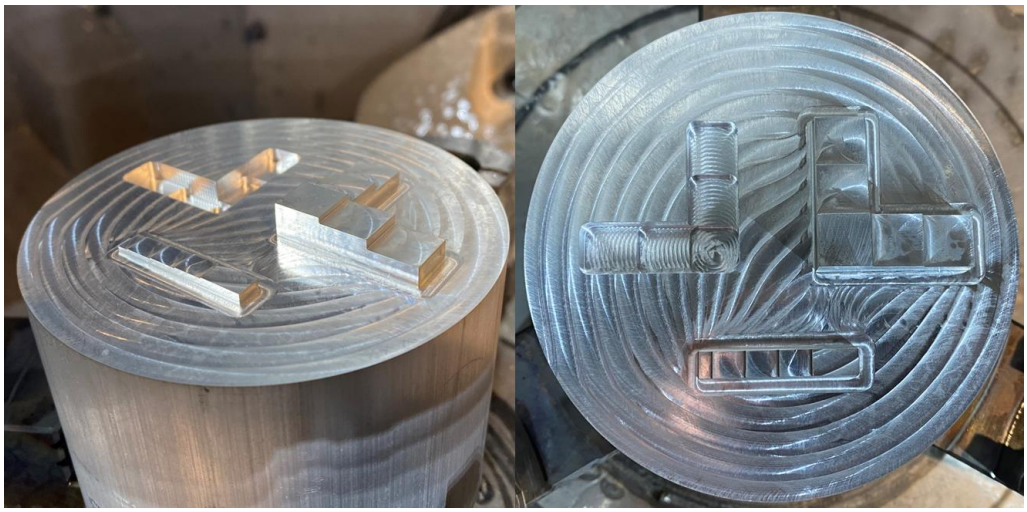

Figure 21: Subtractive NIST Geometry Fabricated Component

A voxel model was produced from the initial G-code instructions, Displayed in Figure 22. However, due to the nature of G-code, the voxel model was a poor approximation of the intended geometry. This is largely due to the fact that G-code only specifies the beginning and ending points of features. The previous line in g-code (corresponding to the current position of the tool) is assumed to be the starting point, location A. The next line of G-code describes the ending point, location B, and the speed at which to traverse the distance between location A and location B. While the mode of operation assumes a linear or circular path (G1 or G2/G3), no information is given between these two points. It is left to the machine controller to determine the interpolation between these two points. Therefore, the model created from G-code instructions does not well describe the exact path between the points, resulting in a poor approximation of the geometry. This lack of information poses significant problems to certification of components with respect to a cybersecurity effort, described in Section 3.7.

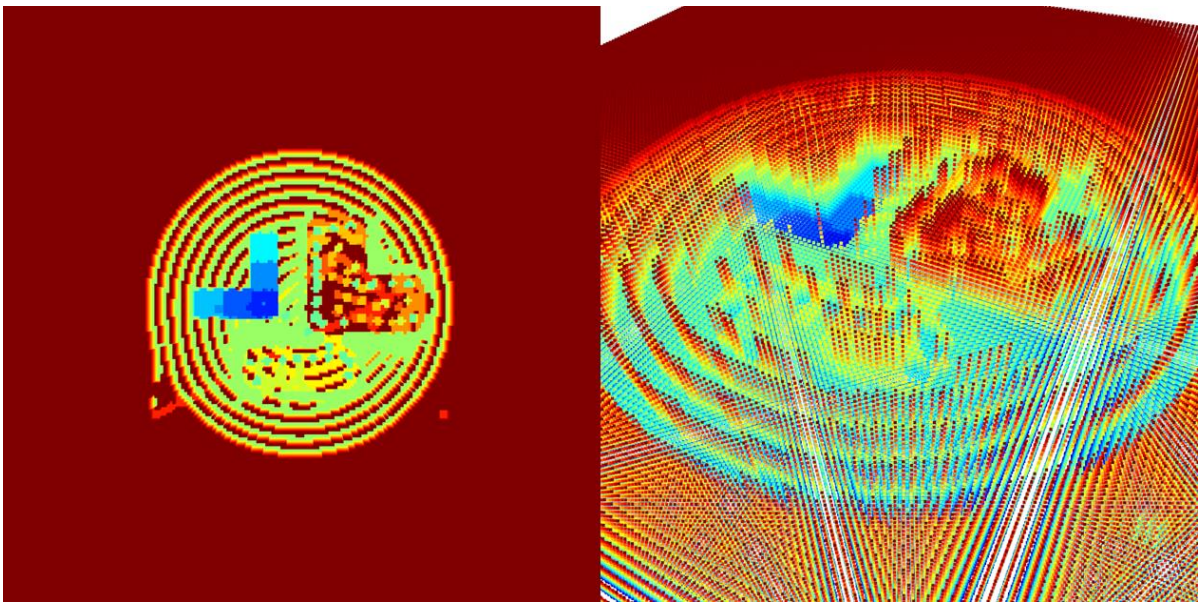

Figure 22: Subtractive NIST Geometry G-Code Voxel Model

MTConnect data produced by the subtractive process was captured and processed as described in section 3.4.2. A voxel model was created from MTConnect data. Three different views of the resulting MTConnect voxel model are shown in Figure 23.

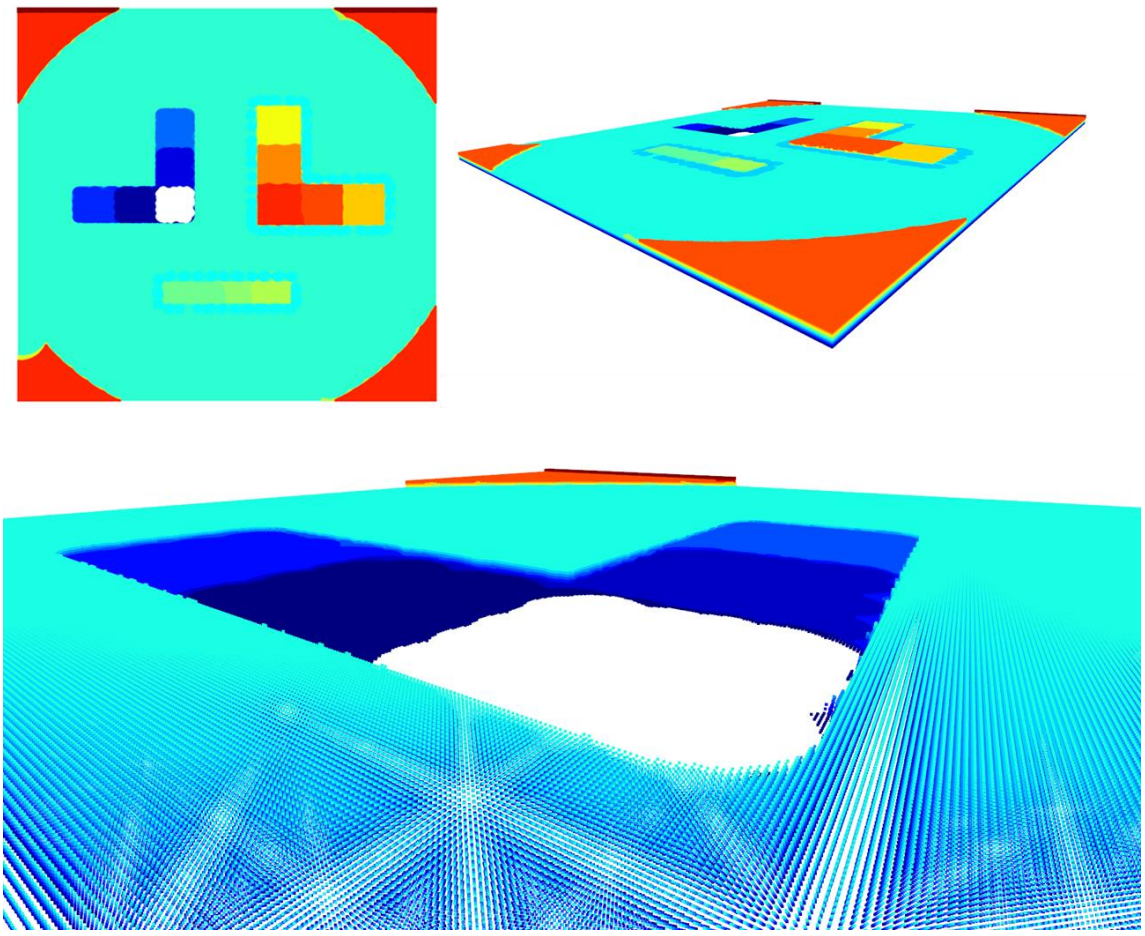

Figure 23: Subtractive NIST Geometry – MTConnect Voxel Model

To determine dimensions from a voxelized model, the following process was used:

1. Points representing the center of each voxel for the area of interest were cropped from the initial dataset. Voxels for a single layer were isolated into a separate dataframe from the cropped subset.
2. A grid was created to match the dimensions of the voxel model's spacing and points from each vertical increment was assigned to a list.

3. Each vertical column was processed to determine the maximum value. These values are stored in the first row of a dataframe matching the voxel grid dimensions.
4. This process is repeated for each layer. The resulting dataframe represents the maximum voxel locations for a single ‘planar’ surface oriented in the Z-direction.

This process was modified to produce the maximum and minimum of a voxel surface in each cardinal direction. For example, to find the maximum voxels of a plane facing the -X direction, the voxels can be distributed into horizontal rows, and the minimum value is recorded. The resulting dataframe is a 2D matrix representing the maximum values of voxel model face. Each of these values were averaged to determine the final dimension. Measurements for Features 1 - 6 of the NIST subtractive geometry voxel model were determined with this process. An example of computing the maximum points from a voxel model is displayed in Figure 24.

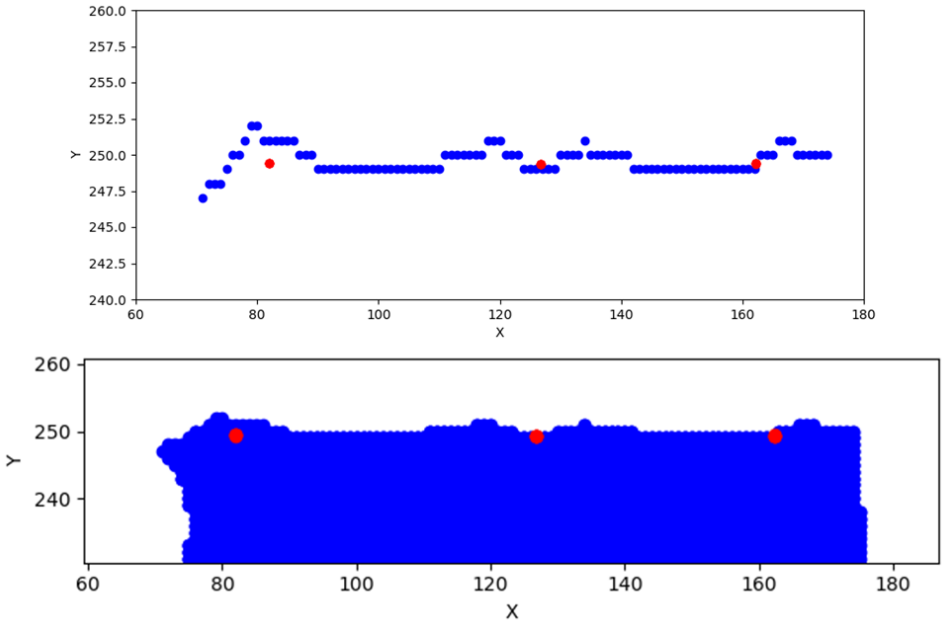

Figure 24: (Bottom) Edge Voxel Points (Top) Initial Z-layer Slice.

The resulting measurements are displayed in Figure 25. Relative measurements were calculated to provide a measure against ground-truth physical measurements, displayed in Figure 26. This calculation is possible with four pairs of measurements on the NIST subtractive geometry. Dimensions for each feature of the NIST subtractive model were verified to be well within the defined tolerance, ±0.1 mm, by both the voxel modelling method and inspection data. However, uncertainty in measurements from inspection data decreased by an average of 67%.

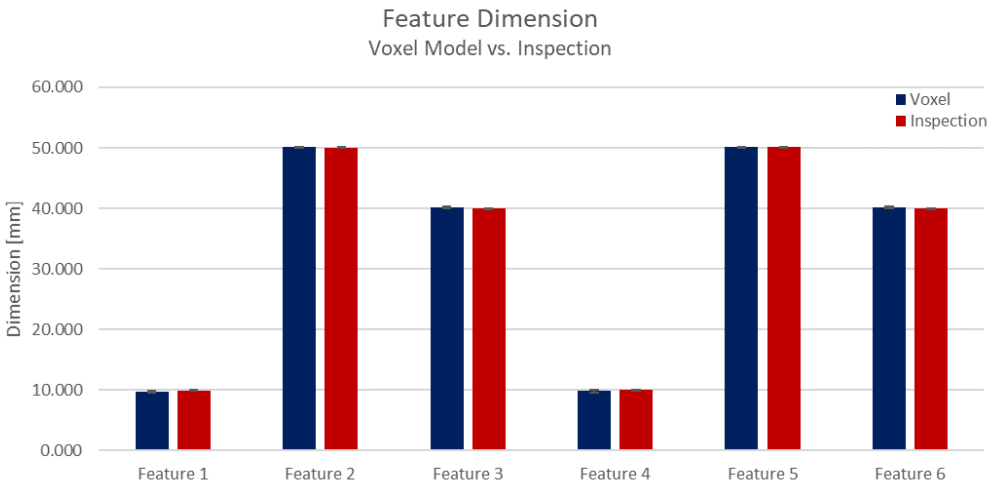

Figure 25: Voxel Model and Specification Dimensions for Subtractive NIST Geometry

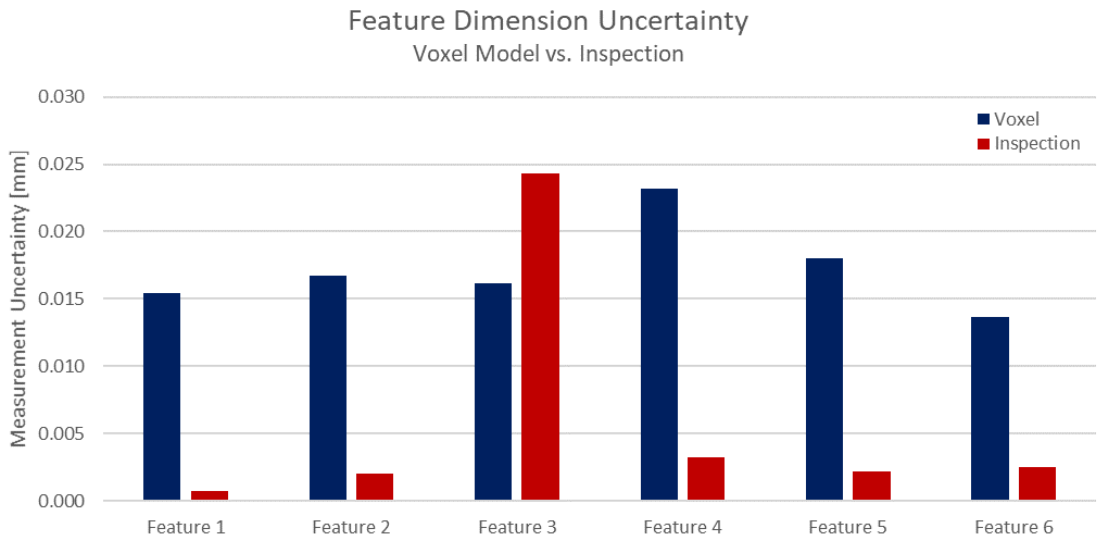

Figure 26: Feature Measurement Uncertainty for Subtractive NIST Geometry

A measure of error from the specified dimensions is presented in Figure 27. Uncertainty values in the figure are calculated with respect to the dimension measurement for each method. They are presented with the error to provide an indication of confidence for voxel and inspection methods, to determine if the true value could be encompassed by

either method alone. For example, the uncertainty in measurements from the voxel model with Features 1, 5, and 6 do not encompass the (more accurate) error given by inspection data. The result is an improvement in accuracy of the part with inspection data is considered. Relative features were measured with calibrated calipers. An increase in accuracy can immediately be seen with the inclusion of inspection data. By including inspection data in the digital model, the error in the digital model was reduced by an average of 52% across each of the four relative feature dimensions. The results of these measurements are displayed in Figure 28.

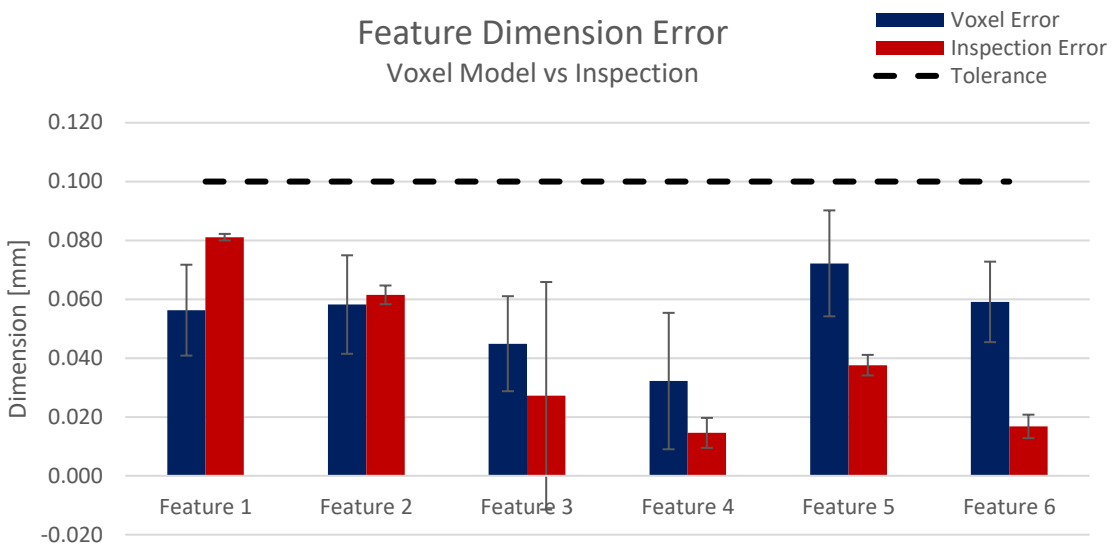

Figure 27: Feature Dimension Error for Subtractive NIST Geometry

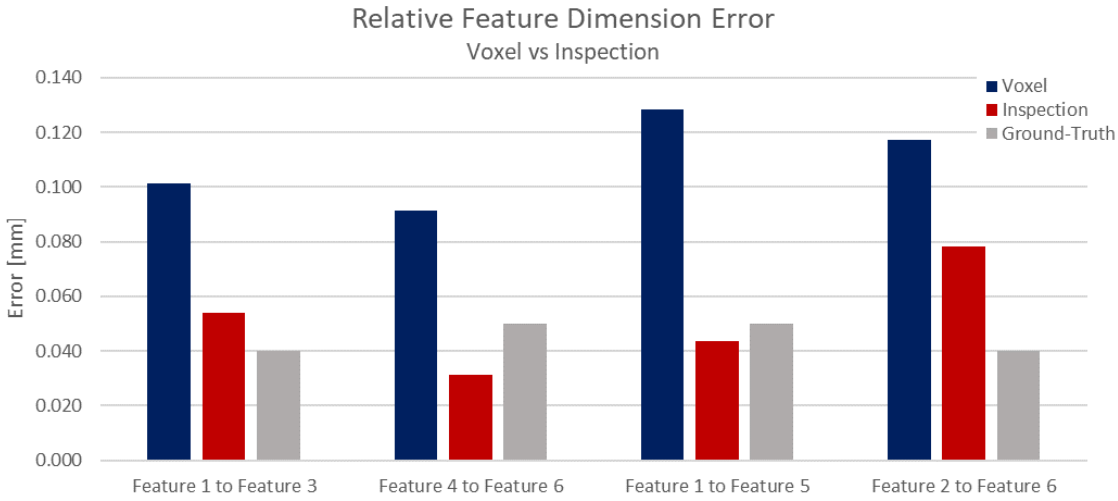

Figure 28: Relative Feature Error for Subtractive NIST Geometry

3.5.2 Additive NIST Geometry

Two versions of the Hybrid NIST Geometry were fabricated as described in Section 3.4.2. The first version was fabricated with only additive operations. A raster toolpath was used beginning in the bottom right hand corner of the geometry, processing horizontally to sweep out the surface area. The toolpath was designed to match geometry specifications – the beginning and end points of the raster fell on the feature boundaries. This was a design choice to measure potentially overbuilt or underbuilt areas (in contrast to the Hybrid NIST geometry, which was fabricated with a 2mm overbuild). The fabricated component is displayed in Figure 29.

Figure 29: Additive NIST Geometry Fabricated Component

MTConnect data was used to create a voxel model, displayed in Figure 30. Methods described in the previous section were used to identify the maximum and minimum points in the voxel model. Resulting edges were compared against probe data and caliper measurements. Data collected to measure additive dimensions are more varied than the NIST subtractive dimensions. However, the scale of the additive component is approximately 50% larger in size.

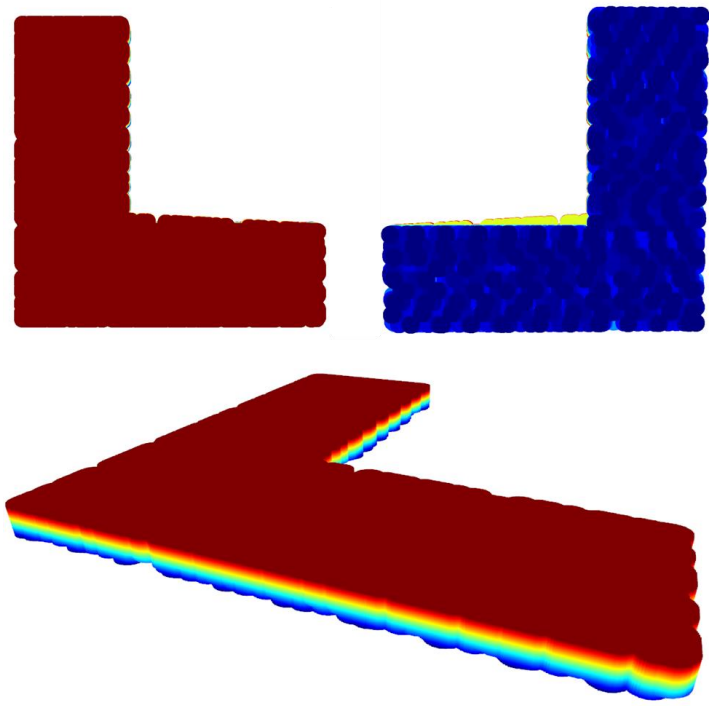

Figure 30: Additive NIST Geometry Voxel Model

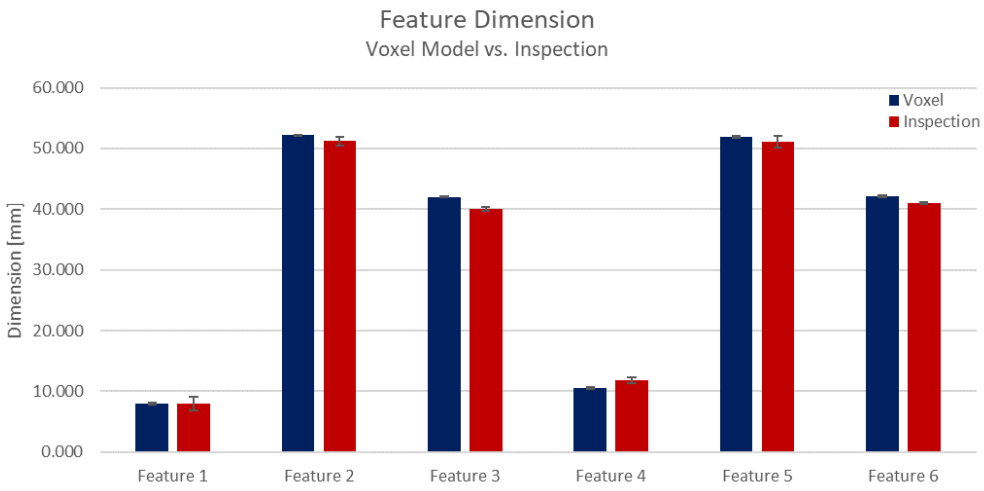

Figure 31: Additive NIST Component Feature Dimensions

It was observed that the probe often hit 'hairs', or bits of wire that did not fully weld to the larger component during the inspection process. This increased the error in inspection data, displayed in Figure 32. Additionally, uncertainty values for the additive NIST component were significantly higher than for the subtractive NIST component, displayed in Figure 33. This can be attributed to the rough surface finish produced by additive manufacturing with Laser Hotwire DED methods. However, the inspection data is on average more accurate than the voxel based data.

Additive manufacturing toolpaths result in a series of raster passes that closely match previous layers, if not a perfect duplication. This results in very uniform buildup in the edges in the voxel model. Therefore, additive may be well modeled by the voxel process whereas subtractive processes are not, due to constantly changing geometric toolpaths.

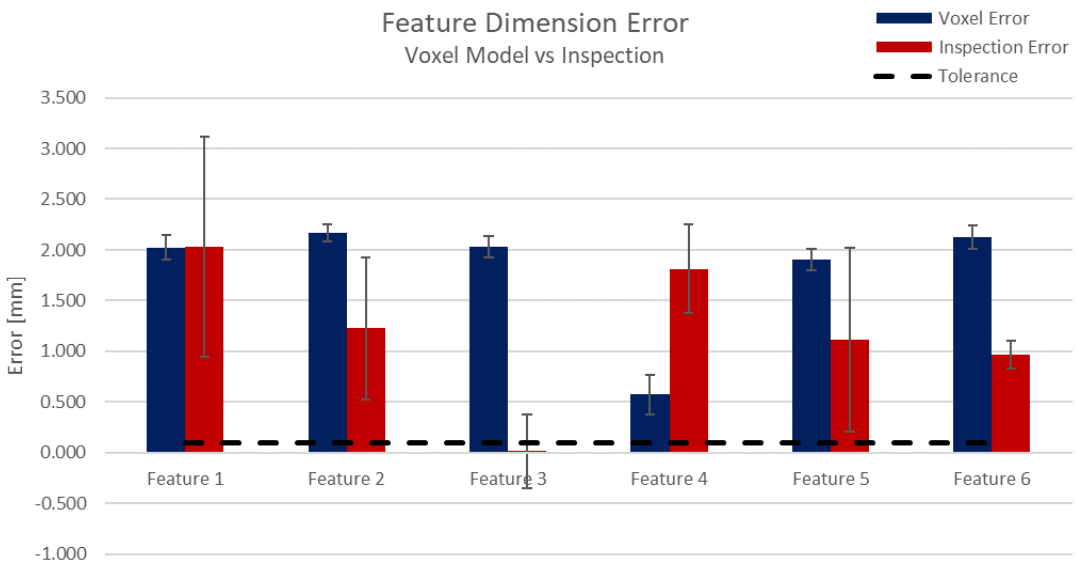

Figure 32: Additive NIST Geometry Dimension Error

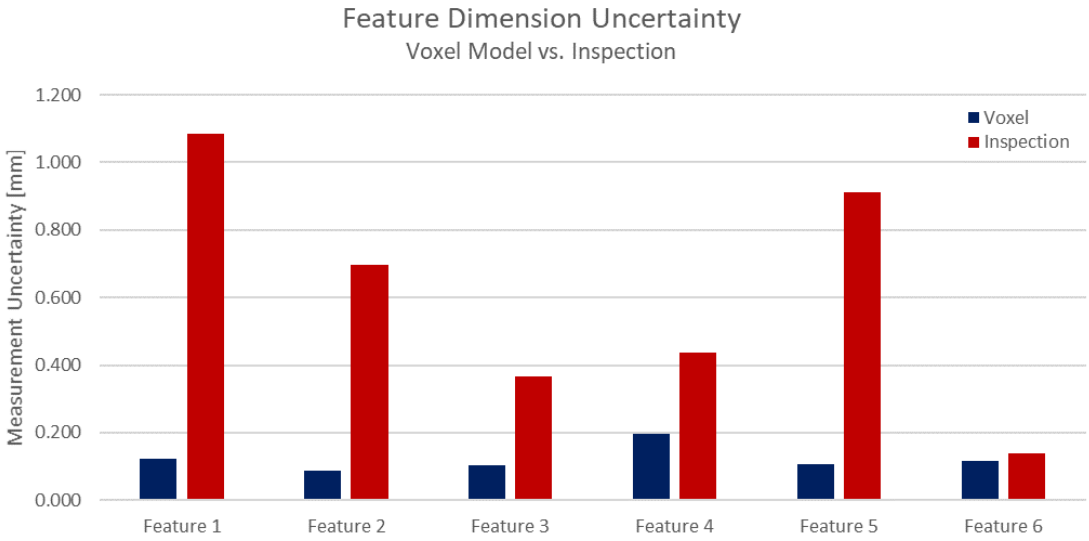

Figure 33: Additive NIST Geometry Uncertainty Measurements

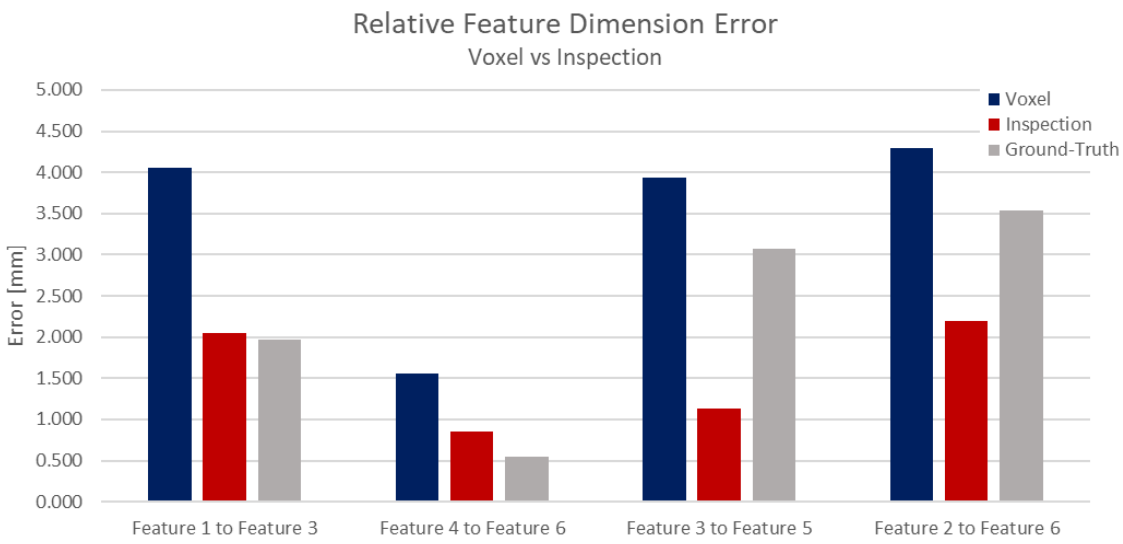

Figure 34: Additive NIST Geometry Relative Feature Dimensions

3.5.3 Hybrid NIST Geometry

The hybrid NIST geometry was produced with both additive operations to fabricate a pre-form geometry, and subtractive operations to fabricate the final features. In contrast to the additive NIST geometry, the additive operation of this component included a 2mm overbuild on each face. This allowed for an investigation of digital detection methods for additively overbuilt features in comparison to subtractive features fabricated to intended geometric specifications. Inspection operations were programmed between the additive and subtractive operations to measure accuracy of the designed 2mm overbuild. The final component is displayed in Figure 35.

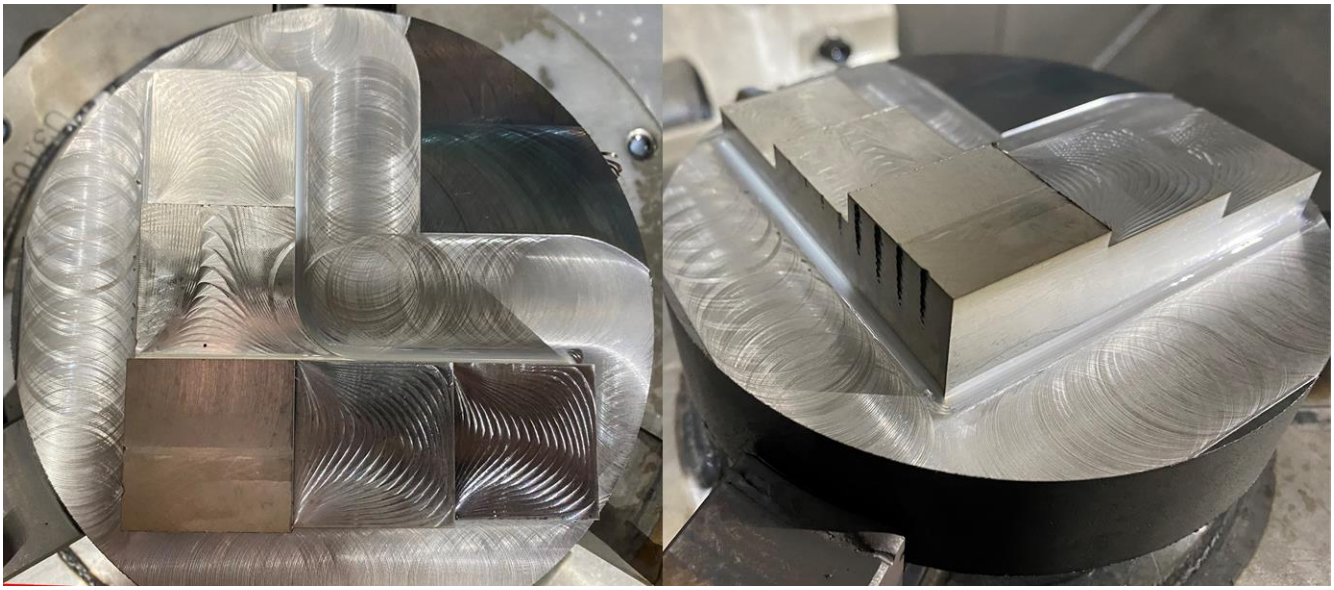

Figure 35: Additive NIST Geometry Fabricated Component

MTConnect data from the production process was used to create a voxel model. The first modelling operations considered additive data to represent the preform geometry. Next, subtractive operations were applied to the additive voxel model to represent the final fabricated component. This process interchangeably used the additive and subtractive methodologies presented in Section 3.4 for selectively adding and removing material in a Digital Twin model. Two views of the resulting voxel model for a component produced with hybrid manufacturing techniques is displayed in Figure 36 and Figure 37.

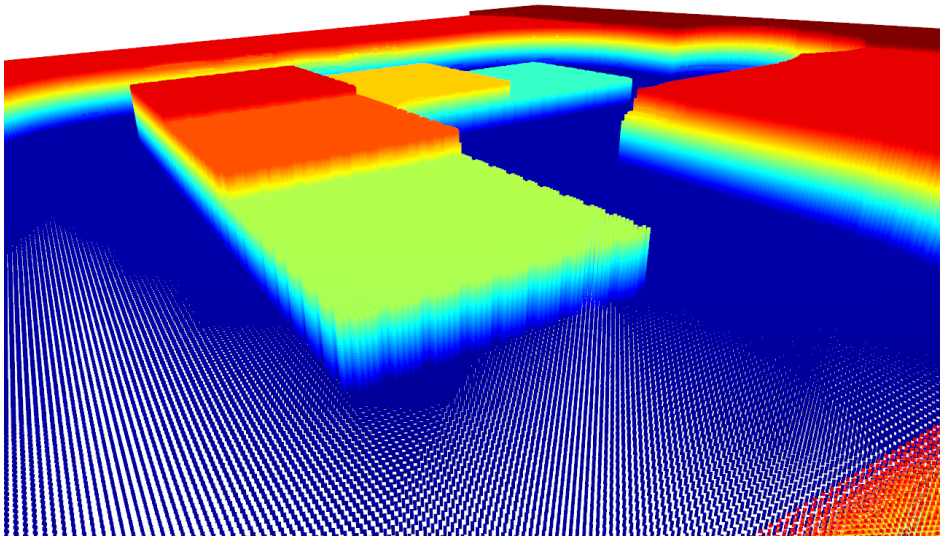

Figure 36: Hybrid NIST Geometry Voxel Model - View 1

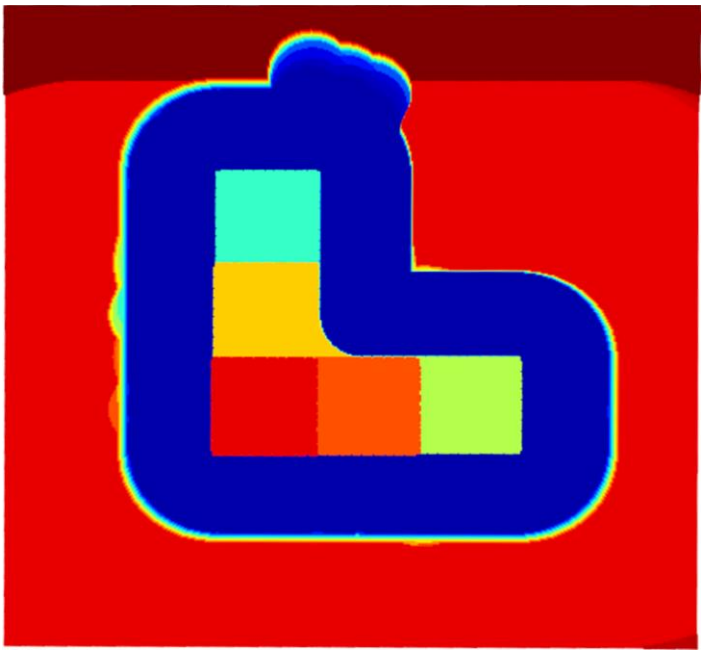

Figure 37: Hybrid NIST Geometry Voxel Model - View 2

Although rectangular stock was used for the voxel model process (compared to the physical component fabricated on cylindrical stock) the voxel modelling methodology developed was successful on true hybrid operations. Interchangeable additive and subtractive operations were successfully modeled.

The hybrid voxel model was used to measure the 6 features as outlined in previous sections, displayed in Figure 38. This component demonstrated a significant increase in accuracy when inspection points were included in the digital model. Dimensional errors calculated from the voxel model indicated that the component exceeded defined tolerances. However, by adding inspection points in the digital model, geometric error was demonstrated the be within defined tolerances, as shown in Figure 39.

The hybrid NIST geometry is distinct in this regard because features measured with both voxel and inspection methods for previous subtractive and additive geometries fell within the defined tolerance. Therefore, this experiment presents a more valuable indication of success, as the addition of information demonstrates a significant decrease in modelling error. A voxel model created from process information alone would have indicated out-of-tolerance features.

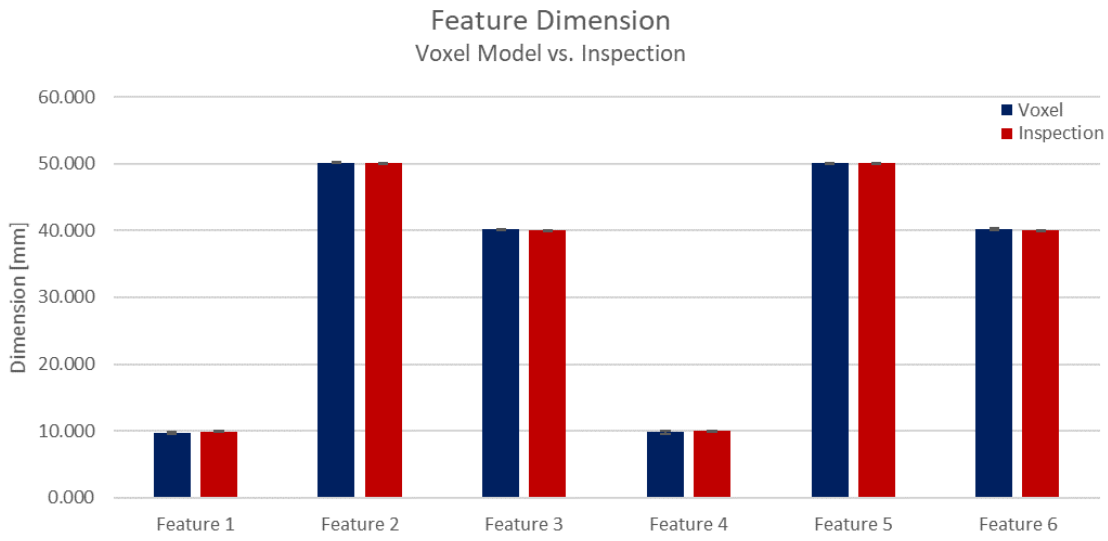

Figure 38: Hybrid NIST Geometry Feature Dimensions

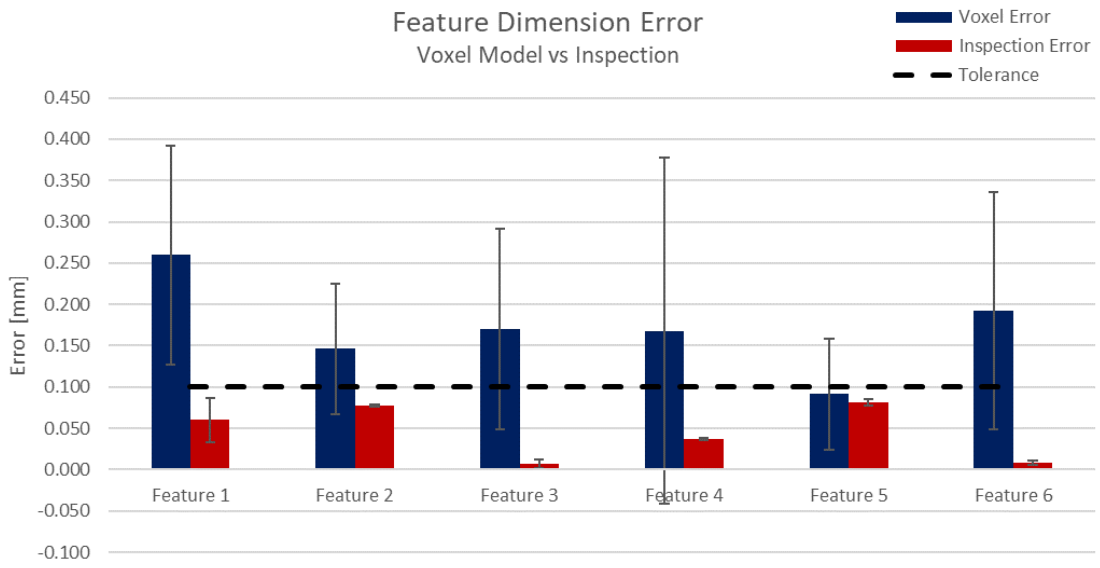

Figure 39: Hybrid NIST Geometry Feature Dimension Error

Dimensional measurement with the hybrid NIST component demonstrated uncertainty values similar to the subtractive component, as displayed in Figure 40. This makes sense as the final inspection surface closely resembles the subtractive NIST component, but at a larger scale. However, a larger error was measured in the process data

voxel model when compared with ground truth measurements, displayed in Figure 41. This could be also be attributed to the scale of the geometry in comparison with the subtractive NIST component.

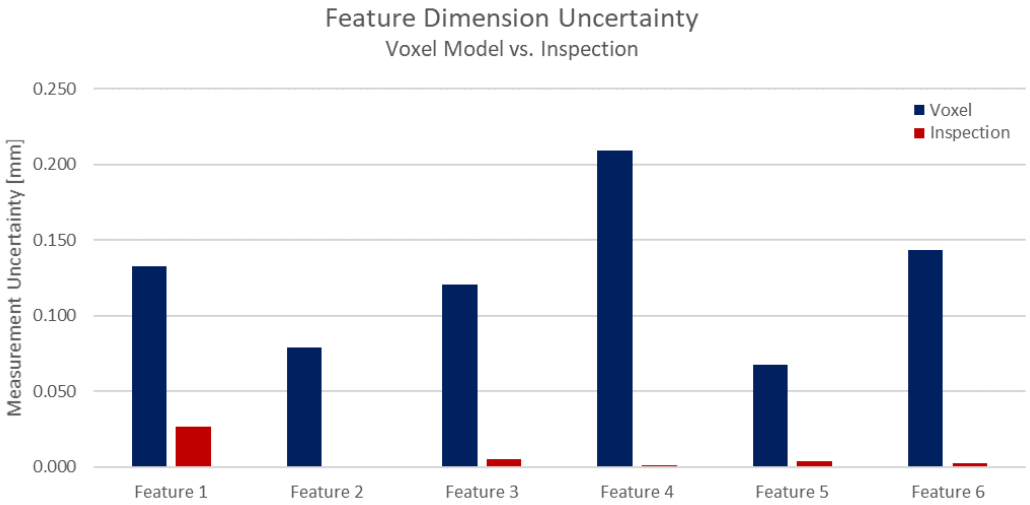

Figure 40: Hybrid NIST Geometry Feature Dimension Uncertainty

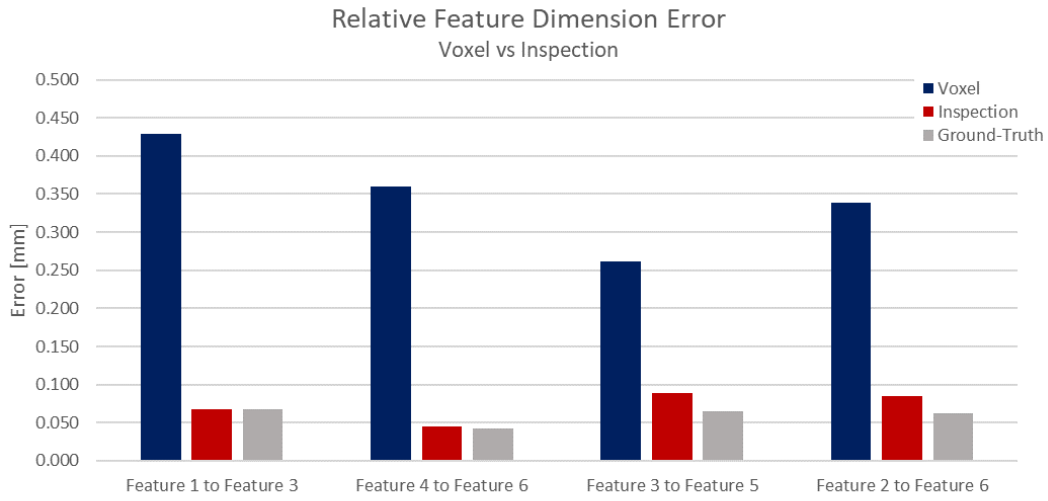

Figure 41: Hybrid NIST Geometry Relative Feature Dimensions

3.5.4 Organic Surface Geometry

The organic surface geometry was fabricated as hybrid component, where a preform geometry was additive manufactured, and the final surface features were subtractively machined. This component was chosen as a test article due to continuously changing radius of curvature in two dimensions. This provided a strategic test of the voxel modelling process to represent smooth geometry, in contrast to the 2.5D shapes that were investigated above. Four different stages in the component's fabrication are displayed in Figure 42.

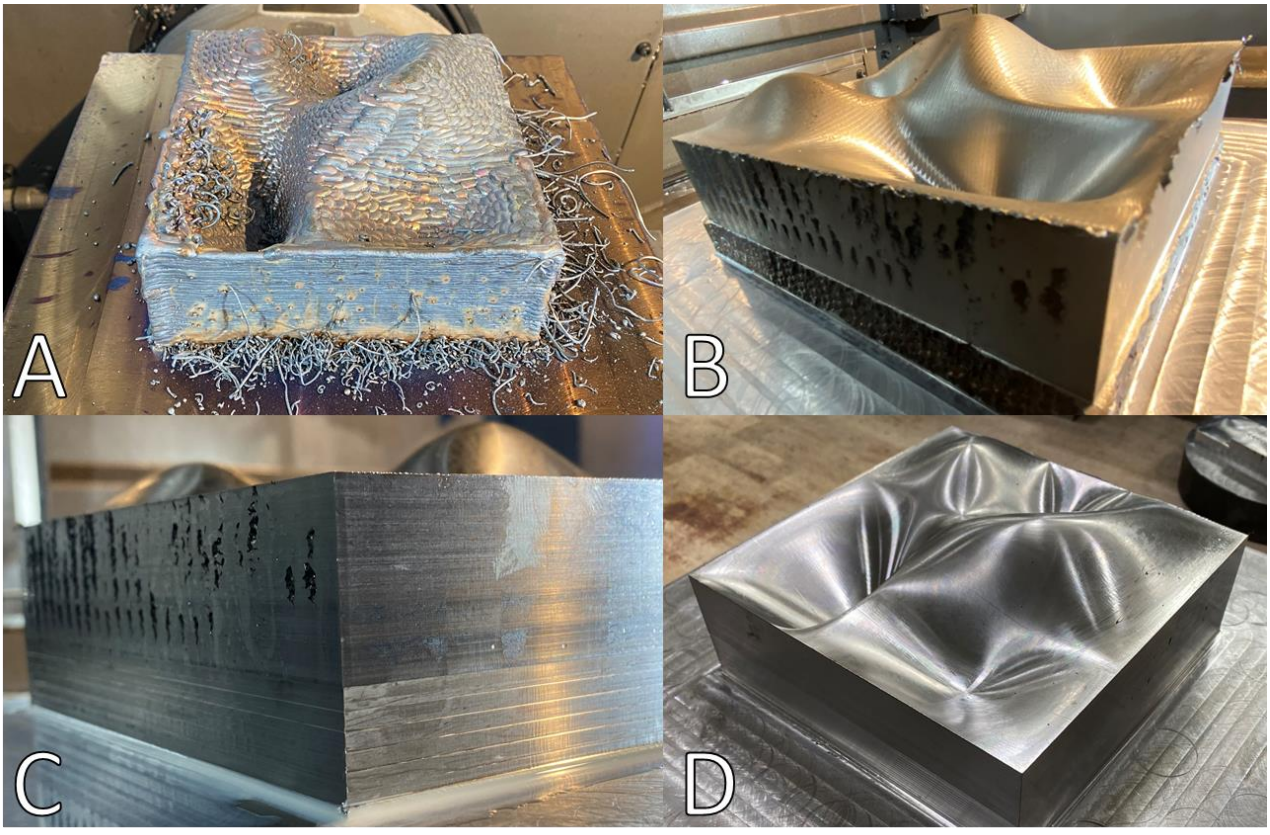

Figure 42: Organic Surface Geometry (A) Additive operations (B-C) In-process Subtractive (D) Final Component

Two voxel models were created to represent this component, each at different points in the fabrication process. The first voxel model was created after additive operations, representing the preform additive geometry, displayed in Figure 43. The second voxel model was created after subtractive operations.

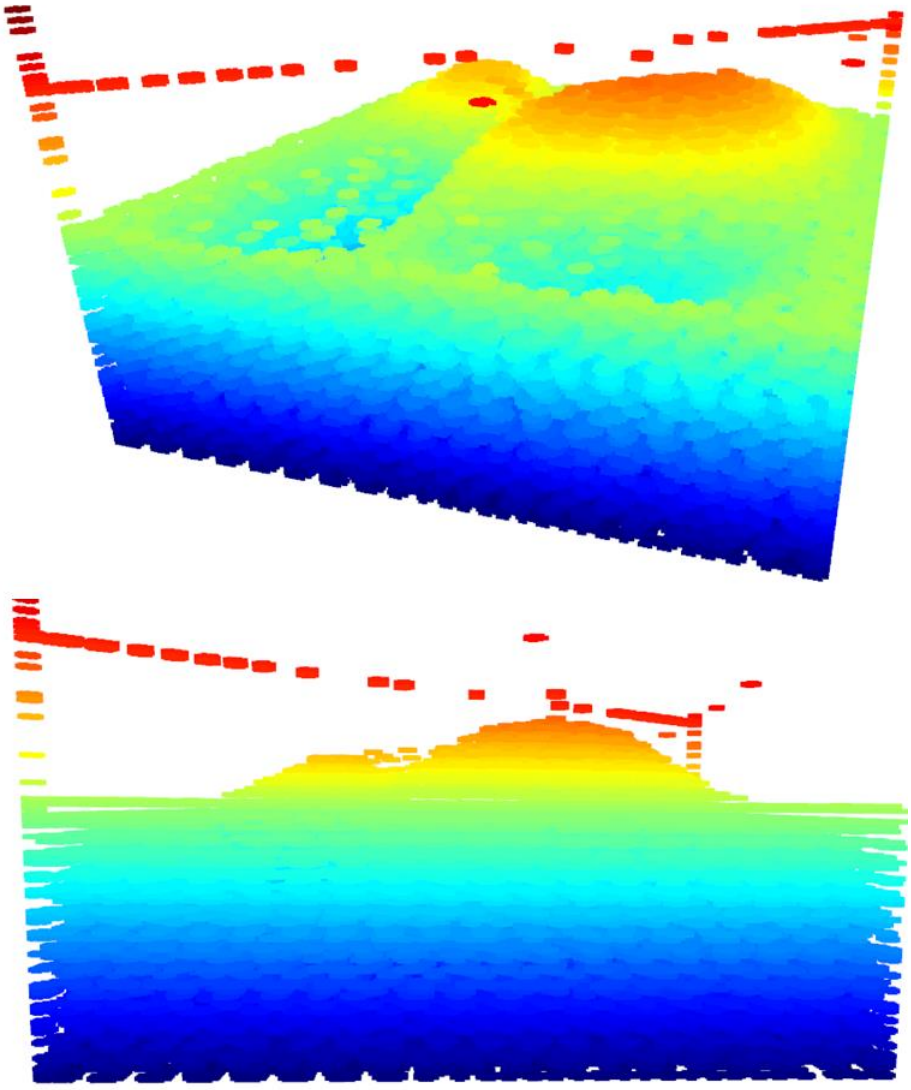

Figure 43: Organic Surface Geometry – Voxel Model

Inspection operation were conducted after both the additive operations and after the subtractive operations. These results are compared against voxel model measurements.

Throughout this research, a design choice was made to have independent resolutions for the XY-axis and Z-axis workspace discretization. This aims in computation efficiency while still preserving planar features A significant decrease in accuracy was expected when measuring features of the organic surface voxel model due to lower resolution discretization in the Z axis in the voxel modelling process.

Six features of the organic surface were measured with the voxel model and with inspection operations. The resulting additive feature dimensions are presented in Figure 44. Uncertainty values for these measurements are displayed in Figure 45.

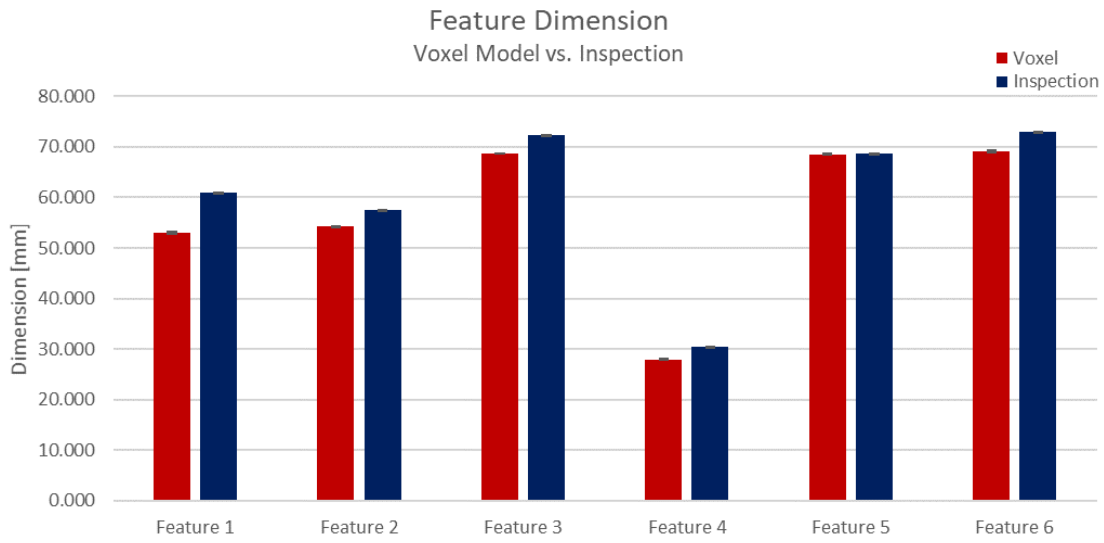

Figure 44: Organic Surface Geometry Additive Feature Dimensions

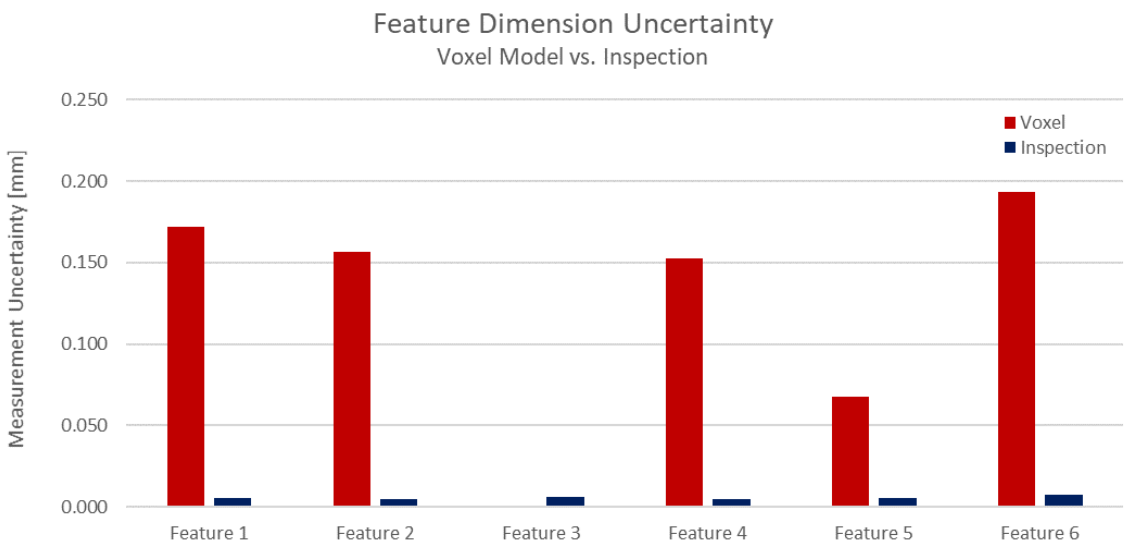

Figure 45: Organic Surface Geometry Additive Feature Uncertainties

A significant disagreement in measurement was found with feature dimensions calculated from the voxel model and those measured via inspection. This confirms expectations that the voxel modelling method would be less suited to model organic surfaces with a constantly changing radius of curvature. Although it is difficult to determine the true accuracy of points on this surface with physical measurements in past experiments, inspection measurement had significantly lower uncertainty values, indicating increased accuracy. However, the voxel modelling performed better than expected when used to model the subtractive process. This may be due to the small stepover values used in subtractive machining (0.1mm) compared with the relatively large stepover value used in additive manufacturing (3.5mm). The small stepover results in more opportunities for MTConnect to register the tool location within a given region, increasing the accuracy of the model. Features dimensions and uncertainty values are presented in Figure 46 and Figure 47, respectively.

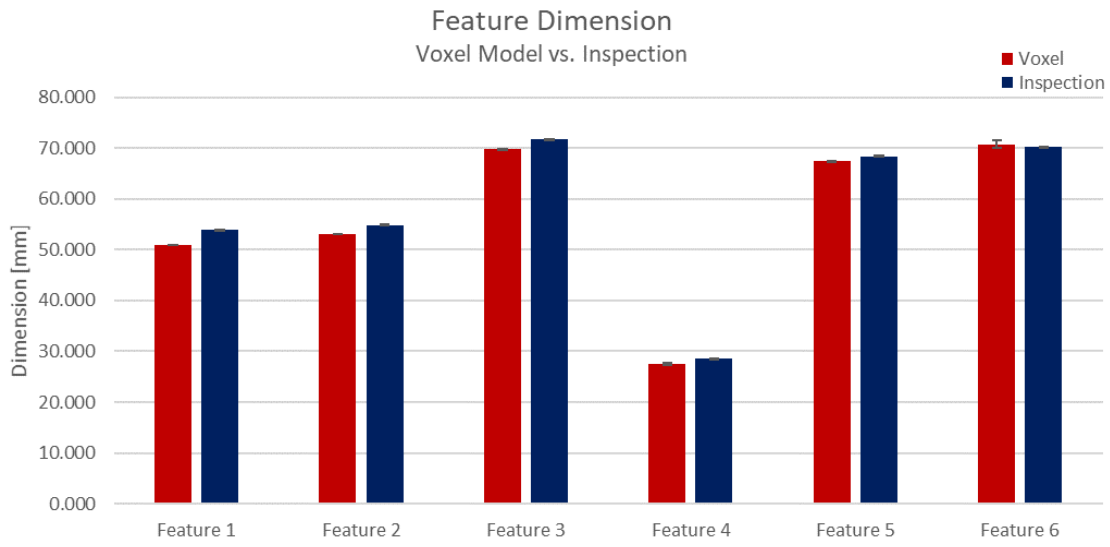

Figure 46: Organic Surface Geometry Subtractive Feature Dimensions

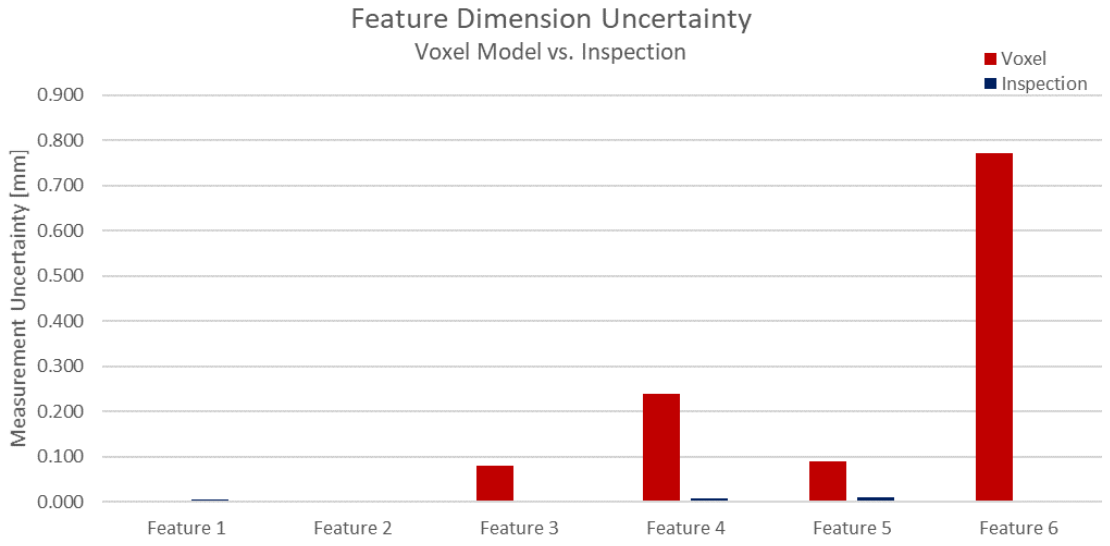

Figure 47: Organic Surface Geometry Subtractive Feature Uncertainties

It is noted that the uncertainty values calculated from inspection points are almost negligible. This may be attributed to the resulting smooth surface of the organic geometry after subtractive machining. In additive components, the rough surface finish may lead to less consistent measurements. However, this should not be confused with accuracy.

Inspection cycles are intended to approach the inspection point on a route that is normal to the surface, as programmed in the previous 2.5D experiments. Inspection cycles for the organic surface geometry were programmed to approach the surface in the negative Z-axis direction due to CAM toolpath constraints. Therefore, while the resulting measurements are therefore repeatable and provide equal metrics against which the voxel model process can be compared, the true accuracy of the dimension is unknown.

3.5.5 ISO-10791-7 Standard Geometry

The ISO-10791 Standard Geometry was fabricated with both additive and subtractive operations on the Mazak VC-500A/5X AM HWD. This experiment served to determine the limits of inspection capabilities with respect to GD&T specifications. The fabricated component is displayed in

Figure 48. Four planes were selected for flatness measurements, displayed in Figure 49.

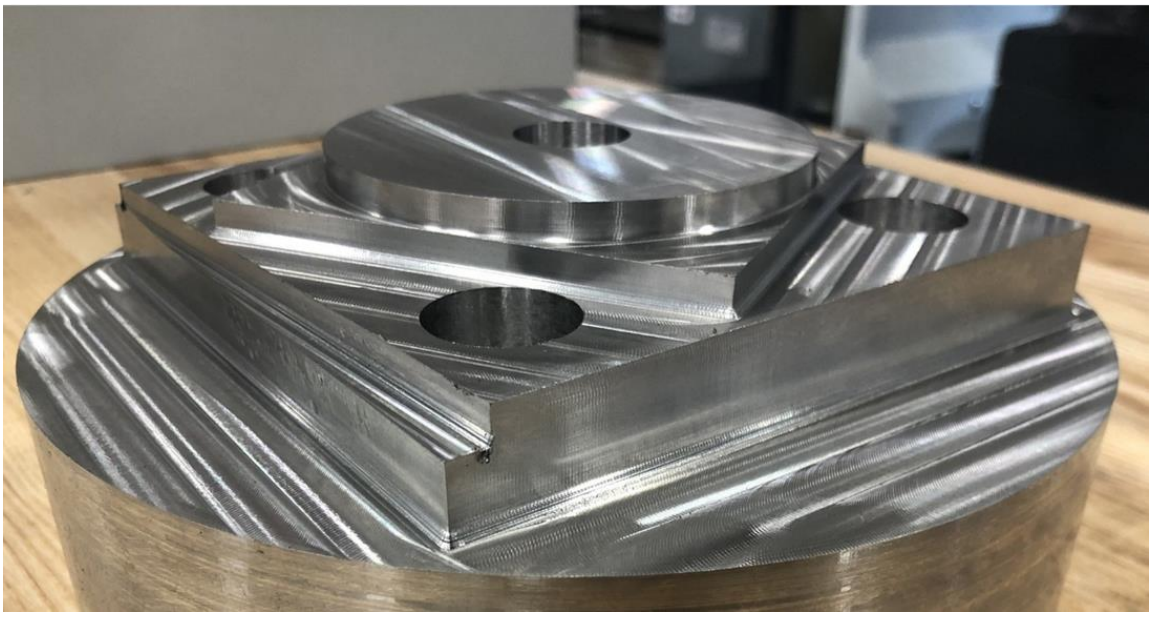

Figure 48: ISO-10791-7 Standard Geometry Fabricated Component

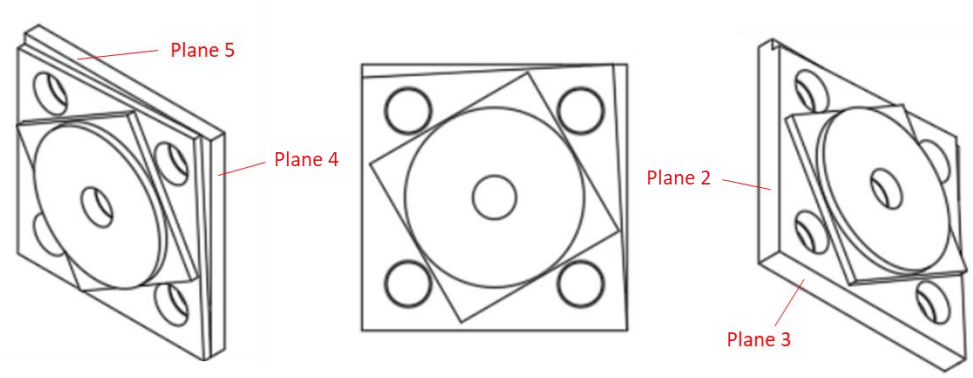

Figure 49: ISO-10791-7 Standard Geometry Inspection Planes

Each of these planes were measured with NIST traceable calibrated CMM to determine the ground truth flatness. The CMM used a serious of continuous measurements

following standard operating procedures. The minimum distance between two parallel planes that encapsulate all points was calculated to provide a measure of flatness.

A series of discrete inspection operations on the were completed with a Renishaw inspection probe on a Haas VF-5 vertical CNC machining center to evaluate the capabilities of CNC inspection operations against calibrated CMM equipment. The inspection probe retained the same repeatability and calibration metrics as in previous experiments.

The resulting points were recorded using the architecture presented in Chapter 4. Two planes fitted to encapsulate the points, in a similar method to computations completed with the CMM. The parallel planes were allowed to rotate by ±3 degrees to minimize the fit error stemming from part perpendicular with respect to the machine coordinate system. A comparison of the resulting flatness measurements is displayed in Figure 50.

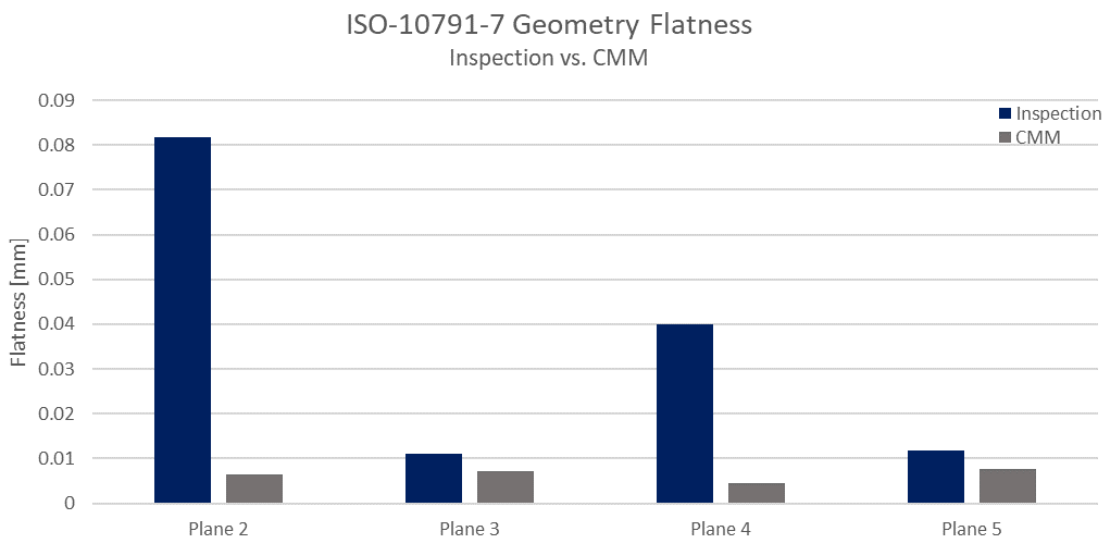

Figure 50: ISO-10791-7 Standard Geometry Flatness Comparison

It is clearly evident that a range of accuracy exists. Flatness measurements for Planes 2 and 4 were significantly different from measured CMM values. Inspection measurements for Plane 2 are nearly an order of magnitude greater than CMM measurements. Inspection measurements for Plane 4 was nearly seven times greater than the CMM value. These measurements indicate that the inspection process used to determine accuracy within GD&T specifications is not valid

However, flatness measurements for Planes 3 and 5 were closer to the CMM values. Inspection measurements for both planes differed from CM values by no more than 0.004 mm. These measurements indicate that the inspection process used to determine accuracy within GD&T specifications is could be valid, with additional development.

It is interesting to note that Planes 2 and 4 were oriented along the CNC machine's Y-axis while Planes 3 and 5 were oriented along the machine's X-axis. It is possible that Haas VF-

5 CNC machine on which these experiments were performed has significantly different accuracy in one axis of motion than the other.

Overall, the results of the ISO-10791-7 Standard Geometry comparison are inconclusive. While some data indicated a successful method for inspection to GD&T specifications, other data indicates a significant difference between measured and true values. Additional experiments are needed to determine the validity of this method.

3.6 Discussion and Limitations

Some limitations in the voxel model exist for the non-uniform bead geometry that is often found with different additive processing parameters. A fundamental contribution of this body of research aims to increase the accuracy of modeled parts by combining additional data sources with the voxel models. A better understanding of bead geometry distributions with respect to processing parameters would significantly improve the modeling capabilities of the voxel-based digital modelling process.

It is also noted that additional computational methods may be more appropriate for computing the average value of non-planar surfaces. For example, the methodology presented above is more accurate when the surface texture and surface finish approaches a true plane. However, additive deposition in hybrid manufacturing commonly produces a rough surface, often related to the bead step-over and layer height parameters. In this sense, the maximum value of each face will be found at the peak of each bead, while the true surface average is somewhere below the peak and base of the surface beads. A weighted average calculation may provide a more useful number to determine dimension for future operations, such as subtractive finishing.

3.7 Conclusion

This chapter evaluated methods to leverage manufacturing data from CNC manufacturing systems for creation of a digital twin model of the *in-situ* fabricated component. Multiple streams of information from hybrid CNC systems were used to create a digital twin model of the part currently in production. This chapter details the following contributions:

1. A method by which digital voxel model can be created through the combination of multiple sensing modalities
2. A method to measure and compare the accuracy of the digital model when to desired feature specifications.
3. An evaluation of this digital voxel methodology against 2.5-axis and 3-axis components produced with subtractive, additive, and hybrid techniques.

This research results enables methodologies for *in-situ* process monitoring, and mechanisms for measuring and comparing *in-situ* features against desired specifications. The results of this work can be used to generate feedback commands to affect the process, studied in Phases II and III.

3.8 Future Work

Computation time is a significant factor in the voxel modelling process. Assuming a standard component of X by Y by Z dimensions, with a digital voxel model of 0.01mm resolution, up to 50 million points must be processed to digitally create the final model. This methodology used Boolean masking and dataframe operations where possible to limit

the number of iterative loops. However, this research focused on the process methodology development. Future work is needed to further refine and optimize the computational implementation of this process.

Additionally, significant work exists to apply this methodology for cybersecurity applications. While these models were created by post-processing batch MTConnect data, the methodology could easily be modified to create the voxel model as the component is fabricated, providing immediate feedback. This foundation for this capability is further developed in the following chapters with feedback control mechanisms.

CHAPTER 4. PHASE II – MULTI-AGENT OPEN ARCHITECTURES

The adoption and use of digital sensors, controls, and communication protocols in modern CNC machines is one of the primary results of the fourth Industrial Revolution [47]. These capabilities provide unparalleled opportunities to monitor the manufacturing process and provide an evaluation of the fabricated component as demonstrated in Chapter 3. However, an underlying information architecture is needed to efficiently govern data produced by the manufacturing systems. Furthermore, a communication architecture is needed to transfer this information efficiently between disparate analysis tools. This chapter investigates multi-agent architecture methodology and compression mechanisms for system information governance to support automated *in-situ* and future feedback control operations.

4.1 Introduction

In the current era of the Fourth Industrial Revolution known as “Industry 4.0”, connected manufacturing equipment, process control equipment, and analysis equipment produce tremendous amounts of data at every stage in the manufacturing process. The ability to take data from all points in the manufacturing process and link them to features and attributes of the resulting product provides an extremely valuable tool for understanding and improving the manufacturing process. Commercial CNC systems often included numerous digital components to support controls, sensing, and path planning operations. Due to the unique combination of capabilities in a hybrid system, multiple

information streams are produced throughout the fabrication process, each with a different format and structure. However, this data is largely wasted due to lack of efficient transmission, storage, and analysis. A supporting information architecture is required to capture this data and govern it in an efficient manner.

Various architectures have been proposed to leverage machine connection mechanisms and extract this data in a logical manner, but many of these architectures rely on proprietary, enterprise software, that restricts the flexibility and adaptability of the architecture. These architectures tend to be static in structure and operation, providing a solution that cannot readily adapt to the current manufacturing needs. However, recent developments in low-cost computational units, high-bandwidth communication protocols, and high-capacity storage units enable information processing to occur physically far away from the information source. Therefore, it is necessary to develop a multi-agent information architecture to support the capture, communication, and analysis of hybrid manufacturing data. It is hypothesized that that the compression ratio and speed can be improved by applying different compression algorithms based on the type of manufacturing data. This study evaluates five compression algorithms against a portfolio of hybrid manufacturing data packages. The result of this work is an information architecture that can efficiently govern different data streams from multiple sources, describing a common manufacturing process. Furthermore, this architecture provides the groundwork for information feedback into the manufacturing systems, supporting adaptive closed-loop operations. The following section discusses relevant literature that enables this work.

4.2 Literature Review

4.2.1 Cyber-Physical Systems and Industry 4.0

Digital Manufacturing technologies, the collection and application of digital information for the enhancement of manufacturing process, have existed in the manufacturing community for the past four decades [3]. While the term Digital Manufacturing once referred the use of digital control components within a manufacturing line (opposed to analog control mechanisms) it now implies a much larger scope, referring to the merging of manufacturing technology, network information technology, and information analysis to provide better understanding, coordination, and control of manufacturing processes [47]. However, recent advances in computational speed, communication protocols, and information storage capacity has influenced the manufacturing industry. The decrease in cost and increase in accessibility for these technologies has enabled manufacturers to integrate advanced sensing and control capabilities in traditional manufacturing equipment. These systems are considered as a new classification of manufacturing equipment, Cyber-Physical Systems (CPS), or systems that are built from and depend upon the synergy of computational and physical components [5].

Across the broad manufacturing industry, the shift toward intelligent and connected manufacturing processes is accepted as the fourth Industrial Revolution, referred to as Industry 4.0. This revolution is a subsequent iteration from the first three major technology advances which focused on mechanization, large-scale production, and automation, respectively [48]. These technologies have provided the foundation

for significant advances in data collection, communication, and analysis across manufacturing processes.

4.2.2 Distributed Computing (Edge-Fog-Cloud)

The third industrial revolution, automation of manufacturing process, served as a steppingstone by providing the mechanisms of information generation and utilization. However, this information typically remained within the same machine or process and was only used for local adjustments. The integration of communication protocols for connectivity between disparate manufacturing and computational equipment is one of the defining accomplishments of the fourth industrial revolution, distinguishing it from previous developments in Digital Manufacturing. Combined with access to high-bandwidth communication protocols, it is now possible to transmit large datasets in practical timeframes for analysis that is physically distant from the point of information generation.

As a result, three primary locations of computation have been developed and discussed in recent literature, Edge computing, Fog computing, and cloud computing. There is significant debate on the most appropriate method to classify computational methods into these three categories [49]. However, physical location of the computing devices forms a convenient method of distinction, as displayed in Figure 51 [50].

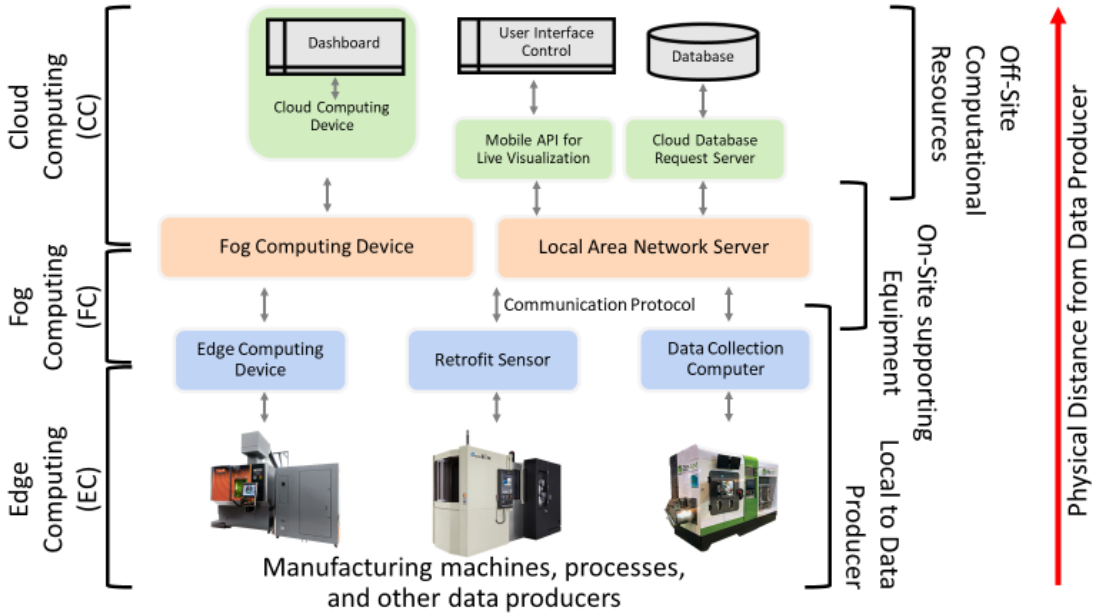

Figure 51: Edge, Fog, and Cloud Computing Diagram [50]

For the purposes of this research, the following terminology will be used [50, 51]:

Cloud Computing (CC): This method of computing refers to processes that take place on-demand at a physically distant location, often relying on centralized shared computing resources. CC is currently the most commercialized method.

Fog Computing (FC): Fog computing included devices that connect cloud and edge computing devices. These are often integrated with supporting networking and traffic control devices. These devices are often physically located within the same building or manufacturing plant, but not immediately next to the information point of origin.

Edge Computing (EC): Edge computing devices are the closest in physical proximity to the information point of origin. These devices act as the first point of contact to collect, format, and begin transmission to other devices. These devices can include low-cost sensors that are designed to monitor a specific aspect of the manufacturing process [52].

4.2.3 Connection frameworks

Multiple connection schemas exist to link different information systems. Modern research has focused on developing high-level connection schemas to connect various information producers and consumers. Some of these methods detail the connection pattern for only two layers of connectivity, such as between Edge and Fog layers, while other methods detail connection patterns between the entre EC, FC, and CC spectrum.

Lee et. Al. proposed a widely-accepted high-level model for connecting CPS that specifies hierarchal levels for communication and use [53]. The "5C Model" describes the different levels of Connection, Data Conversion, Cyber, Cognition, and Configuration necessary to provide a sustainable analytics platform [54, 55].

4.2.3.1 DCS and SCADA Frameworks

The Distributed Control System (DCS) developed in the 1970's enabled reliability in controls. This design enabled continued operation of the manufacturing process, even if one system failed. Under DCS, a multi-layered network is created where granularity of control is related to physical proximity of the controlled device. For example, overall scheduling of production is located at the highest layer while direct control of motion is

located at the lowest layer [50]. This DCS architecture provide the framework for reliability considerations when designing modern information architectures.

Supervisory Control and Data Architecture (SCADA) frameworks have also been considered as a framework for connected devices with CC capabilities. The SCADA structure is an industry-accepted framework for industrial machine control. Recent publications have proposed leveraging this framework for internet connectivity. Zhilenkov et al. discussed a power line communication based on IoT enabling PLC systems [56-58].

4.2.3.2 OSI Interface Model

The Open Systems Interconnection (OSI) model provides a convenience and industry-accepted solution for encryption and authentication techniques. The OSI model is published by the International Organization for Standardization (ISO) that prescribes a 7-layer communication interaction specification by which different applications and protocols may interact [59, 60]. Each layer is assigned its own unique capabilities and uses. Layer 1 (Physical) details electrical characteristics of the network such as the type of the cable and other hardware components that transfers data. Layer 2 (Data Link Layer) details access strategies for signals. Layer 3 (Network) details interaction patterns for multi-source information. For example, the is the layer where standard wireless routers operate. The OSI model can be applied to machine tool communications to increase the security and authorized access to the data [61].

4.2.4 Manufacturing Architectures

There is significant precedence in recent literature for the development of manufacturing architectures. Early research into information architecture for manufacturing focused on local architectures. These systems were intended to govern information in close proximity to the physical manufacturing equipment. Anderson et. al., as part of a US Airforce research initiative, defined a set of specifications in 1993 that must be considered when defining manufacturing architectures. These specifications include Interoperability, Portability, Scalability, and Interchangeability [62]. These specifications were condensed and implemented by Schofield et. al. in 1995 [63]. Schofield outlined a set of guiding principles for information architectures that increase the flexibility and interoperability of any singular architecture component. These guidelines state that architectures must be [63]:

1. *Flexible in hardware and software* allowing for changes in configuration at all levels of control
2. *Standardized* to allow third-parties to develop hardware and software for use within any level of the system
3. *Enables integration with other systems at* any level, i.e. at the system level for multi-machine coordination, and at the process level to integrate sensors and feedback mechanisms

Research by Anderson and Schofield formed the foundation for decentralized manufacturing architectures, where the process could be controlled from a centralized management point within a production facility. Combined with developments of low-

bandwidth communication protocols in the early 21st century, these architectures were adopted for a variety of decentralized control applications. Hillaire documented an open architecture in 2001 to expand CNC capabilities beyond what was traditionally provided through the original manufacturer [64]. Ota also applied a decentralized concept to building efficiency applications, with a wireless demonstrated of HVAC control in 2007 [65].

In the past decade, decentralized architectures have evolved to handle streams of information from multiple sources, each requesting or supplying information as dictated by another device in the system. Andreadis proposed a system in 2014 to logically distribute nodes in a multi-agent architecture based on groupings of information producing agents, information consuming sub-agents, and communication mediators [66]. Palau expanded on this system by proposing a method to define multi-agent architectures based on which nodes have decision-making capabilities [67].

Many modern data communication architectures are intended for static operations. Operations considered static are typically characterized by one-way communication with few, if any, changes to the data monitoring techniques over the production schedule of the machine. Some production facilities deploy an architecture to monitor the state of their machines. This ‘static’ implementation collects the same data, at the same sample frequency and with the same processing tools, regardless of the machine’s operation. Even though the component may change, or the machine may experience downtime, data collection and processing techniques remain constant throughout. An example static implementation is displayed in Figure 52 .

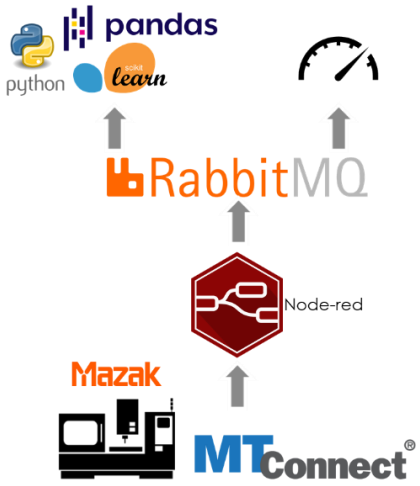

Figure 52: One-Way Communication Process Monitoring Architecture

4.2.5 Compression mechanisms

Information compression mechanisms have existed since information has required storage. It can be argued that one of the first information compression mechanisms included the development of Morse Code, where common letters in the English language such as “e” and “t” were represented with shorter code words for efficiency. With the advent of analog computers in the mid-20th century and digital computers in the late 20th century, information compression mechanism became a focal point of countless research initiatives to optimize computational processes.

Two categories of information compression mechanism exist; (1) lossy compression, where the original information is not fully recoverable from the compressed representation, and (2) lossless compression where an identical copy of the original information can be generated from the compressed representation.

Each of these methods are employed for different uses depending on the underlying principles of information being compressed. For example, audio data is often compressed with lossy methods where sounds that are outside of the normal auditory range of most people are discarded. This results in an audio file that only preserves audio frequencies within a standard range, leaving those outside the range unrecoverable from the compressed file. It is debatable whether or not the lost frequencies improve the overall quality. On the other hand, lossless compressions mechanisms are often used to store financial data, such as digital transaction records and payroll receipts. In this case, loss of any piece of information is detrimental to the account ledger, and therefore must be preserved with lossless methods.

Significant research has been conducted to determine appropriate compression mechanisms with manufacturing data from single-processes systems, such as compression of chemical, subtractive CNC, and additive manufacturing operations. Misra investigated data compression mechanisms via wavelets in 1999 for multi-variate data in chemical processing plants by encoding with [68]. Similar work was completed by Yaman and Dolen in 2013 by evaluating three compression mechanisms for direct command generation with subtractive CNC systems [69]. Salloum investigated lossy compression techniques in 2019 for additive manufacturing data on laser-powder bed systems [70]. This work resulted in methods to compress data used in defect detection mechanisms.

However, limited attention has been given to data compression mechanisms from multi-process systems as found in Hybrid manufacturing. In this paradigm, manufacturing data with different characteristics, formats, and uses must be efficiently compressed. This work is fundamentally different because Hybrid manufacturing looks at compression for

multiple processes in the same system. This work deviates from previous research by investigating methods of lossless compression for datasets that include information from multiple processes within the same system.

4.3 Methodology

4.3.1 Information Sources

A fundamental requirement for process monitoring on hybrid manufacturing systems is the ability to capture, transmit, and store data in multiple formats from multiple sources. This is necessary due to the unique combination of capabilities within a hybrid system, including subtractive machining, additive deposition, and inspection processes, among other potential possibilities. Therefore, an architecture was designed to handle the following types of data.

4.3.1.1 MTConnect

Information about the machine's operations, state, and current position was collected through the MTConnect protocol. The MTConnect protocol is standardized "semantic vocabulary for manufacturing equipment to provide structured, contextualized data with no proprietary format" [12]. The initial version of the MTConnect protocol was released in October of 2009, and subsequent iterations have been released every 1-3 years. Since inception, the MTConnect protocol has been expanded to communicate information from a variety of machine tools including mills, lathes, and hybrid machine tools.

Information provided by the MTConnect protocol begins on the machine's control system in normal motion planning operations. This data is periodically provided to the

MTConnect Adapter. The adapter formats the data into proper structure and makes it available to the MTConnect Agent. The agent is responsible for responding to requests from application clients who wish to receive the machine's current status. This process is displayed in Figure 53 [12].

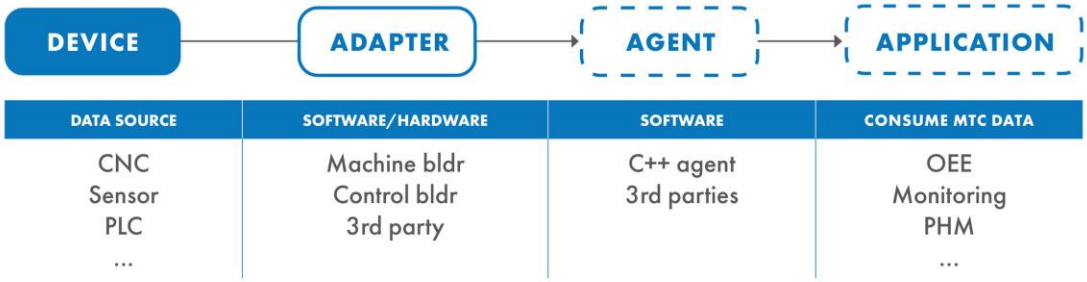

Figure 53: MTConnect Information Flow [12]

There are two primary methods to request data from the MTConnect agent, through polling and streaming. In a polling mode of operation, the client application requests new information from the agent on a periodic basis. For each update, a new request must be sent, acknowledged, and returned. In the streaming option, new information is sent to the client application when it is available at the agent. Polling was used for all MTConnect information in this research to capture all variables at a pre-determined frequency. After polling the machine, the MTConnect information is returned formatted in an eXtensible Markup Language (XML) file. This XML file can be subset for information of interest.

For this research, a select set of 35 MTConnect variables were included in analysis. These variables are presented in Table 3.

Table 3: MTConnect Variables from Mazak VC-500A/5X AM HWD

Category	Variable	Units or Format
Position	X Absolute	mm
	Y Absolute	mm
	Z Absolute	mm
	B Absolute	deg
	C Absolute	deg
	X Workpiece	mm
	Y Workpiece	mm
	Z Workpiece	mm
	B Workpiece	deg
	C Workpiece	deg
Load	X Load	%
	Y Load	%
	Z Load	%
	B Load	%
	C Load	%
Motion	X Feed	mm/min
	Y Feed	mm/min
	Z Feed	mm/min
	B Feed	mm/min
	C Feed	mm/min
	Linear Feed	mm/min
Override	Feed Override	%
	Rapid Override	%
	Spindle Override	%
System State	Laser Power Command	Watt
	Laser Power Output	Watt
	Timestamp	UTC
	Door	String
	Execution state	String
	Controller Mode	String
	Tool Number	Int
	Line Number	Int
	Line Label	String
	Program Name	String
	Program Comment	String

Although the system timestamp is extracted from the XML file generation time, an additional timestamp is collected for each of the position, feed rate, and laser power variables. This timestamp is more accurate to the sample of that specific datapoint than the XML generation timestamp, due to the way variables are passed between the MTConnect adaptor and agent.

4.3.1.2 Infrared Thermal Images

Thermal images are captures by a FLIR A35 infrared camera. While the camera is capable of capturing images at 30 frames/second, the rate of conduction for most components is an order of magnitude slower. Therefore, thermal images were captured at a rate of 0.5Hz for this research. The A35 camera has a resolution of 320 x 256 pixels and a temperature range of -25°C to 135°C. Images were stored in FLIR's sequence file (.seq) proprietary format. A standard thermal image is displayed in Figure 54.

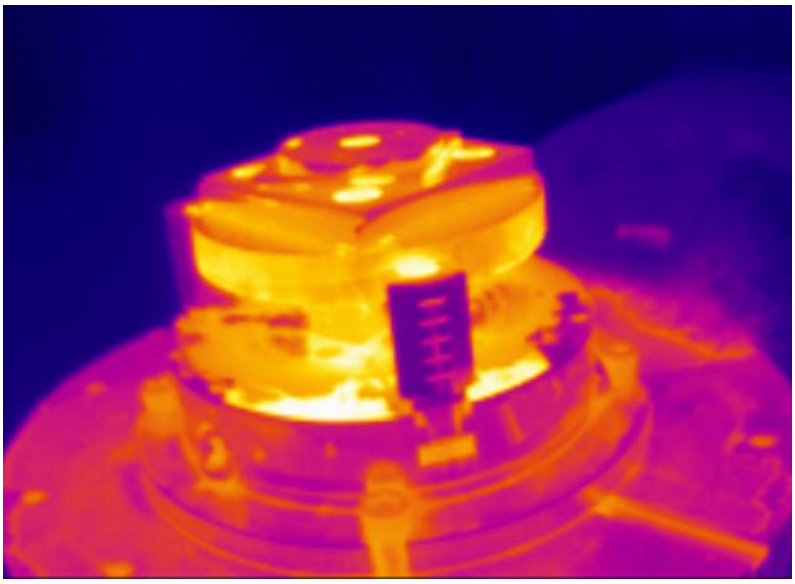

Figure 54: Thermal Image from FLIR A35 Camera

These images were made available to the architecture through networked memory location. The .seq files can be postprocess with open source Python packages. The temperature from ach pixel can be extracted and stored in a common data format. This process is described in section 4.3.2.1.

4.3.1.3 Inspection Data

Inspection data was measured with a Renishaw RMP-60 onboard probing system. Data from the inspection process is stored on the machine in two ways. First, specific inspection points are stored in macro variables that are accessible to the MTConnect protocol. This provides a convenient method of access for a small number of inspection points. Second, the points are also written to a text file that is local to the machine controller. These can be accessed through a network storage system.

For this research, inspection routines were only performed in axial directions. For example, the probe was only instructed to move parallel to the X, Y, or Z axial direction for all points. The inspection location and error from expected location were recorded in the system file.

4.3.2 Architecture Components

4.3.2.1 Summary

An open agent-based architecture for hybrid manufacturing processes was developed. This architecture is capable of capturing, transmitting, and storing the information types and formats discussed in the previous section. The architecture is considered agent-based because each devices connects in one of three configurations, as data producer, a local control unit, or as a supervisor control unit. The architecture is considered open in that any computational unit can connect to the architecture as any of the three roles to produce or consume data as needed, if given the proper credentials. An overview of the connection pattern is shown in Figure 55.

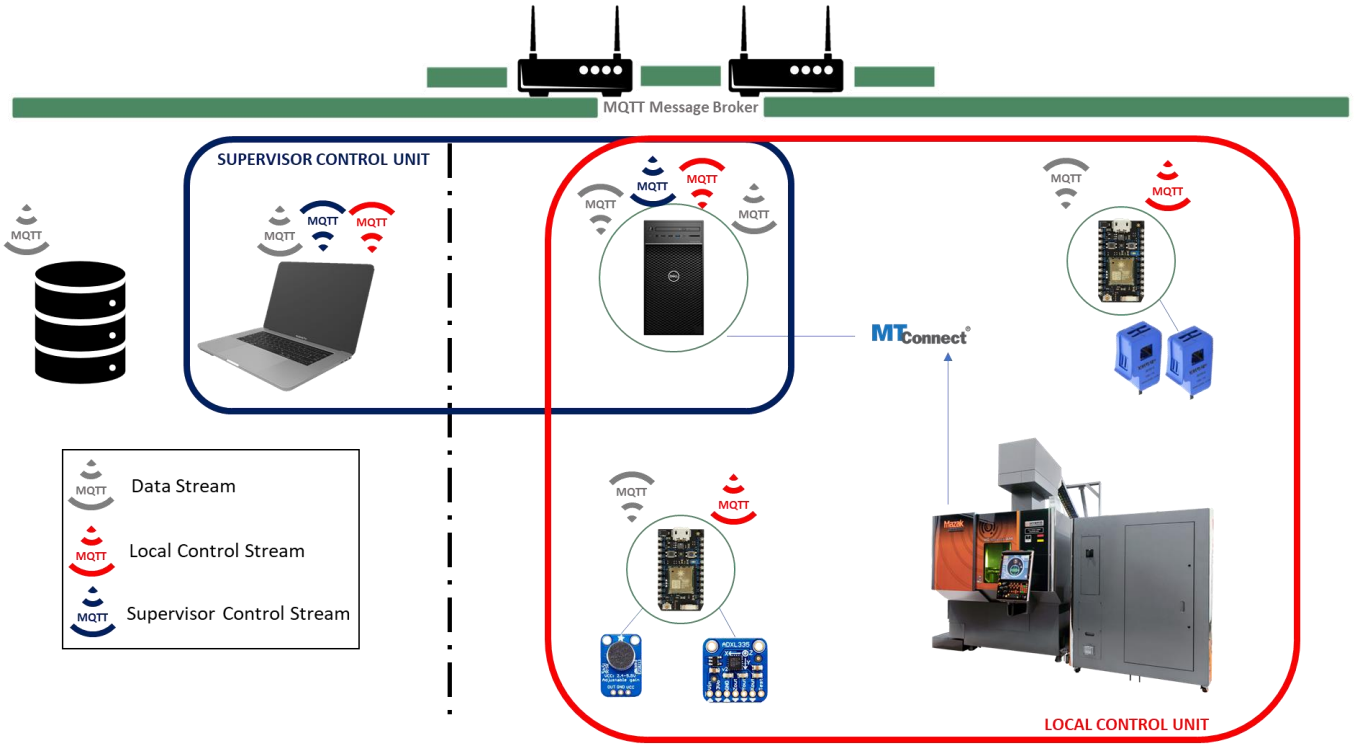

Figure 55: Local Control Unit and Supervisor Control Unit Connections

4.3.2.2 Data Producer

Information about the manufacturing process or environment can be produced at many different points in the hybrid system. A Data Producer (DP) is the first EC device that either (1) measures this information through sensory methods, or (2) captures this information from an information stream inherent to the hybrid machine. The DP node acts as a gateway, measuring or receiving this information and converting it into a common format, before transitioning the data to the local control unit. The data producer is often used to stream discrete values, such as temperature, acceleration, and humidity measurements. The data producer provides all information to the local control unit for further processing. Although it is possible to stream data to any other point in the network (hence, the open network), a specific choice was made to provide a decentralized approach.

Information generated by the data producer can be formatted and transmitted in one of two formats, depending on the measurement size and information type. Measurements of a continuous variable, taken at discrete intervals, are stored in a JSON structure, modified from previous research [71]. Each piece of information is assigned a topic and payload following the convention in Table 4. This structure is designed to handle data from a variety of sources, with different timestamps, and different units or precision, while also keeping a consistent and convenient format for transmission via MQTT.

Table 4: MQTT Payload Specification for Manufacturing Measurements

Field		Description	Format	Notes
	assetId	ID of the machine, sensor, or node generating the data	Integer	
	dateTimeM	Timestamp at time of measurement or data generation	UTC Timecode	
	dateTimeW	Timestamp at time of first gateway receipt, synced with world time.	UTC Timecode	
	dataItemId	Measurement Classification (Xposition)	String	
	value	Data measurement	String	Precision determined by sensor
(optional)	**unit**	Integer corresponding to pr-determined unit (ex. 1=mm, 2=RPM)	String	
(optional)	**optA**	Numerical information	String	
(optional)	**optB**	String information	String	

Measurements of variables in multi-dimensions, such as a thermal field produced by infrared measurements, are converted and stored in the HDF5 format. In effect, this results in an 2D array of values corresponding to temperatures at specific pixels. HDF files can also be sent via MQTT, if they are under a user-specified size limit. In practice, most data generated by a data producer are discrete measurements that can be transmitted via the JSON structure. HDF5 files are more likely generated by processes connected to local control units.

4.3.2.3 Local Control Unit

The local control unit (LCL) is the primary information manager for the hybrid system. It is responsible for collecting, managing, and transmitting data between data producers. The LCL receives information from other data producers, extracts specific pieces for processing, and forwards the information to the larger network. However, the local control unit can also act as a data producer, sampling from the process or recording data from the machine controller when needed. The LCL is the main interface with MTConnect data. Each of the MTConnect variables listed in Table 3: MTConnect Variables from Mazak VC-500A/5X AM HWD is collected, converted, and transmitted by the LCL, as shown in Figure 56.

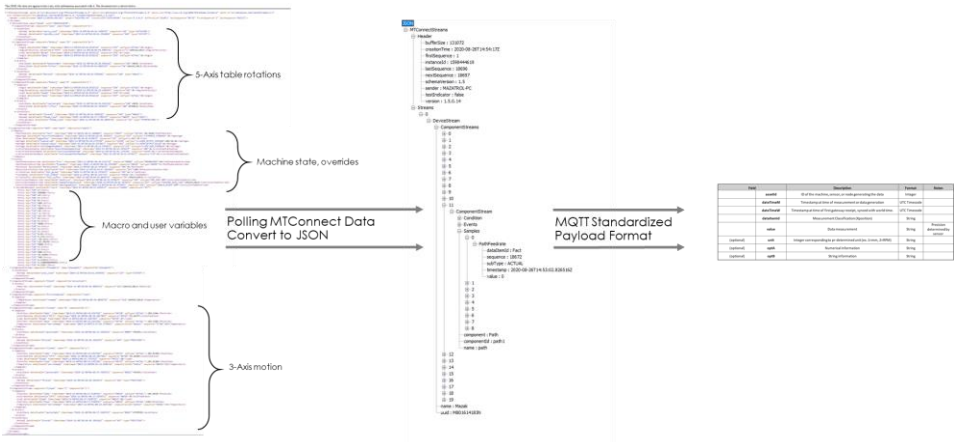

Figure 56: MTConnect, JSON, and MQTT Conversion Flow in LCL

However, the local control unit was designed to support data from any source and link it back to a machine or process. We can accept inputs from almost any output, program, operating software. An example of this is the Local control unit capturing data from the IR

camera and our external sensors while managing the MTConnect stream. This provides us with a thermal image that can be linked to the machine position at a given time.

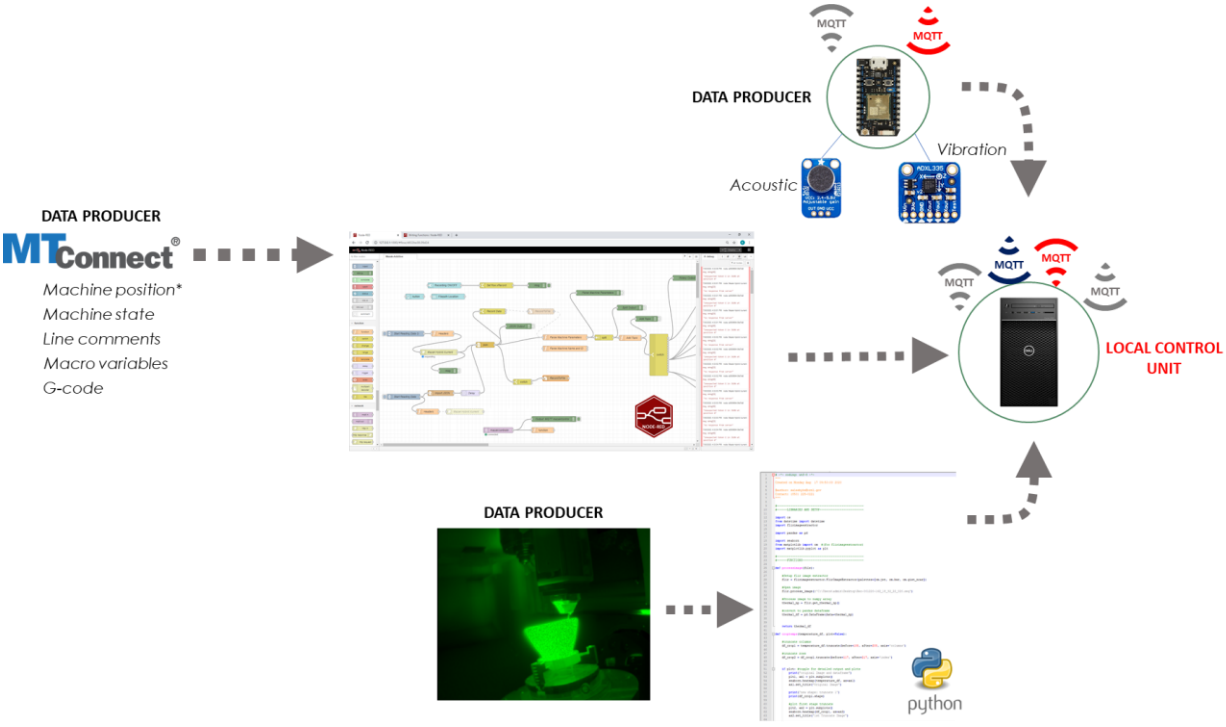

Figure 57: Local Control Unit Information Flow

The Local Control Unit was specifically designed with both data input and output capabilities to support future feedback mechanisms. The development of a feedback mechanisms presented in Chapter 5 are built on this LCL foundation.

4.3.2.4 Supervisor Control Unit

The Supervisor Control Unit (SCU) is a node in the system that is responsible for high-performance computing and intensive feedback analysis. It is distinguished from the LCL due to increased computational, storage, and graphics capabilities. Furthermore, the

SCU does not receive any information directly from DP nodes. It only accepts information from the LCL due to a decentralized communication structure.

The SCU node is intended to provide more in-depth analysis for more accurate corrective actions in the process. LCL units are often standard desktop computer, limited by memory and storage constraints. The SCU enables connections to a larger system that can be leveraged to analyze large data sets that are otherwise impractical for analysis at the LCL node. Furthermore, the SCU controls an overriding command stream, detailed in the following section, to superseded any commands given by the local control unit to the manufacturing system based on the results of its analysis.

4.3.2.5 Control Command Architecture

There are two parallel MQTT streams for control commands. The first is a Local Control Stream (LCS) is intended to pass commands between the local control unit and any sub-nodes that are producing information. This is particularly useful when dealing with low-cost sensors spread around the machine, collecting measurements as DP nodes. From this control structure, we can change the sampling parameters, change operational modes, or check the status of sub-nodes in the system.

The second parallel MQTT stream is the Supervisor Control Stream (SCS). This stream allows for feedback from a node that is outside the primary system of the machine. The supervisor control unit can connect to the local control unit to provide high-level direction, information, or updated instructions. The supervisor control computer and stream were setup to mimic a shop supervisor. This allows the local control unit to handle

operations for analysis of the right scale but provide an opportunity to increase analytical and computational power when needed.

4.3.2.6 Data Historians

Data Historians (DH systems) for archiving manufacturing information are included as a fourth class of device nodes. DH systems can be used to temporarily store files related to a single component, or information collected over multiple production runs. Common formats for data historians are SQL databases that insert MQTT messages into matching relational tables. Although historians are not the focus of this research, they provide power opportunities for future creation of a Digital Passport during the fabrication of an arbitrary hybrid component.

4.3.3 Compression Analysis

The architecture presented in Section 4.3.2 was used to collect data throughout the experiment performed in Chapter 3 – Phase I. A significant roadblock in the usage of data for process analysis is the size of data collected for a single component. There is a significant need to provide mechanisms for data compression to efficiently transmit and store manufacturing information. This capability is a keystone in successful industry adoption of component certification technologies.

A subset of data collected in Chapter 3 experiments was used to evaluate compression mechanisms for efficient transmission and storage of Hybrid manufacturing data. The datasets used are listed in Table 5.

Table 5: Datasets for Compression Analysis

Dataset	Type	Motion	Operation	Filesize (Mb)
1	Subtractive	2.5-Axis	ISO-10791-7 Standard Subtractive Machining	380.6
2		3-Axis	Organic Surface Geometry Subtractive Machining	318.7
3		5-Axis	Turbine Blade Subtractive Machining	130.4
4	Additive	3-Axis	Organic Suface Geometry Additive Toolpath	1194.2
5	Hybrid	3-Axis	Organic Surface Geometry Additive and Subtractive Toolpath (Dataset 2 and 4 combined)	1287.4

Each of the datasets chosen were designed to provide a representative sample of the different process within hybrid manufacturing. Three categories of datasets were used, subtractive processes, additive processes, and hybrid processes.

Three datasets were chosen to represent subtractive machining, subtractive toolpaths from the ISO-10791-7 Standard geometry experiment, operations from the organic surface geometry experiment, and operations from subtractive machining of a mock geometry high-pressure turbine blade. One dataset was chosen to represent additive deposition, additive operations from the organic surface geometry. Two of the previous datasets were combined to represent Hybrid processes, the additive and subtractive operations from the organic surface geometry.

Each of these datasets were saved in two different formats for analysis:

Format 1: Raw MTConnect Data - The full MTConnect XML output was captured and converted to a JSON format. This results in one complete JSON structure for each sample of data. Every sample was stored on a single line in a text file with ASCII formatting.

Format 2: CSV MTConnect Data Subset - The MTConnect output was process with the method described in Section 4.3.1.1. A total of 35 MTConnect variables

were extracted and stored in a Comma-Separated Value (.csv) format with ASCII encoding. Each line of the .CSV format corresponds to a single sample of the concatenated 35 variables. The resulting file was used as the compression dataset.

Each of these datasets in both storage formats were compressed with five common compression algorithms. The algorithms were evaluated by compression speed and ratio to determine the most appropriate method for each process. The selected algorithms are presented in Table 6.

Table 6: Compression Algorithms

Acronym	Full Name	Type	Initial Release
GZIP	GNU GZIP Algorithm	Lossless	1992
ZLIB	ZLIB Algorithm	Lossless	1995
LZMA	Limpel-Ziv-Markov Chain Algorithm	Lossless	1996
BZ2	BZIP2 Algorithm	Lossless	1996
LZ4	LZ4 Algorithm	Lossless	2011

Most algorithms offer a user-selectable tradeoff between compression speed and compression rate. For these tests, all algorithms were set at the maximum level of compression to provide an equal comparison.

4.4 Results

4.4.1 Architecture Evaluation

The architecture described in section 4.3 was successfully implemented with a Mazak VC-500A/5X AM HWD hybrid machine. The architecture included a local control unit, supervisor control unit, and data producers with auxiliary sensors. A total of five experiments were performed to evaluate the architecture. The first experiment was a simple

investigation and demonstration of the dynamic sampling characteristics of the architecture, detailed below. A primary goal of the architect is to provide a foundation for adaptive feedback control of the hybrid manufacturing. Thus, the remaining four experiments are detailed in Chapter 5.

The first experiment conducted on this architecture implementation was designed to investigate and demonstrate dynamic data collection capabilities. The goal of this experiment was to verify the dynamic sampling mechanisms of the architecture components. An example program was setup on the Mazak Hybrid to serve as the manufacturing operation. The experiment was conducted as follows:

1. Local Control Unit (LCU) monitoring Mazak under low data rate state via MTConnect. Minimal data recording during operation pause.
    a. LCU polling current status every 0.5 seconds.
    b. LCU watching for “ACTIVE” command via MTConnect to trigger high data rate sampling
    c. Once triggered, LCU send notification to Supervisor Control Unit (SCU) for measurement decision
2. SCU enables high data rate capture settings
    a. SCU sends command to LCU to enable high data rate sampling
    b. SCU sends command to Photon 1 (Accelerometer) to enable high data rate sampling
3. Data capture continues for duration of manufacturing operation
4. LCU monitoring Mazak via MTConnect for end of cycle

    a. LCU watching for “READY” command signifying the end of the cycle
    b. LCU sends notification to SCU
5. SCU disables standard capture settings
    a. SCU sends command to LCU to disable high data rate
    b. SCU sends command to Photon 1 (Accelerometer) to disable high data rate capture
6. LCU returns to monitoring Mazak under low data rate state via MTConnect.

The results of the experiment indicate a successful execution of the architecture’s dynamic data collection system. After a period of in activity, a user began the example program. The LCU correctly identified the start of operations and notified the SCU, which in turn triggered the high data rate sampling characteristics. Machine process data and accelerometer data was collected accordingly, displayed in Figure 58.

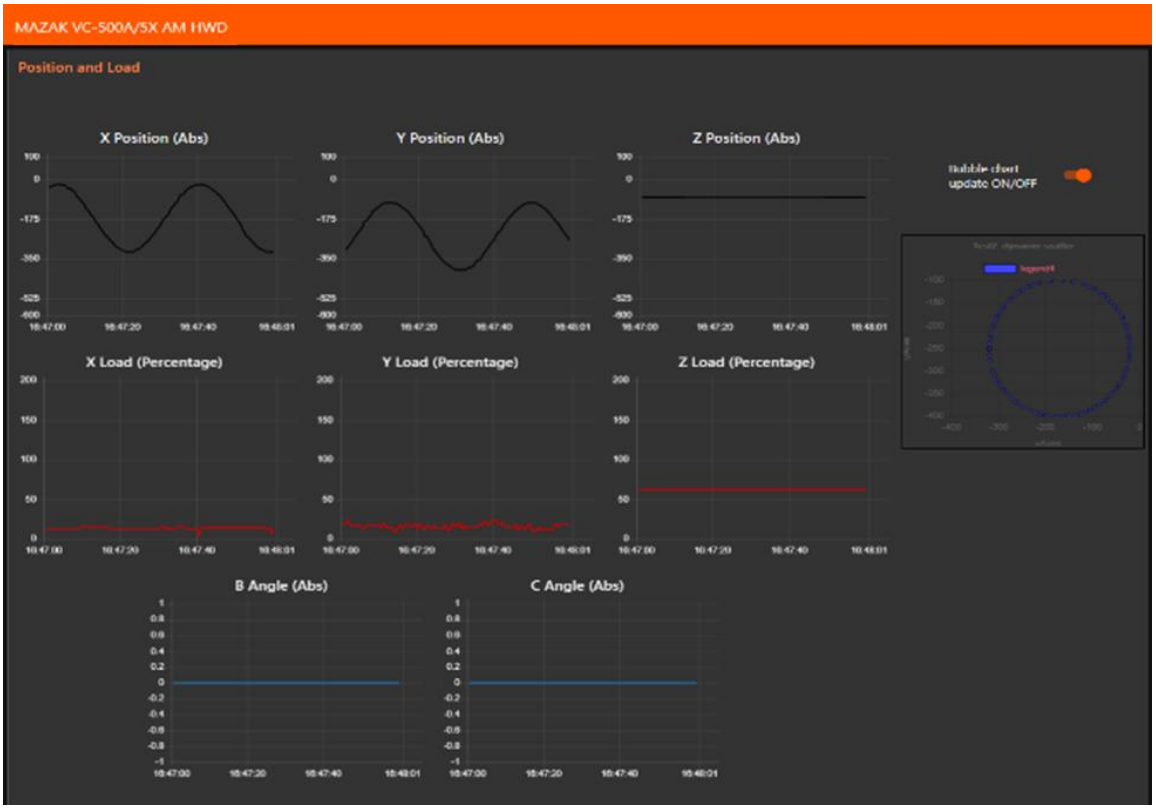

Figure 58: LCL displaying process data from Mazak hybrid system

FFT analysis was conducted on the accelerometer data. Two peaks at approximately 70 Hz and 190 Hz are observed in the frequency spectrum. The 70 Hz frequency corresponds to a spindle speed of 4200 RPM. The nominal spindle speed set by the program was 4000 RPM, confirming this result when accounting for error and operator override. The 190 Hz frequency corresponds to a rotational speed of 11,400 RPM, which is above the maximum spindle speed of the machine. Upon closer inspection, the accelerometer was placed on the machine casting near a cooling fan. 11,400 RPM is a reasonable speed for the fan frequency and large amplitude to its operation during the process.

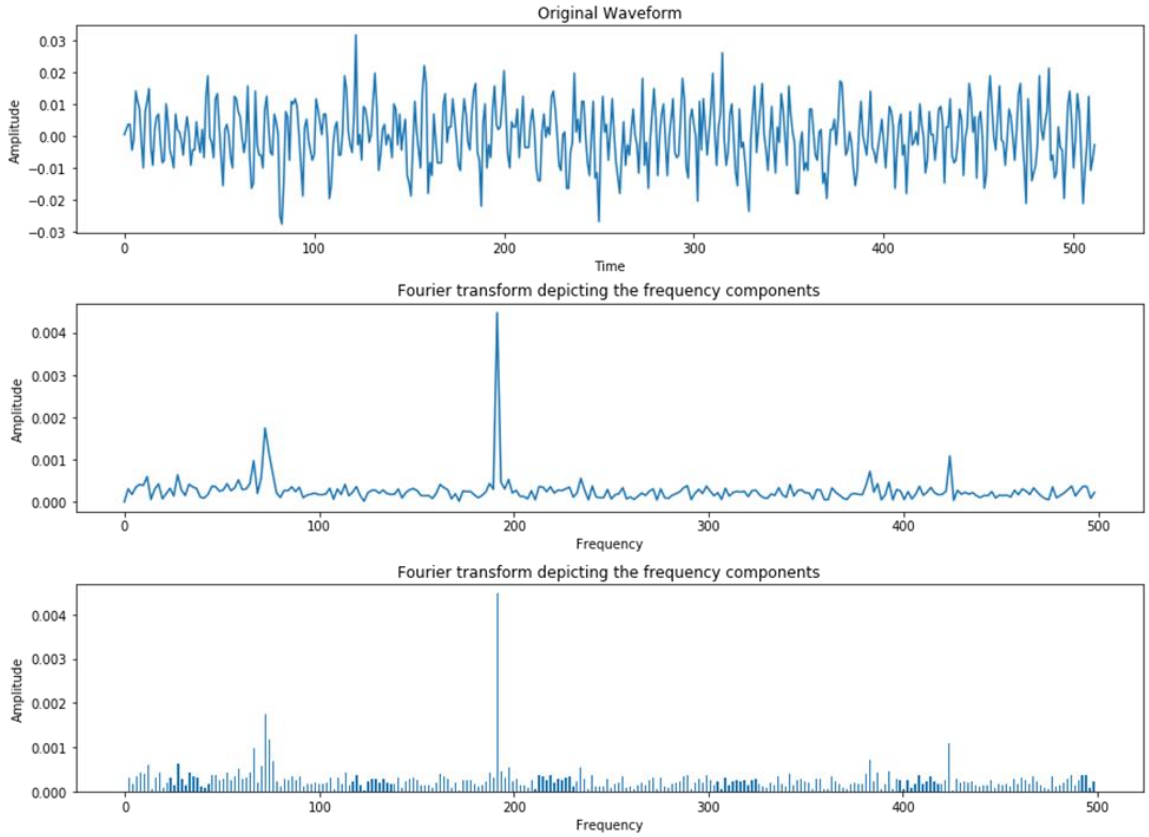

Figure 59: FFT analysis of accelerometer data

The successful implementation of an adaptable architecture for dynamic sampling parameters was demonstrated. A control mechanism was implemented to allow both Local Control Units and Supervisor Control Units to modify the data collection parameters on the fly. This capability provides a foundation to collect, analyze, and transmit data with dynamic sampling parameters as local and supervisor control structures adapt to current monitoring needs. The result of this work will enable significant improvements in the manufacturing process including analysis driven machine actions and machine feedback control mechanisms.

4.4.2 Compression Analysis

Each of the five datasets were evaluated against the five compression algorithms. Both raw MTConnect data and subset MTConnect data were evaluated to determine any differences in the resulting compression ratio and compression time.

The LZMA algorithm demonstrated the lowest compression ratio (highest amount of compression) out of the five algorithms evaluated for raw MTConnect data. An average compression ratio of 0.004 (0.4% of original file size) was achieved across all five datasets. However, it also required the greatest amount of time to achieve this level of compression in all cases. It is noted that all other compression algorithm performed within the same range of each other with respect to compression range across all datasets. The maximum difference in compression ratio between any two algorithms and datasets is between the ZLIB algorithm compressing the subtractive 5-axis dataset and the LZMA algorithm compressing the Additive 3-axis dataset, resulting in a difference of 0.016 in compression ratio. All compression algorithms achieve a compression ratio of 0.02 (2% of the original dataset size) or better, displayed in Figure 60.

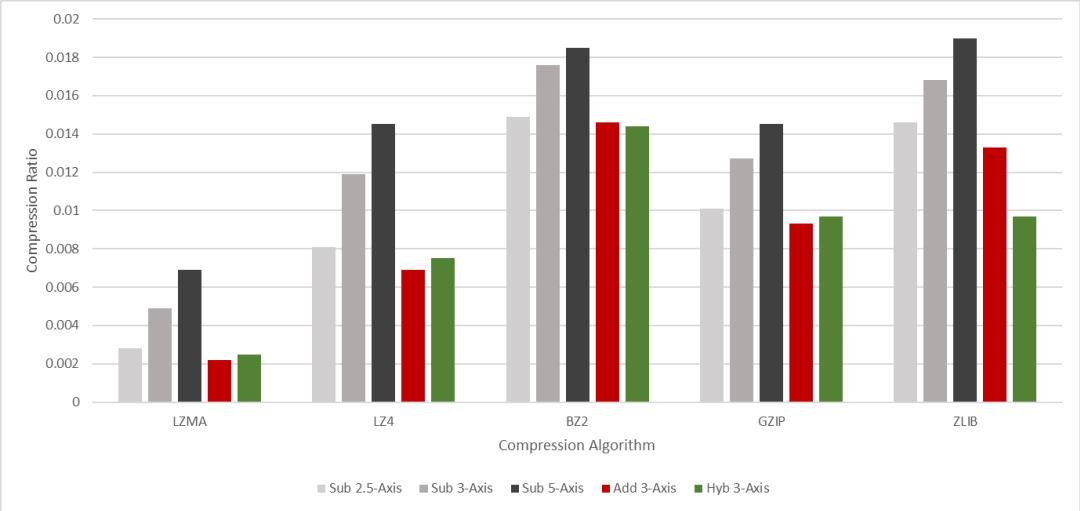

Figure 60: Raw MTConnect Compression Ratio

Although all compression algorithms performed reasonably well on Raw MTConnect data, there was a significant difference in computational time. While the LZMA algorithm outperformed the other algorithms in compression ratio, it took two orders of magnitude longer to reach that level of compression. The average compression time across datasets from all processes was 116 seconds. The maximum compression time was 225 seconds while compressing the Hybrid 3-axis dataset. The LZ4 and ZLIB algorithms were the best performing with respect to compression time, resulting in an average compression time of 3.72 seconds and 3.97 seconds, respectively. A summary of the compression times are displayed in Figure 61 and Figure 62. Note a different scale is presented in Figure 62 to easily compare the top performing algorithms.

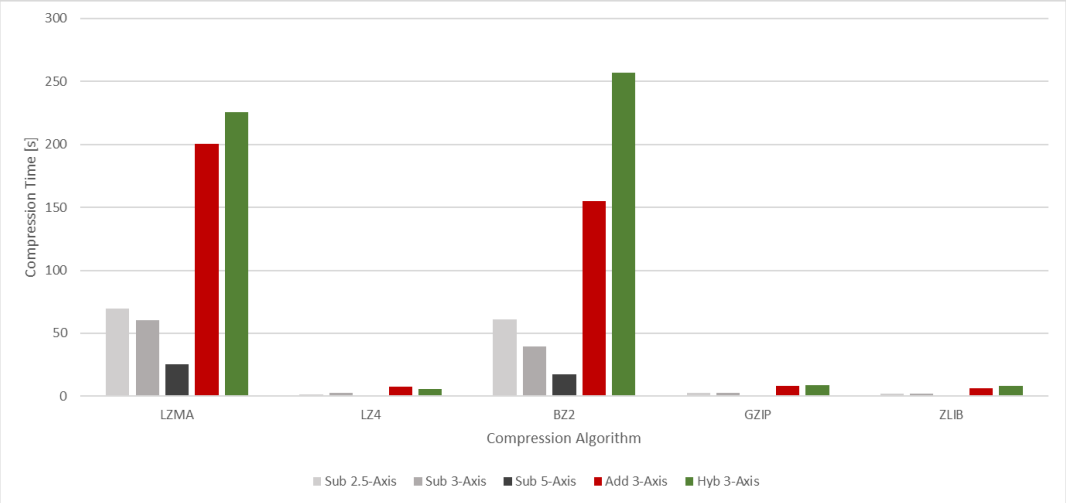

Figure 61: Raw MTConnect Compression Time – All algorithms

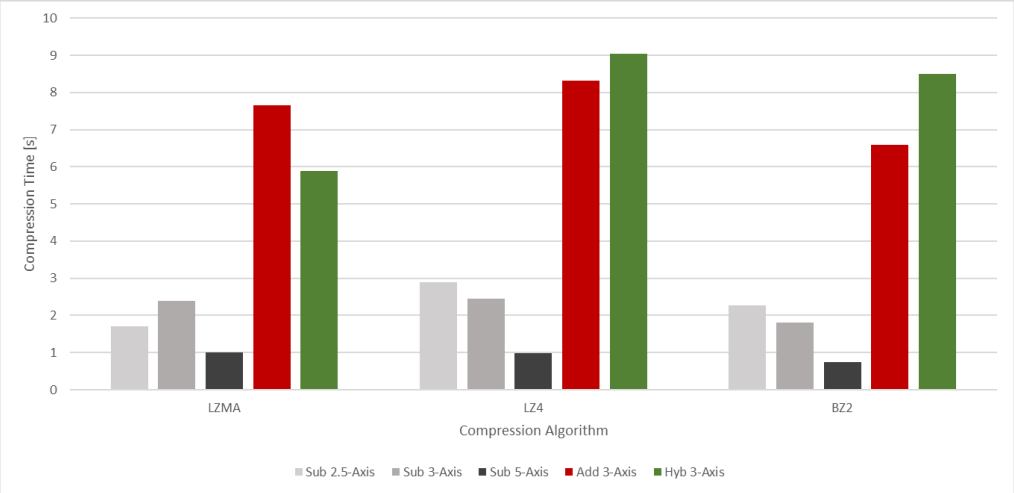

Figure 62: Raw MTConnect Compression Time – Top Algorithms

A common method of evaluating compression algorithms is to determine the relationship between compression ratio and compression time for datasets of different sizes and formats. From this plot, optimal datasets for each algorithm can be identified. The top

performing algorithms for time and compression ratio with raw MTConnect data (LZMA and LZ4) are displayed with scatter plots in Figure 63 and Figure 64.

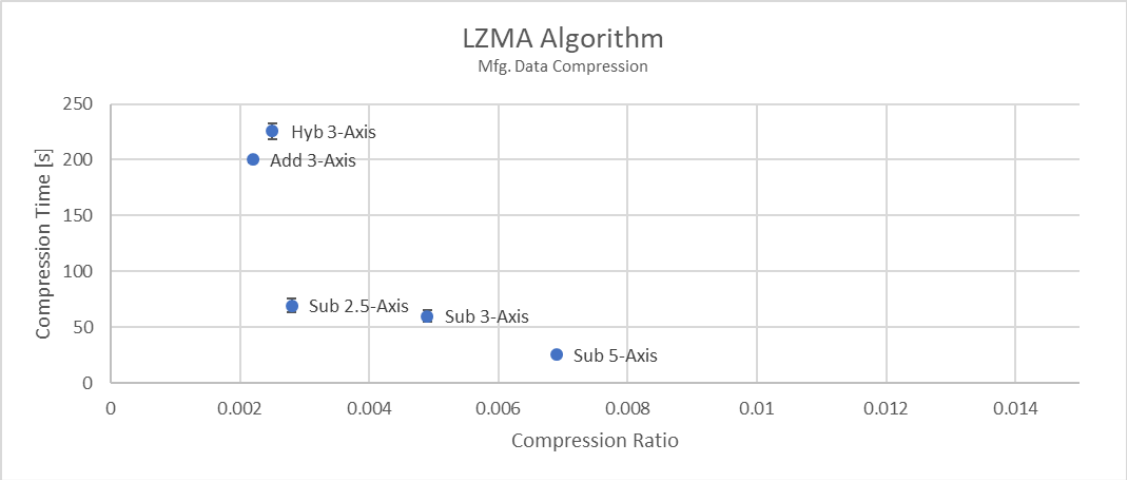

Figure 63: LZMA Algorithm – Compression Ratio vs. Compression Time for Raw MTConnect Data

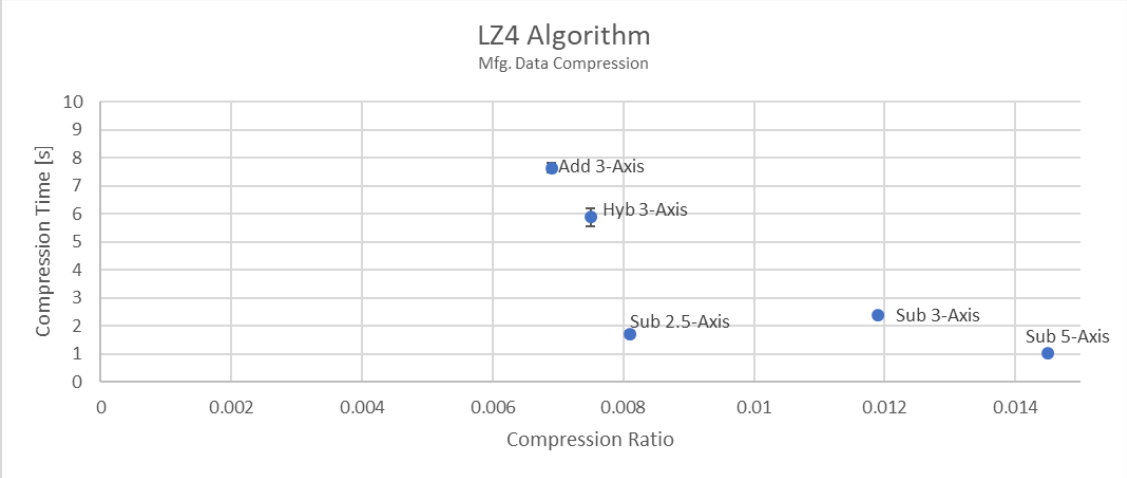

Figure 64: LZ4 Algorithm – Compression Ratio vs. Compression Time for Raw MTConnect Data

For both algorithms, the subtractive 2.5-axis dataset struck the best balance between final compression ratio and compression time. Surprisingly, any data set that included additive operations resulted in higher compression times, but lower compression ratios. This may

be attributed to the layered nature of additive toolpaths, where there is significant repetition in Z values for discrete layers. As repetition enables higher compression, these processes stand in contrast to subtractive 5-axis tool paths where each motion variable is constantly changing, which resulted in a higher compression ratio.

The same experiment was performed with subset MTConnect data, where significant variables were extracted from the initial MTConnect XML file and stored as a concatenated CSV string. The results are displayed in Figure 65 and Figure 66.

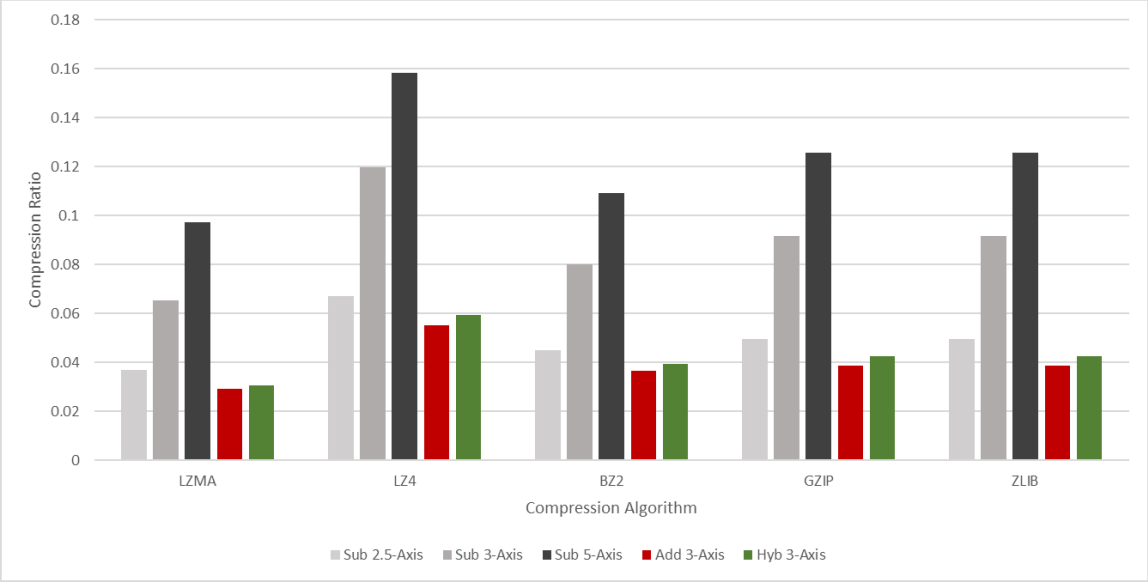

Figure 65: Subset MTConnect Data Compression Ratio

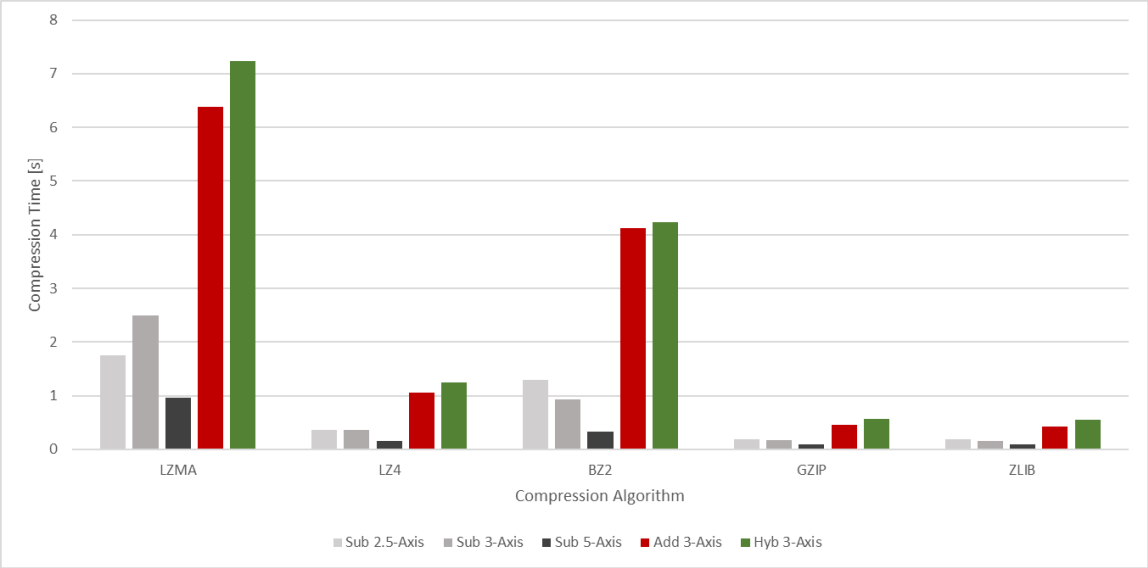

Figure 66: Subset MTConnect Data Compression Time

The subset MTConnect data provided a more equal distribution of results for compression ratio and compression time. The ZLMA algorithm once again provided lowest compression ratio. While the time required was still greater than all other algorithms, all compression times were the same order of magnitude. Additionally, The GZIP and ZLIB algorithms outperformed the LZ4 algorithm with respect to time.

A less significant tradeoff between compression time and compression ratio was observed in this experiment. Noted above, final compression ratios from all algorithms were comparable. The maximum span in compression time was less than 6 seconds between compressing subtractive 5-ais data with the GZIP algorithm and compressing hybrid 3-axis data with the LZMA algorithm. Therefore, there is less benefit to optimizing the choice of compression algorithm with this dataset format. It is hypothesized that the significant reduction in initial file size affected the results.

4.5 Discussion and Limitations

The results of this research provide a methodology for designing, implementing, and evaluating a multi-agent architecture for manufacturing processes.

Additionally, the research results in a process that can be used on an arbitrary computational unit in the multi-agent architecture to determine the best compression method for this system, given a representative dataset. It is noted that the computer processor and available RAM play a significant factor in this experiment. While these results are valid for the specific system on which the experiment was conducted, they are expected to vary significantly from system to system. Additionally, it is interesting to note that while the compression time differ slightly for each iteration of the compression experiment, the resulting compressed file was identical in size and ratio for each iteration. This is attributed to the deterministic nature of lossless compression methods.

It is also acknowledged that decompression speed is an important factor in selecting the most appropriate algorithm for efficient storage and transmission of manufacturing data. An intentional decision was made to defer this research as computational units in EC and FC layers are more often limited by processing power and RAM storage. However, the LCL nodes and SCL units who receive the information (and therefore are responsible for decompressing it) typically have more processing capabilities. Therefore, an argument can be made that decompression rate is not as significant as compression rate due to increased computational power.

Finally, it is acknowledged that there are countless methods of data pre-processing and formatting that can significantly influence the results of this research. For example, a

design choice was made to evaluate compression batch files, datasets that describe the complete process from start to finish. There is a significant body of research to evaluate incremental compression of information streams that was not considered in this research. Furthermore, information stream compression often relies on lossy data post processing methods, invalidating one of the foundation assumptions that each piece of information must be preserved. Future work remains to investigate these methods and applications to manufacturing data.

4.6 Conclusion

The successful implementation of an adaptable architecture for dynamic sampling parameters was demonstrated. A control mechanism was implemented to allow both Local Control Units and Supervisor Control Units to modify the data collection parameters on the fly. This capability provides a foundation to collect, analyze, and transmit data with dynamic sampling parameters as local and supervisor control structures adapt to current monitoring needs. The result of this work will enable significant improvements in the manufacturing process including analysis driven machine actions and machine feedback control mechanisms.

CHAPTER 5. PHASE III – FEEDBACK METHODS FOR ADAPTIVE PROCESSING

Hybrid manufacturing systems provide unparalleled manufacturing flexibility by combining additive and subtractive capabilities within the same build chamber. However, numerous challenges exist to fabricating components to geometric specifications on the first attempt. Effects such as geometric distortion, thermal overheating, and losses in efficiency have been well documented [19]. While these effects can be mitigated with iterative testing, commercial operations demand a repeatable process with reliable results on the first attempt. This phase of research explores and develops closed-loop control mechanisms for commercial hybrid manufacturing systems, enabling dynamic processing conditions.

5.1 Introduction

Feedback control is a fundamental field of science and engineering. The ability to recognize deviations from a desired path, determine the appropriate amount of corrective action to take, and executive the compensation is common to countless applications within electrical, mechanical, and chemical engineering. Although there are many types of control systems, schemas, and methodologies, a few commonalities exist. Simple process controllers can be classified into two main categories: open-loop control (without process modification) and closed-loop control (process monitoring and modification). Hybrid manufacturing systems provide a unique platform where standard open-loop control is used to drive processes that demand close-loop control. This body of work results in a method

for discrete, *in-situ* closed-loop control of commercial Hybrid CNC systems to enhance resulting components.

5.2 Literature Review

5.2.1 Control systems

An open-loop control system is defined as one where "the output has no effect on the control action" [72]. These systems are prevalent in many household electronics, automotive devices, and even manufacturing equipment. Open-loop control systems rely on a setpoint to determine the resulting system outpoint, displayed in Figure 67. While the operator can manually adjust the setpoint, the system itself has no capabilities for self-regulation to account for disturbances that change the ultimate output.

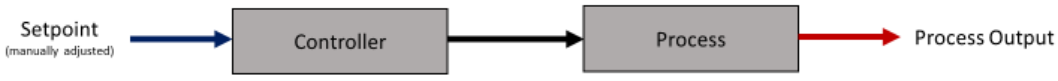

Figure 67: Open-Loop Control System

Standard manual subtractive mills and lathes can be represented as open-loop systems. The operator enables the spindle before manually adjusting the position to the desired point. Each change in action must be driven by the operator. Modern CNC systems developed as part of the 3rd industrial revolution (focusing on automation), implemented feedback mechanisms for motion planning [1]. This resulted in closed-loop control systems, defined as a system "that maintains a prescribed relationship between the output

and the reference input by comparing them and using the difference as a means of control" [72]. Motion and control systems developed in pursuit of automation are well studied and understood. In the simplest configuration, a sensor monitors the process output, computes necessary correction actions, and updates the input accordingly. A standard form of closed-loop control is displayed in Figure 68.

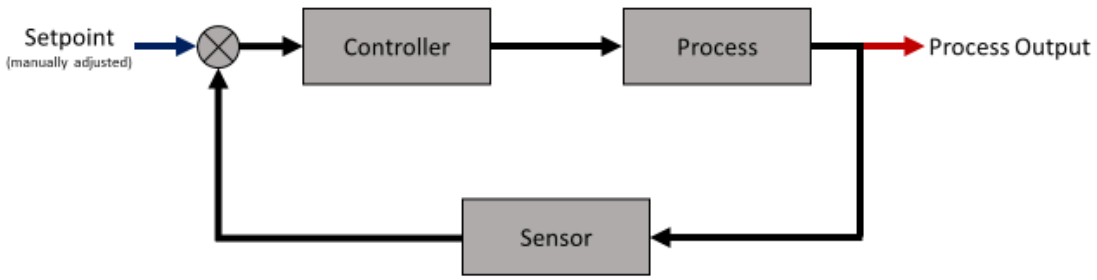

Figure 68: Closed-Loop Control system

These systems have been implemented in commercial machining equipment as early as the 1940's with the invention of CNC machines by John Parsons [73]. However, while closed loop control systems are used for motion control, they are not used for system and process control.

5.2.2 Hybrid Manufacturing

Modern CNC systems are notoriously repeatable and reliable systems. They are designed to execute precision motion paths with minimal positional error. These commands are provided by G-code, a text-based low-level programming language that describes incremental motion positions. While extremely advanced low-level closed-loop

control systems exist for the motion planning within a CNC system, there is no commercial method to dynamically control the overall process. Commercial CNC machines rely on the operator to manually update the g-code when new instructions are required.

This mode of operation is sustainable for a subtractive machining paradigm, where stock is within defined tolerances and the same component is fabricated thousands of times. However, the inclusion of additive capabilities in Hybrid CNC machines drives a need for enhanced process control.

Additive processes are often plagued with geometric errors due to overbuilding or underbuilding. Feldhausen demonstrated that significant distortions can occur during the hybrid process as a result of repeated heating and cooling cycles [19]. Feldhausen also demonstrated that there is not a single set of processing parameters for arbitrary geometries. Appropriate processing parameters are dependent on material, substrate, and geometry. These parameters may require adjustment over time to account for machine wear, decay, and other environmental factors. Hybrid CNC systems provide a unique opportunity to account for geometric errors due to the combination of additive and subtractive capabilities within a single system.

Other benefits can be achieved through closed-loop control of hybrid manufacturing processes. Thermal overheating is often experienced with thin-wall structures. Higher power for material deposition is needed when the build begins to heat the substrate. Once the substrate reaches thermal equilibrium, the power can be reduced to prevent overheating. While thermal time constants can be simulated for pre-programmed power modulations, environmental factors and machine error prevent complete accuracy of the model. A

method of feedback control is required to sustainably leverage hybrid manufacturing processes. Development of a closed-loop control system for commercial hybrid CNC systems will increase their repeatability and improve industry adoption.

5.3 Methodology

This section details the methodology used to design and investigate a method for discrete feedback control of a commercial Hybrid CNC system for commercial hybrid manufacturing systems. An evaluation of the current information input and output pathways is conducted. The resulting communication pathways are investigated for dynamic control mechanisms. Finally, three methods of control are designed for different time scales. The resulting techniques are implemented and leveraged for dynamic process control of three experiments, two additive experiments and one subtractive experiment.

5.3.1 Information Input and Output

An evaluation of the information input and output (I/O) capabilities was conducted for Mazak's VC-500A/5X AM HWD hybrid vertical machining center (Mazak hybrid system) [8]. A significant amount of data output opportunities exists for this system, as described in depth in Chapter 3, Phase 1. Information available directly from the controller consists of process monitoring data through the MTConnect protocol [12]. This information includes current machine position, state, macro and user variables, and the g-code command currently being executed. An I/O diagram is displayed in

Figure 69.

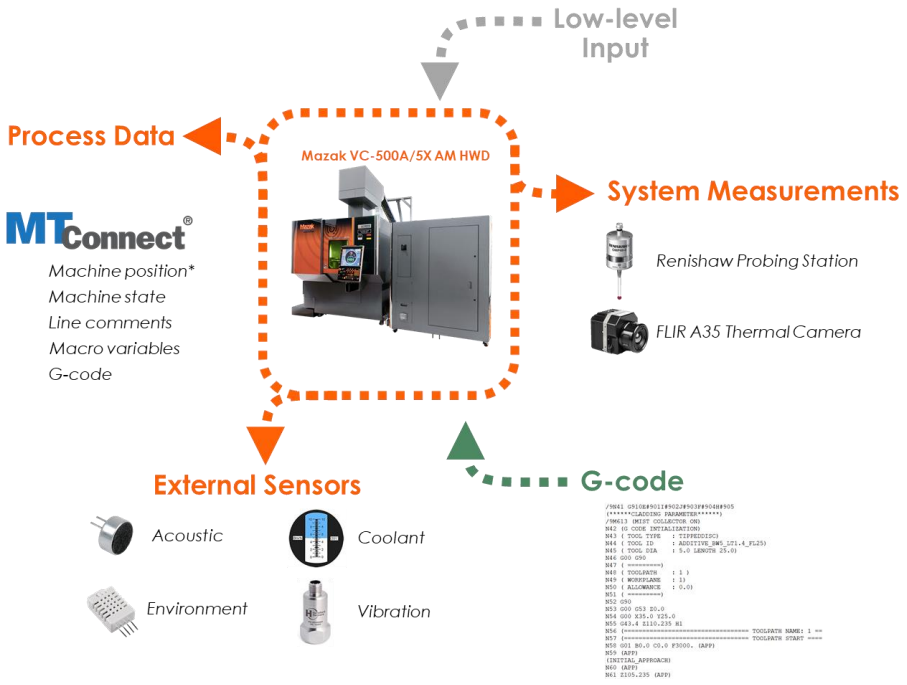

Figure 69: Information input/output diagram for commercial hybrid manufacturing systems

Additional information sources are available from external systems, retrofitted on the hybrid system. Many modern machining centers include a geometry inspection suite. The Mazak hybrid system includes a Renishaw RMP-60 probing system with Renishaw's Set and Inspect software [24]. Thermal monitoring systems are often used in additive manufacturing monitoring systems. A FLIR A35 camera was included to provide thermal information *in-situ* [74].

Although numerous information output sources are present, very few information input pathways exist. The primary pathway for information input is through G-code, a set of text-based instructions that commands machine motion. G-code is described in depth in Chapter 2, Phase I. CNC machines are designed to run repeatably, time and time again, without any input. Most machine tool manufactures go to great lengths to prevent

disturbances or outside influences from changing the process, aside from static, fixed, and pre-compiled G-code. While this information setup is logical in a subtractive-only paradigm, it is not scalable for additive or hybrid manufacturing.

It must be noted that one other low-level information input pathway exists. Many commercial CNC systems utilize a combination of non-real time systems for the HMI system, with real-time system for motion control. This enables the opportunity to overwrite selective memory locations to affect the current process actions. This approach typically requires support from the machine tool manufacture for safe implementation. However, this information input pathway has the potential to enable high-speed dynamic feedback processes.

5.3.2 Supporting Architecture for Feedback Control

To sustainably implement feedback methods utilizing the information I/O paths identified above, three major framework components are required. Each of these three components have been described in depth at different sections in this dissertation. The third and final component, feedback methods, is described in this chapter. A short summary of the three components is provided below:

1. A process monitoring architecture is needed to collect data. This architecture captures everything produced on the data input/output slide. This data must be collected, transmitted, synchronized, and stored for efficient analysis. This process is documented in Chapter 4, Phase II.
2. A coordinated analysis process is needed to process and compare data against desired outcomes. Geometric and thermal analysis is needed, depending on the

feedback control application. Geometric analysis methods for hybrid manufacturing are documented in Chapter 3, Phase I. Other supporting software used in this process are open-source python libraries including Pandas, Numpy, and FlirImageExtractor [75].

3. A communication pathway is needed to make actionable changes on the machine. These mechanisms are the core contributions for this chapter. Although implemented and tested on the Mazak hybrid system, they must be applicable to any commercial hybrid manufacturing system.

5.3.3 Levels of Feedback Control

Three levels of feedback control have been developed as a result of this research. These levels are classified by timescale of communication. Actions appropriate for these feedback levels and timescales are displayed in Figure 70.

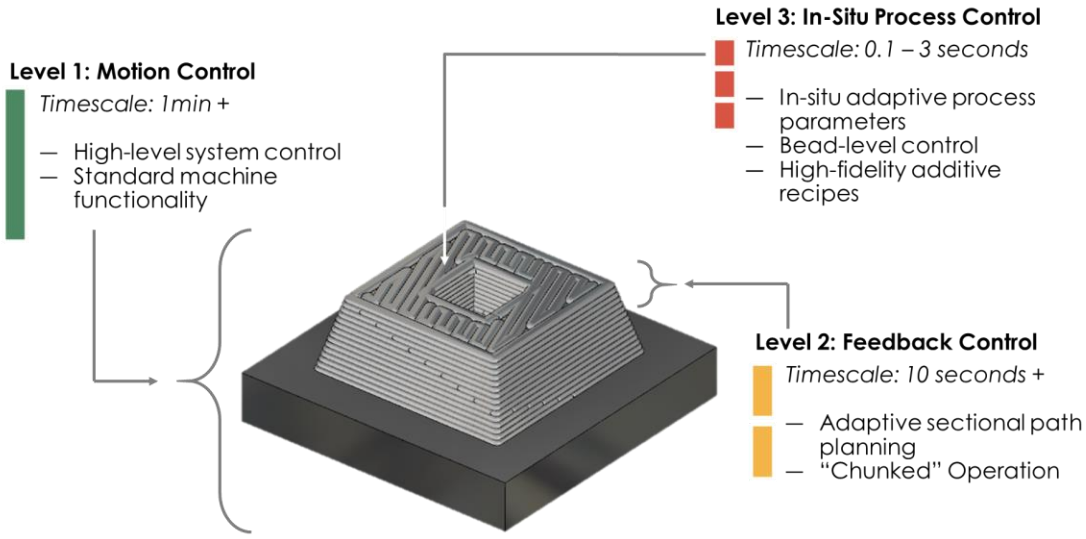

Figure 70: Levels of feedback control with corresponding timescales

Level 1 control is focused on primary machine functions. This control is designed to command any standard machine setup or pre-programmed operations such as tool changes, program file changes, and static G-code programs. Level 1 control operates on a minimum time scale of 10 seconds and greater.

Level 2 control is designed to handle segmented operations. This level of control is applicable to dynamic processes, where a small segment of the desired operations are executed, the status of the process is monitored for desired results, and subsequent sections are modified for any corrective actions. For example, this level of control is appropriate for dynamic layer-by-layer additive operations to change process parameters on the next deposition path. Level 2 control operates on a minimum timescale of 3 seconds. This level of control provides most capabilities that we currently use in dynamic hybrid manufacturing operations.

Level 3 control in designed to handle high-frequency process parameters changes within a single deposition path, such as dynamic laser power, hotwire power, and wire feed rate. Level 3 control is the most difficult, requiring a low-level feedback pathway on the hybrid system. This level of control operates on a minimum timescale of 0.01 seconds. Level 3 control has significant opportunities for future work in controlling material properties during the hybrid manufacturing process, it was not the focus of this research.

5.3.4 Feedback Mechanisms

An analysis of the information input and output pathways was completed to determine possible mechanisms by which machine instructions could be updated. Two key functionalities were identified:

(1) The underlying operating system of the machine controller operates on the Windows 7 platform. This is an embedded system without flourishes reserved for standard desktop systems. However, it retains full standard functionality and networking capabilities.

(2) The MTConnect output of the Mazak hybrid system includes current macro variable values as well as the current line number and in-line comments from current G-code command.

The combination of these two capabilities enables a discrete two-way communication system between the Mazak hybrid machine and an external computer. Since the underlying operating system of the Mazak controller is a windows machine, various memory locations internal and external to the controller can be mapped and networked. This enables a pathway to feed information back into the machine. Furthermore, current values of macro variables can be changed via G-code commands during live operations. This enables a pathway for information output that can be leveraged to signal an external source and request updated instructions. Together, these capabilities allow for discrete updates to the machine's G-code instructions.

5.3.5 Integration with Information Architecture

The multi-agent architecture developed in Chapter 4 – Phase II was instrumental in enabling discrete closed-loop control for the Mazak hybrid system. A Local Control Unit (LCU) was configured to receive MTConnect information produced by the machine. The primary hard drive of the Mazak's controller was networked to the LCL such that the LCL could read and write files in a specific directory. Finally, The LCL was connected with

other external sensors as documented in Chapter 4 – Phase II. The enabled a connected feedback loop, where the LCL could read the current status of the Machine via MTConnect and transfer updated G-code to the machine via the networked hard drive. A diagram of this configuration is shown in Figure 71.

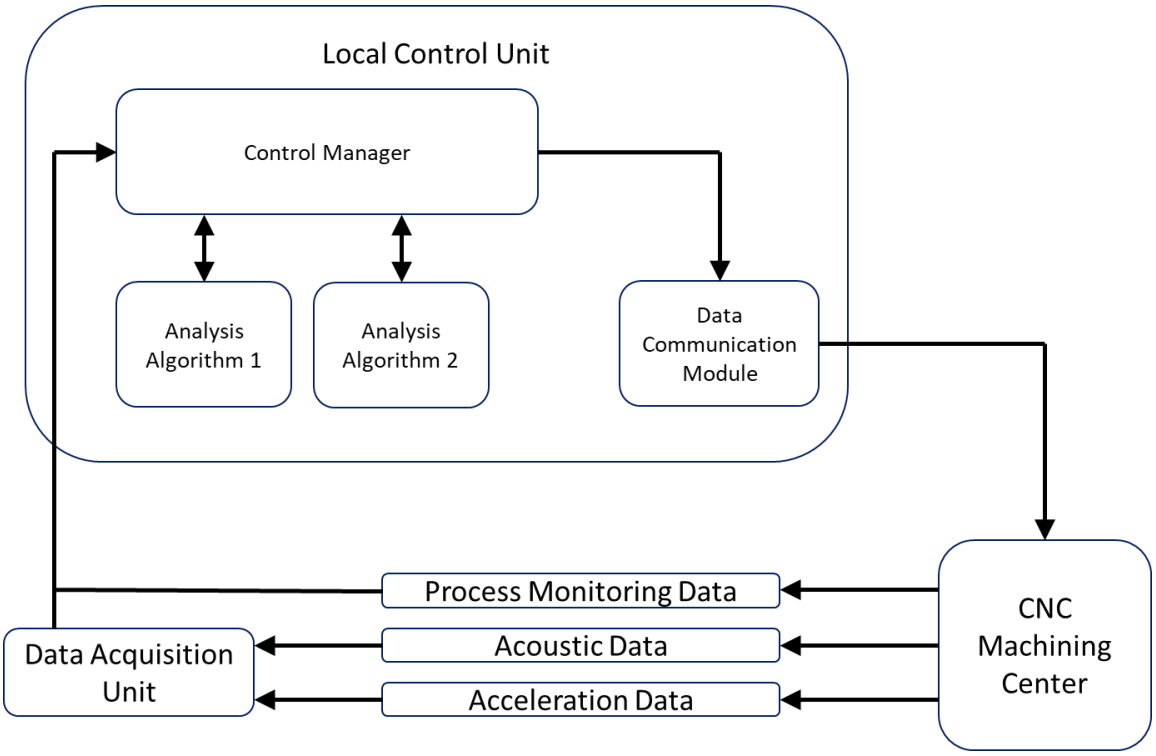

Figure 71: System setup for feedback communication with local control unit

Two G-code programs were used to operate the CNC machine, a primary control program and a sub-program. The primary control program was enabled by the user. This program set appropriate macro variables to signal that the Mazak machine had entered closed-loop control mode. A variable delay was used to provide computation time for the LCL. The LCL polled the macro variable's status at a rate of 2 Hz. When the variable signalled closed-loop control mode, the LCL transferred a new set of instructions to the networked memory location on the Mazak controller's hard drive. This new set of instructions can

include any commands enabled by standard G-code. After the delay expired, the controller entered the sub-program and executed the G-code statements. Finally, the sub-program returned to the main program, and the flag was reset to indicate that updated instructions were requested. This loop completes until a termination signal is given by the LCL. A timing diagram is provided in Figure 72.

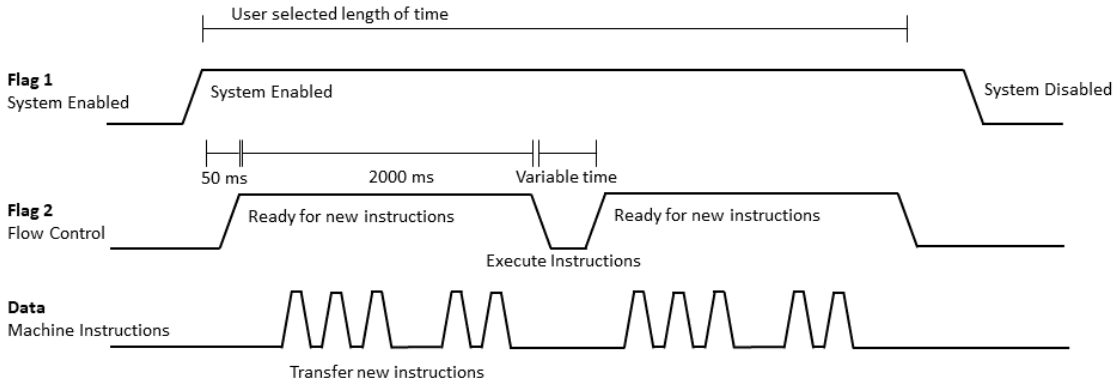

Figure 72: Timing Diagram for Closed-Loop Control System

This process was designed to work on any commercial CNC system with a standard operating system as the foundation of the machine's control. A generic operational flow is presented in Figure 73. The specific implementation flow for the Mazak hybrid machine is presented in Figure 74.

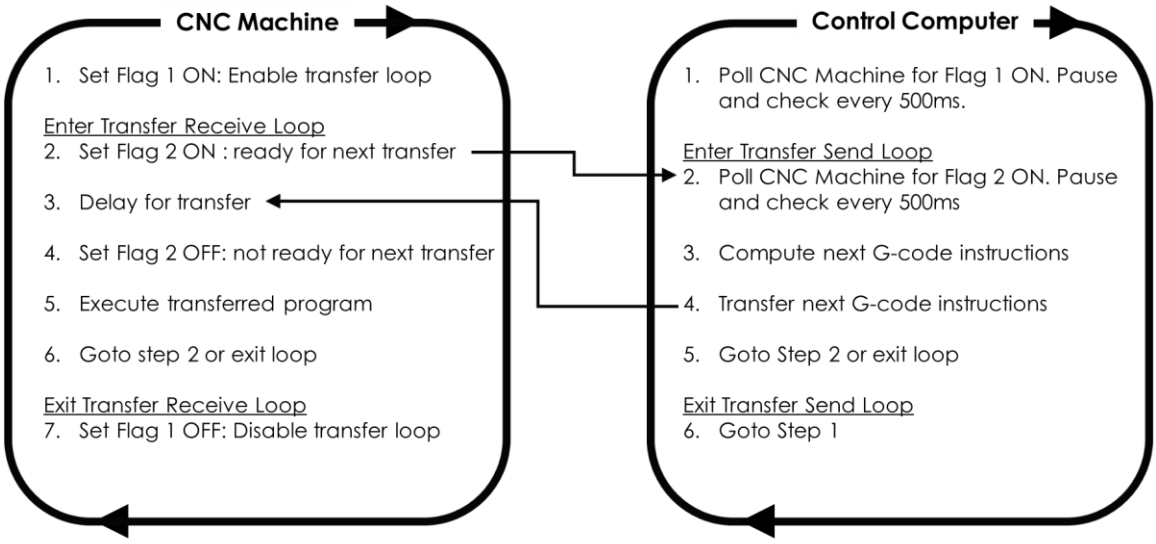

Figure 73: Generic Level 1 and 2 Closed-Loop Control for Arbitrary Commercial CNC System

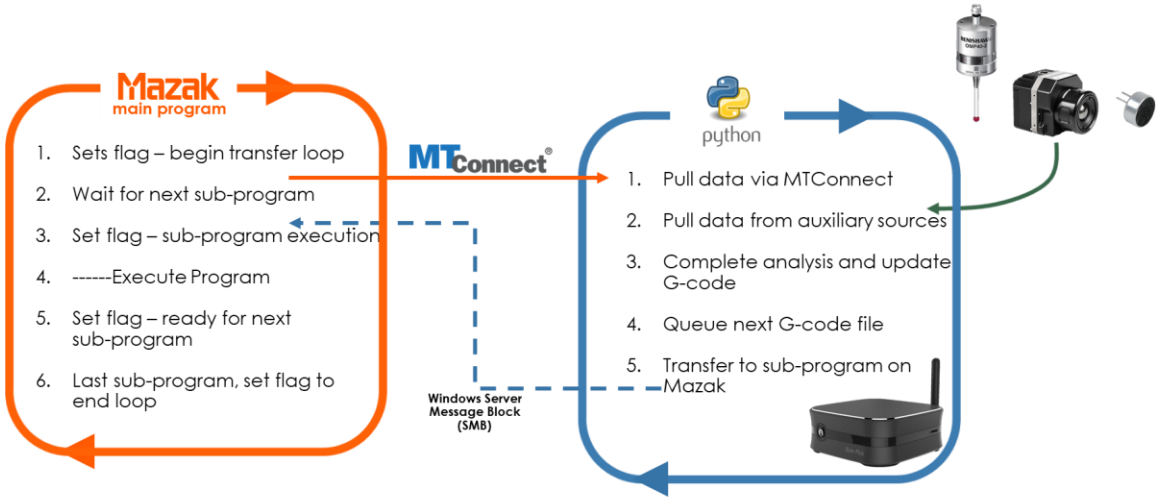

Figure 74: Level 1 and 2 Closed-Loop Control Implementation for Mazak Hybrid

5.4 Results

A series of three experiments were performed to evaluate the capabilities of the Closed-Loop Control System. These three experiments were designed to test different capabilities of the hybrid manufacturing system under a closed-loop control regime. The experiments performed are as follows:

1. Dynamic dwell control to prevent thermal overheating of a thin-wall structure during additive material deposition
2. Multiple part fabrication based on thermal control
3. Continuous inspection for *in-situ* distortion monitoring during cooling

5.4.1 Experiment 1 – Dynamic Dwell

Thermal control of additive processes is critical for the successful fabrication of thin-wall structures. This is increasingly difficult when the bead geometry for deposited material is of similar size to the thickness of the structure. Previous experiments attempting to print a thin-wall structure with a 15 degree overhang have failed due to thermal overheating. An example of a failed component is displayed in Figure 75.

Figure 75: Thin-Wall Structure Overhang Failure from Thermal Overheating

The closed-loop control methodology was used to dynamically change dwell times between deposition of each layer. The FLIR A35 thermal camera was used to monitor the maximum temperature within the part. A dwell was commended until the temperature fell below a threshold value of 135 C. A chart of dwell times per layer is displayed in Figure 76. It can be seen that the dwell times were consistent for layers 1-6. This is attributed to a cold substrate. However, once the substrate reached thermal equilibrium, the dwell time increased and the closed-loop control algorithm waited until the maximum temperature fell below the threshold. The thin-wall geometry was successfully printed with the closed-loop control methodology, displayed in Figure 77.

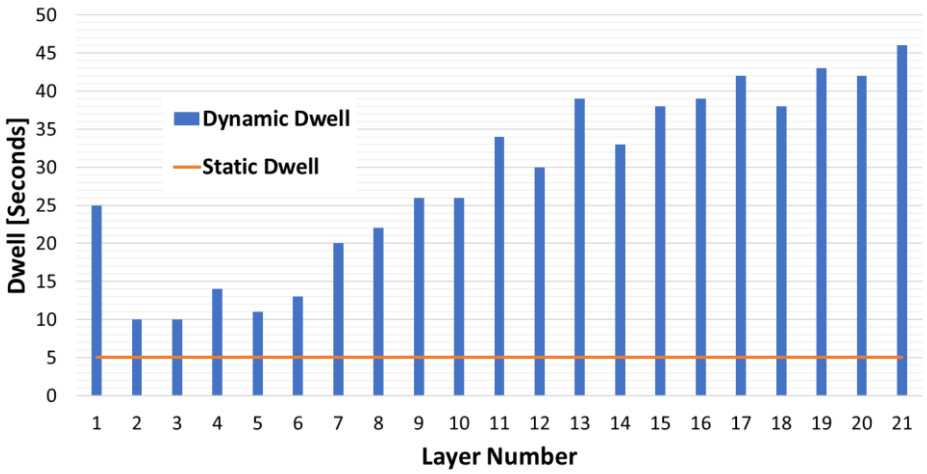

Figure 76: Dwell Times for Thin-Wall Overhang Geometry

Figure 77: Thin-Wall Structure Overhang Fabricated with Closed-Loop Control

5.4.2 Experiment 2 – Multi-Part Operations

A second plug-in was developed as part of the closed-loop control capabilities to coordinate separate operations on multiple components. This capability enables the independent fabrication of N number of distinct parts within the same build chamber. A specific application of this capability is the increase in machine efficiency while operating under thermal management conditions in metal additive manufacturing.

A multi-part experiment was setup to test and demonstrate this capability. A FLIR A35 thermal camera was positioned to monitor temperatures over two sections of a cast iron substrate, as shown in Figure 78.

Figure 78: Multi-Part Thermal Camera Experiment Setup

The closed-loop control plug-in captured the thermal image and evaluated the maximum temperature on both halves of the substrate, as displayed in Figure 79. G-code for two 5-bead walls measuring 50mm in height (total of 26 layers) was created. The closed-loop control framework with multi-part plugin evaluated the thermal image and identified the section with the lowest temperature. The machine instructions were subsequently updated to continue operations on that part. Throughout the fabrication of these parts, the left side was favored. While layers 1-10 alternated between the left and right parts evenly, the left part cooled faster and was therefore favored by the algorithm for subsequent layers. The left part was completely fabricated while over 10 layers remained on the right part, as shown in Figure 3. A standard "1-2-3 block" is provided in the picture for scale.

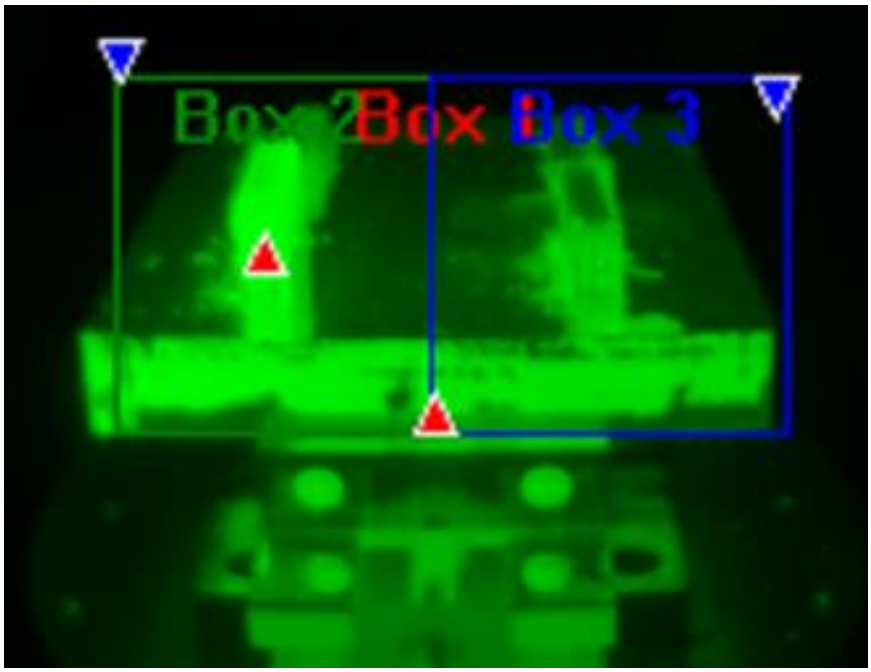

Figure 79: FLIR A35 Thermal Image Segmented for Multi-Part Fabrication

Figure 80: Multi-Part Fabrication of Two Walls through Closed-Loop Control

Although the demonstration of multi-part fabrication was successful, further development of the closed-loop control algorithm is needed. Additional logic should be added to monitor the differential between layers of separate parts. If one part is allowed to build beyond a certain number of layers with respect to the other components, the potential for a machine crash becomes significant. Additionally, while the algorithm is currently capable of multi-part fabrication with both additive and subtractive operations, it is not capable of the preparatory tasks required to make such changes. For example, automatic fan cycles could be triggered to follow all subtractive operations, clearing coolant and other chips from the substrate before additive operations continue.

5.4.3 Experiment 3 – Geometric Distortion Detection

One of the fundamental technical challenges in additive manufacturing is the production of geometrically accurate components. In additive manufacturing with fused deposition modeling (FDM) techniques, components are often underbuilt or overbuilt. A benefit of hybrid manufacturing is the ability to add and subtract material at will, enabling corrective operations for components not printed within desired specifications. However, a closed-loop control framework is required to measure, analyze and repair component efficiently.

A plug-in for geometric inspection process was developed as part of the closed-loop control capabilities. A Renishaw RMP-60 inspection probe was used with the Mazak hybrid machine to provide inspection capabilities. This probe allows for geometric inspection with full 5-axis motion. However, for this demonstration probing cycles were created for 3-axis planar inspections.

A python script was developed that generates G-code corresponding to planar probing cycles for the Mazak / Renishaw RMP-60 combination. The python script can generate probing cycles for a single point or generate a grid of points for surface inspection. A set of G-code instructions is generated that probes the surface in either the ±X, ±Y, or -Z axial directions. The resulting inspection points are collected by the Local Control Unit.

An experiment was performed to deposit a conical structure, displayed in Figure 81. Immediately after deposition, the closed-loop control architecture was used to continuously monitor distortions over a period of three hours. A series of 12 points around

the circumference of the cylinder were measured. These points were collected by the Local Control Unit following the process described in Chapter 4 – Phase II.

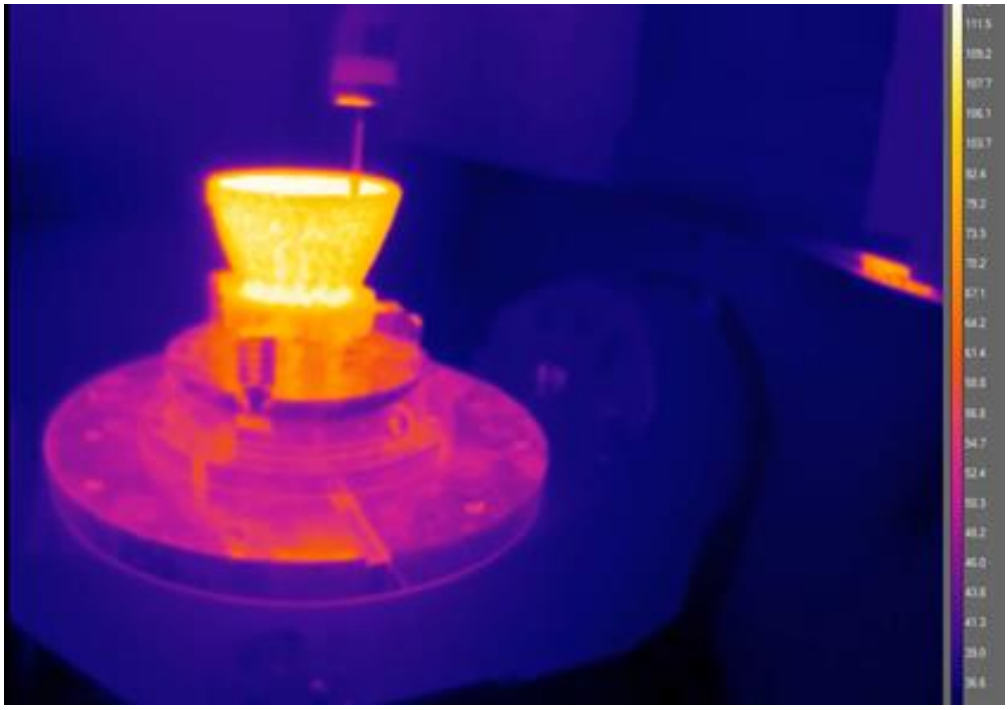

Figure 81: Conical Structure Fabricated with Mazak Hybrid Machine

Distortion points were collected and plotted as shown in Figure 82. This capability allows for immediate comparison of the fabricated component against the CAD model. By integrating this capability with the closed-loop control framework, corrective action can be triggered to repair features that are underbuilt or overbuilt.

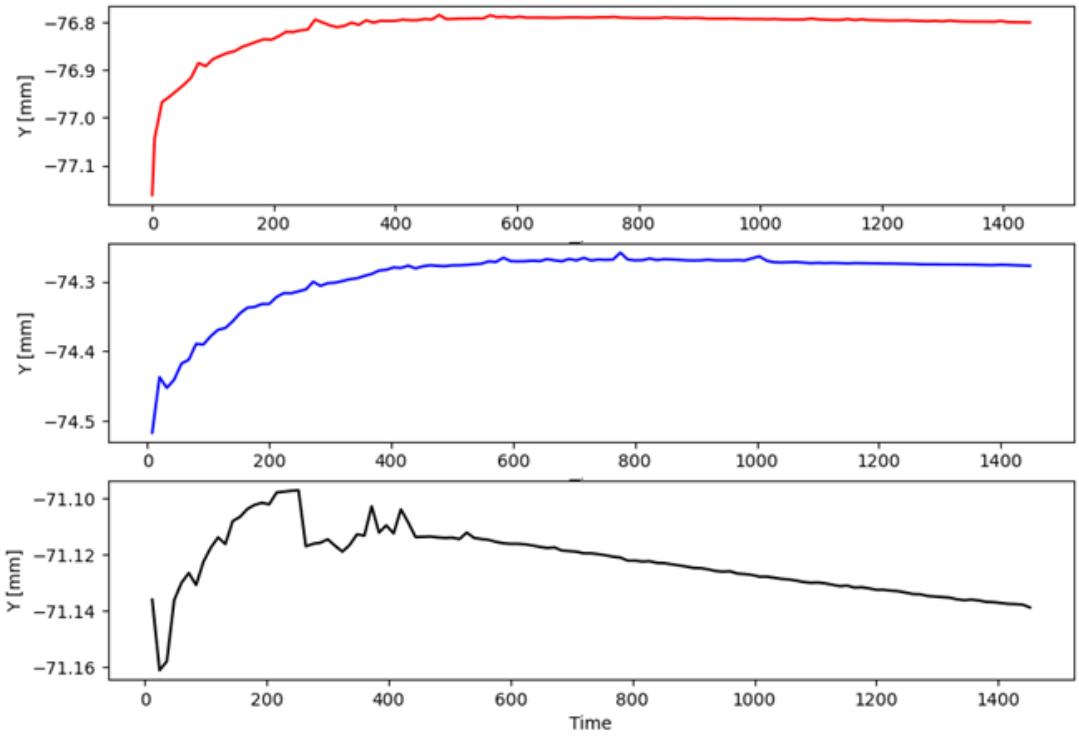

Figure 82: Distortion in Y-axis for Three Points in Cylindrical Geometry

5.5 Discussion and Limitations

The development of a closed-loop control methodology for hybrid operations enables an enhanced set of operational flows for fabrication of hybrid components. Fabrication processes are no longer limited to open loop systems, where the operation cannot be salvaged if errors occur. However, there is a fundamental reliance on machine information and access to enable the closed-loop control methodology.

The methods presented above were developed without significant access to the underlying machine structure. Vulnerabilities in the operational structure of the machine were identified and leverages for enhanced control. In a way, machine instructions were updated on the machine by writing to a specific memory location when it was safe to do so

and the file was not in active use. In other words, machine data was overwritten when "the machine was not looking." There is a significant need for increased access to the machine controller to enable a more formalized approach to Closed-Loop Control operations.

Additionally, there is a need for higher frequency feedback methods to support Level 3 control, high-frequency updating of process parameters sch as laser power and standoff distance. There is also a need for fast data output capabilities for higher fidelity monitoring. Standard MTConnect implementations are often limited to 1-5Hz in output frequency to prevent overloading the machine controller. MTConnect itself was originally intended to be used for machine efficiency calculations, and overall statistics. However, it was leveraged to create a digital twin of the process, requiring higher frequency data. Improving the output frequency of MTConnect would significantly increase the capabilities provided by the Closed-Loop Control methodology.

5.6 Conclusion

The closed-loop control framework is a powerful and essential addition to standard Hybrid manufacturing centers. The ability to trigger and control a variety of operations for more intelligent manufacturing process flows provides flexibility increases and efficiency gains. While the closed-loop inspection and multi-part fabrication capabilities were demonstrated in this special problem, significant work is still needed to refine the existing framework and include additional capabilities, decision logic, and expanded controls. In time, the closed-loop control framework has the potential to be an integral component in commercial hybrid manufacturing operations.

CHAPTER 6. CONTRIBUTIONS

This body of work was conducted to advance the understanding and applications of digital monitoring technologies with feedback methodologies for commercial CNC systems, with broad applications to the manufacturing industry. The strategic combination and synchronization of information from multiple sensing modalities was investigated to improve the accuracy of *in-situ* digital twin components. Three key contributions were completed through this research:

> **Contribution 1:** Development of a method to monitor, measure, and compare geometric feature error by use of existing manufacturing data streams.
>
> **Contribution 2:** Investigation of multi-agent architecture methodology and compression mechanisms for system information governance to support automated *in-situ* modelling and feedback control operations.
>
> **Contribution 3:** Development of a method for discrete, *in-situ* feedback control of commercial hybrid CNC systems to enhance resulting components.

These technologies are investigated and demonstrated with hybrid CNC machining centers manufacturing; however, they are applicable to any CNC manufacturing process. These contributions further enable verification of component accuracy on multiple manufacturing platforms through digital twin modelling techniques.

CHAPTER 7. CONCLUSION

This dissertation investigated the strategic combination and synchronization of information from multiple sensing modalities to improve the accuracy of digital twin models. A voxel modelling methodology was developed and investigated to create a digital twin of the component being produced. Information describing the machine's current operations was strategically combined with information from additional sensing modalities, improving the accuracy of *in-situ* digital twin models by up to 52%. This research resulted in (1) a method to geometrically compare features of *in-situ* components from multiple sensing modalities against desired specifications, (2) a multi-agent architecture to support efficient communication, storage, and use of this information, resulting in (3) feedback methodologies for commercial CNC systems to affect the *in-situ* manufacturing process and correct geometric deviations.

CHAPTER 8. FUTURE WORK

8.1 Part Certification

The results of this research focused on geometric verification of CNC fabrication methods. These results are applicable to both standard subtractive machining methods as well as hybrid manufacturing methods. However, the inclusion of additive processes in hybrid manufacturing demands attention with respect to the underlying material properties of fabricated components. Significant work remains to control and verify material property characteristics for components produced with hybrid manufacturing techniques.

Previous research has demonstrated the benefits of microstructure control in additive manufacturing [76]. Localized microstructure control of the final material has been achieved by applying non-standard scan strategies to laser powder bed fusion techniques. A similar strategy could be applied to additive processes in hybrid manufacturing, enabling non-uniform material properties in different regions of geometry.

8.2 Cybersecurity Applications

The integration of CPS in the manufacturing industry enable advantageous opportunities to better understand and control production processes, while simultaneously providing a pathway for malicious digital attacks intended to adversely affect equipment and fabricated components. While cybersecurity has long been a concern in the national security and finance industry, the need for secure manufacturing processes is quickly becoming evident [77].

An evaluation of the information input and output capabilities for CNC manufacturing systems conducted as part of Phase II and Phase III revealed numerous high-level vulnerabilities. These systems are prone to attack for unintended operations due to current design, operational flow, and software vulnerabilities. A diagram for the high-level vulnerabilities beginning with a CAD model to process feedback opportunities is displayed in Figure 83.

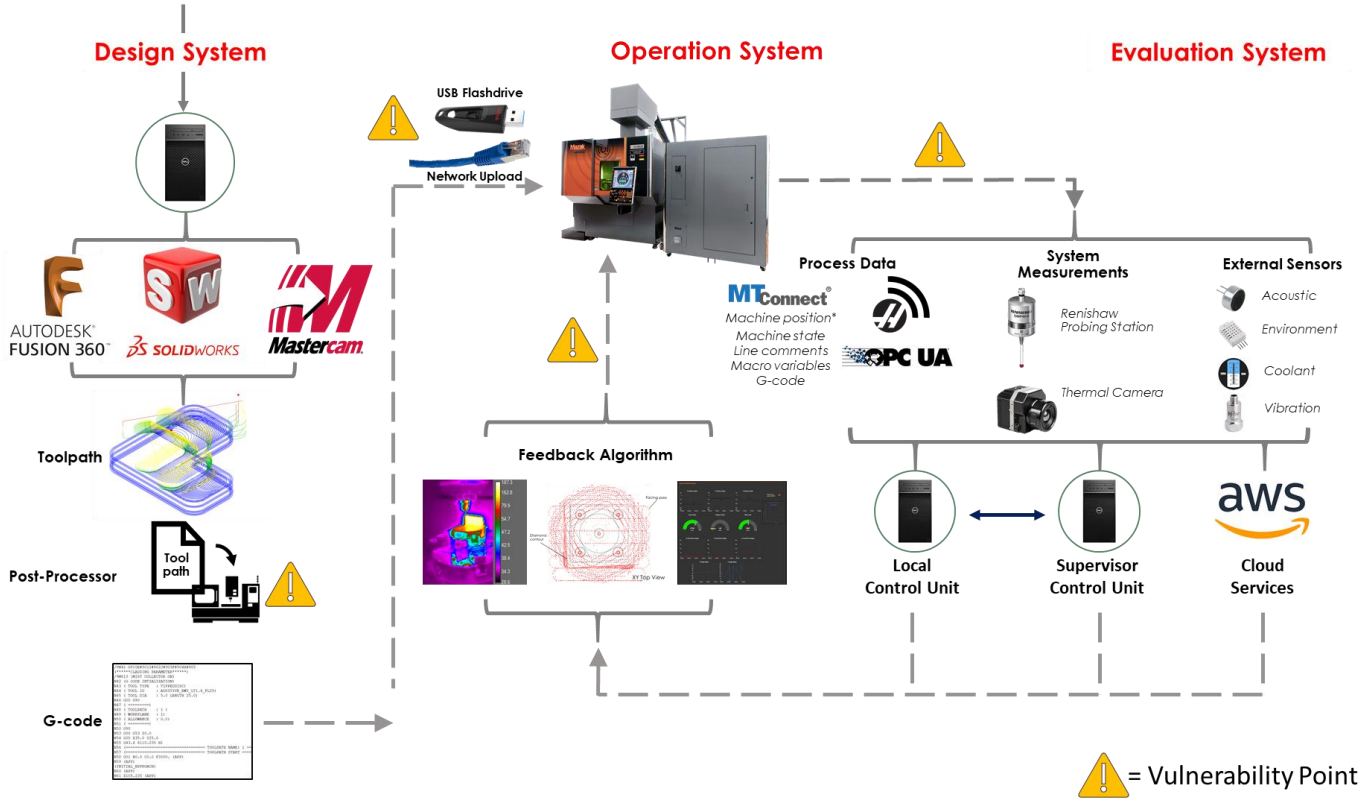

Figure 83: Vulnerabilities in CNC Manufacturing Information Flow

These vulnerabilities range from modification opportunities during transmission of G-code instructions to adverse feedback commands during *in-situ* process monitoring operations. Significant work is needed to protect existing production processes with update operational flows designed to increase secured information transfer. It is acknowledged that due to the

age of many manufacturing machines, upgrade opportunities may be limited. Therefore, the next generation of manufacturing equipment must be rapidly developed with consideration to modern cybersecurity practices. Among other common practices, it can no-longer be acceptable to transfer G-code information through USB-sticks from the CAD/CAM designer's computer to manufacturing equipment without additional anti-tampering checks. Other subtle opportunities for malicious intent must be mitigated by integrating cyber-secure practices with the next generation of manufacturing equipment.

8.3 Spinning the Digital Thread

The hybrid manufacturing platform provides unparalleled opportunities to 'spin the digital thread' with data-driven, modularly interleaved operations [78]. The digital thread concept refers to an extension of Digital Twin modelling methods where a comprehensive timeline is created to detail the actions, events, processes, and inspection operations used to affect or measure a uniquely identifiable component from cradle to grave [79]. A visualization of a components' digital thread is presented in Figure 84.

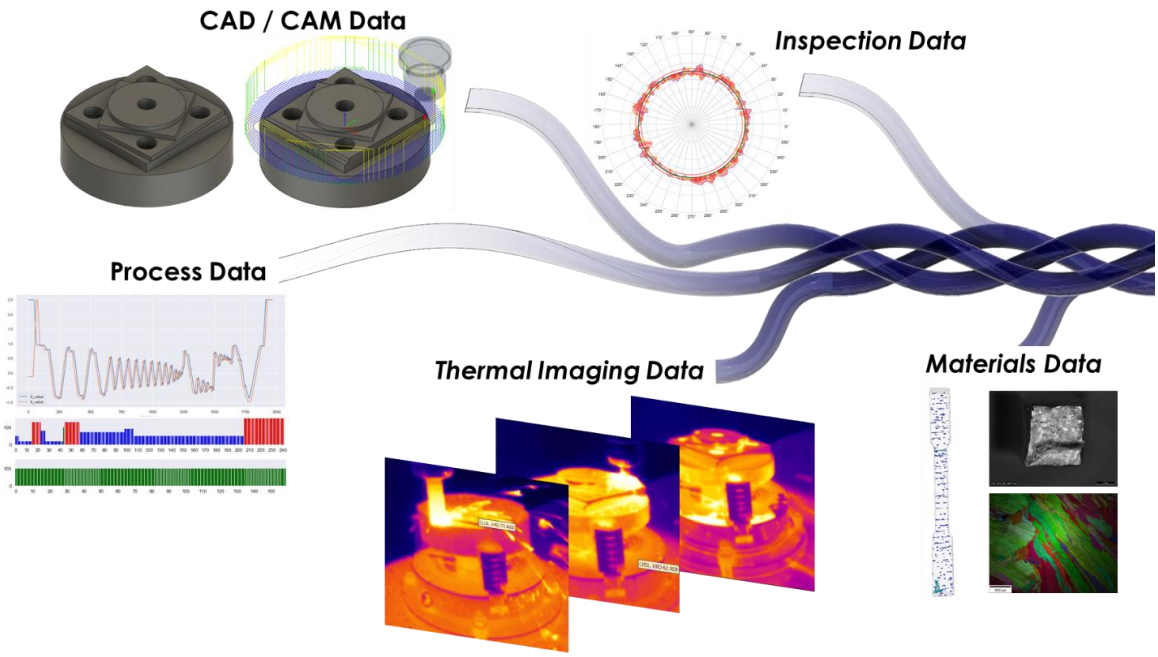

Figure 84: Spinning the Digital Thread with Hybrid Manufacturing [78]

When combined with *in-situ* verification methods, non-destructive testing operations, and process monitoring of component repairs, the digital thread has the potential to serve as a digital passport of authenticity that can accompany a physical component. This passport can aid in assuring part quality and performance capabilities.

8.4 The Future of Advanced Manufacturing

CNC manufacturing systems are well equipped to produce digital threads of all fabricated components. A powerful combination of process monitoring techniques, information analytics, and feedback mechanisms enable unparalleled fabrication and verification opportunities. Hybrid CNC manufacturing systems further enable the fabrication for complex geometries within a single system. Together, the combination digital manufacturing methods with the next generation of manufacturing machines will propel the advanced manufacturing industry for decades to come.

REFERENCES

[1] Oliveira, L. E. S., and Álvares, A. J., 2016, "Axiomatic Design Applied to the Development of a System for Monitoring and Teleoperation of a CNC Machine through the Internet," Procedia CIRP, 53, pp. 198-205.

[2] Bibby, L., and Dehe, B., 2018, "Defining and assessing industry 4.0 maturity levels – case of the defence sector," Production Planning & Control, 29(12), pp. 1030-1043.

[3] McFarlane, D., Brintrup, A., "What is Digital Manufacturing?," https://www.ifm.eng.cam.ac.uk/research/digital-manufacturing/what-is-digital-manufacturing/.

[4] Garza-Reyes, J. A., Eldridge, S., Barber, K. D., and Soriano-Meier, H., 2010, "Overall equipment effectiveness (OEE) and process capability (PC) measures: A relationship analysis," The International Journal of Quality & Reliability Management, 27(1), pp. 48-62.

[5] Dumitrache, I., and Caramihai, S. I., 2013, "The Enterprise of Future as a Cyber-Physical System," IFAC Proceedings Volumes, 46(9), pp. 1310-1315.

[6] Lorenz, K., Jones, J., Wimpenny, D., and Jackson, M., "A review of hybrid manufacturing."

[7] Mori, D., 2012, "LASERTEC 65 DED hybrid," https://us.dmgmori.com/products/machines/additive-manufacturing/powder-nozzle/lasertec-65-ded-hybrid.

[8] Corporation, M., 2019, "VC-500A/5X AM HWD."

[9] Corporation, O., 2018, "MU-8000V LASER EX," https://www.okuma.com/products/mu-8000v-laser-ex.

[10] Jones., J. B., "World's first commercially available hybrid CNC," https://hybridmanutech.com/our-history/.

[11] Kottman, M., Zhang, S., McGuffin-Cawley, J., Denney, P., and Narayanan, B. K., 2015, "Laser Hot Wire Process: A Novel Process for Near-Net Shape Fabrication for High-Throughput Applications," JOM, 67(3), pp. 622-628.

[12] Institute, M., 2018, "MTConnect Standard," MTConnect Institute.

[13] Foundation, O., "OPC Unified Architecture," https://opcfoundation.org/developer-tools/specifications-unified-architecture.

[14] Haas, 2020, "HaasConnect: Remote monitoring," Haas.

[15] Radhakrishnan, R., and Balamurugan, P., 2011, "Six Sigma Based Control Chart for Fraction Defectives," Journal of testing and evaluation, 39(4), pp. 1-4.

[16] "Machinery's handbook. : 1914C."

[17] Karandikar, J., Honeycutt, A., Schmitz, T., and Smith, S., 2020, "Stability boundary and optimal operating parameter identification in milling using Bayesian learning," Journal of manufacturing processes, 56, pp. 1252-1262.

[18] Shamsaei, N., Yadollahi, A., Bian, L., and Thompson, S. M., 2015, "An overview of Direct Laser Deposition for additive manufacturing

Part II: Mechanical behavior, process parameter optimization and control," Additive manufacturing, 8, pp. 12-35.

[19] Feldhausen, T., 2020, "DEVELOPMENT AND EVALUATION OF INTERFACIAL STRUCTURES FOR HYBRID MANUFACTURING," Doctoral, Georgia Institute of Technology.

[20] Saleeby, K. S., Kurfess, T., Feldhausen, T., and Love, L., 2020, "Production of Medium-Scale Metal Additive Geometry With Hybrid Manufacturing Technology."

[21] S.P. Moylan, J. A. S., A.L. Cooke, K.K. Jurrens, and M.A. Donmez, "Proposal for a standardized test artifact for additive manufacturing machines and processes," Proc. International Solid Free Form Symposium, pp. 902 - 920.

[22] Organization, I. S., 2020, "Test conditions for machining centres," Part 7: Accuracy of finished test pieces, Switzerland, pp. 7-29.

[23] Gene, R. C., 2011, Geometric Dimensioning and Tolerancing for Mechanical Design, Second Edition, McGraw-Hill Education, New York.

[24] Renishaw, "RMP60 radio transmission probe," https://www.renishaw.com/en/rmp60-radio-transmission-probe--19257.

[25] Haas, "Haas VF-5/40," https://www.haascnc.com/machines/vertical-mills/vf-series/models/medium/vf-5-40.html.

[26] Lee, K.-J., Lee, T.-M., and Yang, M.-Y., 2007, "Tool wear monitoring system for CNC end milling using a hybrid approach to cutting force regulation," The International Journal of Advanced Manufacturing Technology, 32(1-2), pp. 8-17.

[27] Imtiaz, J., and Jasperneite, J., "Scalability of OPC-UA down to the chip level enables “Internet of Things”," Proc. 2013 11th IEEE International Conference on Industrial Informatics (INDIN), IEEE, pp. 500-505.

[28] Xu, X. W., and Newman, S. T., 2006, "Making CNC machine tools more open, interoperable and intelligent—a review of the technologies," Computers in Industry, 57(2), pp. 141-152.

[29] Nsiah, K. A., Schappacher, M., Rathfelder, C., Sikora, A., and Groza, V., "An open-source toolkit for retrofit industry 4.0 sensing and monitoring applications," Proc. 2018 IEEE International Instrumentation and Measurement Technology Conference (I2MTC), IEEE, pp. 1-6.

[30] Halsey, W., Ferguson, J., Plotkowski, A., Dehoff, R., and Paquit, V., 2020, "Geometry-independent microstructure optimization for electron beam powder bed fusion additive manufacturing," Additive Manufacturing, 35, p. 101354.

[31] J. K. Nagel, F. W. L., 2021, "Hybrid Manufacturing System Design and Development," Manufacturing System: IntechOpen.

[32] Kerschbaumer, M., and Ernst, G., 2004, "Hybrid manufacturing process for rapid high performance tooling combining high speed milling and laser cladding," International Congress on Applications of Lasers & Electro-Optics, 2004(1), p. 1710.

[33] Klocke, F., Wirtz, H., and Meiners, W., "Direct Manufacturing of Metal Prototypes and Prototype Tools."

[34] Jones, J. B., "The Synergies of Hybridizing CNC and Additive Manufacturing."

[35] Autodesk, 2020, "Autodesk Fusion 360," Autodesk, pp. Integrated CAD, CAM, CAE, and PCB software.

[36] MIND, O., 2020, "hyperMILL," OPEN MIND.

[37] Feldhausen, T., Raghavan, N., Saleeby, K., Love, L., and Kurfess, T., 2021, "Mechanical properties and microstructure of 316L stainless steel produced by hybrid manufacturing," Journal of Materials Processing Technology, 290, p. 116970.

[38] Cai, Y., Starly, B., Cohen, P., and Lee, Y.-S., 2017, "Sensor Data and Information Fusion to Construct Digital-twins Virtual Machine Tools for Cyber-physical Manufacturing," Procedia Manufacturing, 10, pp. 1031-1042.

[39] DebRoy, T., Zhang, W., Turner, J., and Babu, S. S., 2017, "Building digital twins of 3D printing machines," Scripta Materialia, 135, pp. 119-124.

[40] Knapp, G. L., Mukherjee, T., Zuback, J. S., Wei, H. L., Palmer, T. A., De, A., and DebRoy, T., 2017, "Building blocks for a digital twin of additive manufacturing," Acta Materialia, 135, pp. 390-399.

[41] LincolnElectric, and Tucker, T., 2020, "SculptPrint."

[42] Lynn, R., Contis, D., Hossain, M., Huang, N., Tucker, T., and Kurfess, T., 2017, "Voxel model surface offsetting for computer-aided manufacturing using virtualized high-performance computing," Journal of Manufacturing Systems, 43, pp. 296-304.

[43] Lynn, R., Dinar, M., Huang, N., Collins, J., Yu, J., Greer, C., Tucker, T., and Kurfess, T., 2017, "Direct Digital Subtractive Manufacturing of a Functional Assembly Using Voxel-Based Models," Journal of Manufacturing Science and Engineering, 140(2).

[44] DeWitte, L. N., Saldana, C. J., Feldhausen, T. A., and Kurfess, T. R., 2020, "Initial Process Planning of a Hybrid Multi-Tasking Platform."

[45] Stenerson, J., 2007, Computer numerical control : operation and programming / Jon Stenerson, Kelly Curran, Upper Saddle River, N.J. : Pearson Prentice Hall, Upper Saddle River, N.J.

[46] Renishaw, "RMP60 - Radio Macine Probe Installation Guide," https://resources.renishaw.com/en/details/installation-guide-rmp60--58782.

[47] Zhou, Z., Xie, S., and Chen, D., 2012, "Introduction," Fundamentals of Digital Manufacturing Science, Z. Zhou, S. Xie, and D. Chen, eds., Springer London, London, pp. 1-18.

[48] De Oliveira, L., and Alvares, A., 2016, "Axiomatic Design Applied to the Development of a System for Monitoring and Teleoperation of a CNC Machine through the Internet," Procedia CIRP, 53.

[49] Elazhary, H., 2019, "Internet of Things (IoT), mobile cloud, cloudlet, mobile IoT, IoT cloud, fog, mobile edge, and edge emerging computing paradigms: Disambiguation and research directions," Journal of network and computer applications, 128, pp. 105-140.

[50] Kurfess, T. R., Saldana, C., Saleeby, K., and Dezfouli, M. P., 2020, "A Review of Modern Communication Technologies for Digital Manufacturing Processes in Industry 4.0," J. Manuf. Sci. Eng, 142(11).

[51] Tao, F., Zhang, M., and Nee, A. Y. C., 2019, "Chapter 8 - Digital Twin and Cloud, Fog, Edge Computing," Digital Twin Driven Smart Manufacturing, F. Tao, M. Zhang, and A. Y. C. Nee, eds., Academic Press, pp. 171-181.

[52] Saleeby, K. S., and Kurfess, T. R., "Low cost wireless accelerometer sensor platform with internet-of-things for manufacturing (IOT4MFG) applications," Proc. Micro-and Nanotechnology Sensors, Systems, and Applications XI, International Society for Optics and Photonics, p. 1098210.

[53] Lee, J., Kao, H.-A., and Yang, S., 2014, "Service Innovation and Smart Analytics for Industry 4.0 and Big Data Environment," Procedia CIRP, 16, pp. 3-8.

[54] Lee, J., Bagheri, B., and Kao, H.-A., 2015, "A Cyber-Physical Systems architecture for Industry 4.0-based manufacturing systems," Manufacturing letters, 3, pp. 18-23.

[55] Bagheri, B., Yang, S., Kao, H.-A., and Lee, J., 2015, "Cyber-physical Systems Architecture for Self-Aware Machines in Industry 4.0 Environment," IFAC-PapersOnLine, 48(3), pp. 1622-1627.

[56] Li, B., Ling, Y., Zhang, H., and Zheng, S., 2016, "The design and realization of cherry tomato harvesting robot based on IOT," International Journal of Online and Biomedical Engineering (iJOE), 12(12), pp. 23-26.

[57] Zhilenkov, A. A., Gilyazov, D. D., Matveev, I. I., and Krishtal, Y. V., "Power line communication in IoT-systems," Proc. 2017 IEEE Conference of Russian Young Researchers in Electrical and Electronic Engineering (EIConRus), IEEE, pp. 242-245.

[58] Daneels, A., and Salter, W., 1999, "What is SCADA?."

[59] Briscoe, N., 2000, "Understanding the OSI 7-layer model," PC Network Advisor, 120(2).

[60] Handel, T. G., and Sandford, M. T., "Hiding data in the OSI network model," Proc. International Workshop on Information Hiding, Springer, pp. 23-38.

[61] Torrisi, N. M., and de Oliveira, J. F. G., 2012, "Remote monitoring for high-speed CNC processes over public IP networks using CyberOPC," The International Journal of Advanced Manufacturing Technology, 60(1-4), pp. 191-200.

[62] Schofield, S., and Wright, P., 1998, "Open Architecture Controllers for Machine Tools, Part 1: Design Principles," Journal of Manufacturing Science and Engineering, 120(2), pp. 417-424.

[63] Anderson, B. M., Cole, J. R., and Holland, R. G., 1993, "An Open Standard for Industrial Controllers," Manufacturing Review, 6(3), pp. 180-191.

[64] Hillaire, R. G., 2001, "New Machining Strategies with Open Architecture Controllers," Doctor of Philosophy Dissertation, University of California, Berkeley, Berkeley, CA.

[65] Ota, N. K., 2007, "The Application of Wireless Sensor Networks to Residential Energy Efficiency and Demand Response," Doctor of Philosophy Dissertation, University of California, Berkeley, Berkeley, CA.

[66] Andreadis, G., Klazoglou, P., Niotaki, K., and Bouzakis, K.-D., 2014, "Classification and Review of Multi-agents Systems in the Manufacturing Section," Procedia Engineering, 69, pp. 282-290.

[67] Salvador Palau, A., Dhada, M. H., and Parlikad, A. K., 2019, "Multi-agent system architectures for collaborative prognostics," Journal of Intelligent Manufacturing, 30(8), pp. 2999-3013.

[68] Misra, M., 1999, "On -line multivariate chemical data compression and validation using wavelets," ProQuest Dissertations Publishing.

[69] Yaman, U., and Dolen, M., 2013, "Direct command generation for CNC machinery based on data compression techniques," Robotics and computer-integrated manufacturing, 29(2), pp. 344-356.

[70] Salloum, M., Salloum, M., Johnson, K. L., Johnson, K. L., Bishop, J. E., Bishop, J. E., Aytac, J. M., Aytac, J. M., Dagel, D., Dagel, D., van Bloemen Waanders, B. G., and van Bloemen Waanders, B. G., 2019, "Adaptive wavelet compression of large additive manufacturing experimental and simulation datasets," Comput Mech, 63(3), pp. 491-510.

[71] Tritschler, N., Dugenske, A., and Kurfess, T., 2021, "An automated edge computing based condition health monitoring system: with an application on rolling element bearings," J. Manuf. Sci. Eng, pp. 1-10.

[72] Ogata, K., 1990, Modern control engineering, Englewood Cliffs, N.J. : Prentice Hall.

[73] Xu, X. X., 2009, Integrating Advanced Computer-Aided Design, Manufacturing, and Numerical Control : Principles and Implementations, IGI Global, Hershey, UNITED STATES.

[74] FLIR, "FLIR A35 Thermal Camera," https://www.flir.com/products/a35/.

[75] Drones, N., 2020, "FLIR Image Extractor," National Drones.

[76] Halsey, W., Ferguson, J., Plotkowski, A., Dehoff, R., and Paquit, V., 2020, "Geometry-independent microstructure optimization for electron beam powder bed fusion additive manufacturing," Additive manufacturing, 35(1), p. 101354.

[77] Thames, L., and Schaefer, D., 2017, Cybersecurity for industry 4.0: analysis for design and manufacturing, Springer.

[78] Feldhausen, T., Saleeby, K., and Kurfess, T., 2021, "Spinning the Digital Thread with Hybrid Manufacturing," Manufacturing Letters(Under Review).

[79] Kurfess, T., "Smart Manufacturing at Oak Ridge National Laboratory: Integrating Hybrid Manufacturing Processes via the Digital Thread," Proc. Smart Manufacturing Experience (SMX), Society of Manufacturing Engineers (SME).